University of Pécs
Faculty of Engineering
and Information Technology

Investigation of Building Materials Containing Algae-Prone Properties: Perspectives for Sustainable Façade Design

Doctoral-Thesis

submitted for the degree of

Doctor of Philosophy (PhD)

by

Holger Heinrich

24th of April 2024

Supervisor:
Dr. habil. Adél Len, University of Pécs
External Tutor:
Prof. em. Dr. rer. nat. Dr.-Ing. habil. Helmuth Venzmer, Wismar

“A discovery is to see something that everyone has seen and to think of something that no one has ever thought of.”

(Albert von Szent-Gyorgyi, 1893-1986)

Abstract

During the last decades, research has been concerned with the topic of microbial colonisation of building components. Algae are in focus of investigations, as they occur worldwide and are conspicuous for the intense colouring of their photopigments. As a successful model of evolution, these autotrophic microorganisms can adapt quickly to new and extreme living conditions. It is therefore no surprise that algae have recognised and conquered the large areas of façades for themselves. As water is the most important basic prerequisite for biological life, building physics countermeasures focused on preventing condensation on façades – not only on external thermal insulation composite systems (ETICS).

Architects and building planners are called upon to avoid algae infestation through constructive measures and the combination of suitable building materials as the visual aesthetics and long-term serviceability of building façades must be maintained. Investigations into the influence of coating formulations have so far primarily focused on binder systems, biocides, constructive and hygrothermal properties. Research on the algal susceptibility due to magnesium-containing fillers is not to be found, but these regularly constitute a large proportion of final coatings on building surfaces. The present work investigates the role of magnesium-containing fillers in the process of algal colonization of façade coatings.

The effect of in-situ generated protons on the development of algal biofilms in the outdoor weathering experiment was investigated as a possible defence strategy by water-activated filler composition. Architectural engineering not only takes place on a large scale but begins on the micro scale of functional fillers, whose creative design has the potential to solve problems on a bigger scale. Understanding the mechanisms can help to avoid causes rather than fighting symptoms of algal colonization with organic biocides and high environmental risks.

Practical measurement methods are needed that can be used in the laboratory and on site. The results achieved in this PhD thesis are based on the development of a novel application of the mobile fluorescence measurement system.

The focus of current research is no longer only on control, but also on targeted establishment of algal biofilms on building surfaces. Recognizing that algae contribute to CO_2 sequestration and climate control, the development of bio-receptive façades gained in research importance. Less complex and reliable methods for the detection of algal biofilms are required to reveal influencing factors in all cases that can be considered for more sustainable future façade design.

Abbreviations

AES	Atomic Emission Spectroscopy
ATP	Adaptation to Technical and Scientific Progress
AUC	Area under the curve
A24	Autobahn 24 / Highway 24
BPR	Biocidal Product Regulation
BTo	BenthoTorch
Ca	Calcium
ca.	circa
CAS	Chemical Abstracts Service
°C	Degree Celsius
Chl-a	Chlorophyll a
cm	centimetre
CO_2	Carbon Dioxide
DIN	Deutsches Institut für Normung
ECHA	European Chemicals Agency
Ed.	Editor
EDX	Energy Dispersive X-Ray
EN	European Norm
et al.	et alii / and others
etc.	et cetera

ETICS	External Thermal Insulation Composite System
EU	European Union
Fig.	Figure
g	gram
GmbH	Gesellschaft mit beschränkter Haftung
h	Hours
HBW	Hellbezugswert / light reflective value
HSD	Honestly Significant Difference
i.e.	id est / that is
ICP	Inductive Coupled Plasma
IEP	Iso-electrical point
Incl.	inclusive
IR	infra-red
ISBN	International Standard Book Number
ISO	International Organisation for Standardisation
K	Kalium/Potassium
kg	Kilograms
km	Kilometre
L*	colour distance value
LED	light emitting diode
log	logarithm

m	mass
max.	maximum
Mg	Magnesium
min.	Minimum
ml	Milliliter
mm	Millimeter
Mo	Molybdenum
µm	Micrometer
µg	Micro Gram
n	count
Na	Sodium
NIR	near infrared
nm	nanometre
No.	number
O	oxygen
OH	hydroxyl group
PAM	pulse amplitude modulation
PAR	Photosynthetically Active Radiation
PC	personal computer
PCM	phase change material
pH	pondus hydrogenii

PM10	particulate matter < 10 micrometre particle size
pp.	pages
®	registered trademark
R^2	coefficient of determination
RH	relative humidity
s	standard deviation
Si	silicon
spp.	species pluralis
Tab.	Table
TiO_2	titan dioxide
TSR	total solar reflectance
USB	universal serial bus
UV	ultraviolet
vs.	versus
WDVS	Wärme-Dämm-Verbund-System
w/w	weight by weight
Y*	brightness reference value
Zn	zinc

Table of Contents

1. Introduction

1.1. Aspects of supramural algal biofilms

Building façades offer a large contact surface for the ubiquitous algae species and in the case of external thermal insulation composite systems (ETICS) the thermal decoupled façade enables an increased presence of moisture films [1]. To avoid thermal stresses in today's polymer-modified coatings, light reflective colours are used. White surfaces have significantly lower absorption coefficients and therefore heat up less in sunlight than dark surfaces. Such surfaces dry more slowly, and the duration of water availability is greatly extended for algal growth [2]. The lighter surfaces enhance the contrast and are ideal indicators of biogenic discoloration on façades. Algae infestation affects an important part of the architectural design elements of façades. With the thermal and structural decoupling of the façade from the load-bearing structure of a building, the individual and material-independent colour scheme has been given more leeway. In comparison to the material visibility of classicism, modern façade designs have developed into unique features. The representative function must be retained and must not be allowed to develop into a petri dish for microbial processes due to unsuitable building materials. Reflection behaviour and water absorption are changed and, in symbiosis with destructive fungal cultures, lichen systems develop that lead to biocorrosion.

Coatings, that are applied to protect façades, become substrates due to an unfavourable combination of ingredients. The combination of mineral fillers and pigments in a polymer-based binder matrix provides a water barrier and gains condensation effects. The polymer content is particularly pronounced in outdoor areas for protective purposes. Airborne algae mainly get onto vertical surfaces by wind and wet deposition [3]. As a result of climate change, algae have access to increasing concentrations of carbon dioxide. In combination with the decrease of disinfecting sulphur dioxide from exhaust gases [4], this results in favourable living conditions. The pronounced scientific interest in algae species relevant to

building components and their economic and ecological consequences deserves its own classification. The author of this work introduced the term supramural for algal biofilms of this purpose in 2020 [5]. Planners and contractors have the task and the contractual mandate to plan a building project that is in a specific environment in such a way that it can withstand these environmental conditions. The infection load comprises the sum of all microorganisms in a habitat and is therefore initially a one-sided offer by nature. Whether this supply develops into a biofilm on a component is determined by the physico-chemical properties of the surface. The potential infection load of the environment should therefore also be considered for future building designs. The findings of this work applies both to the avoidance of algae and to the targeted colonization of bio-receptive facades.

2. Aim of the work and research questions

The constructive and hygrothermal measures to prevent moisture on building material surfaces have not yet had the desired long-term effects. Airborne algae cells still conquer façades and develop biofilms. The complete isolation of a building envelope from its environment is impossible and toxic biocides are still used to compensate for the deficits of the construction and measures [6]. The current EU directives force the manufacturers of building materials to restrict the use of biocides and to defuse the existing formulations regarding their negative ecological impacts [7]. Climate change and the role of the greenhouse gas carbon dioxide pose great challenges to mankind. The important contribution of algae to global oxygen production and carbon dioxide sequestration must be preserved - even on façades.

During the theoretical studies and the research work, the following specific research questions had to be answered in connection with the microbial colonisation of building material surfaces:

- Which advanced fluorescence measurement methods can be used to monitor algae biofilms on building component surfaces?
- What is the role of bioadsorption in the process of algae colonisation on building material surfaces?
- Which alternative sources of essential magnesium-based minerals result from the coating formulations?
- What are the long-term effects of magnesium-containing fillers on algae susceptibility of building materials?
- How to determine the area-related algae adsorption on building materials?
- What is alternative biocide-free control strategies without toxic intervention to algae and environment?

The present work pursues the approach of identifying further essential colonisation factors for algae on building component surfaces, which are available as a control element of functional façades.

2.1. Applicability of a benthic detection device for the determination of algal biomass on building material surfaces

The further development of chlorophyll-fluorescence spectrometers in the field of water body monitoring has led to interesting instrument configurations. One of these instrument developments is the BenthoTorch® (BTo) model from the company bbe Moldaenke GmbH, Germany [8]. The mobile fluorometer enables the non-destructive detection and estimation of area-related chlorophyll-a content of benthic algae in riparian and littoral zones of water bodies [8]. The manufacturer calibration by means of reference microorganisms permits the expression of the cell numbers per square millimetre. The present work examines the formation of new biofilms on component surfaces without previous algae infestation. In this early phase, the cell numbers and layer thicknesses are very low. Self-shadowing through multiple cell-layers in the biofilm is avoided and the linear measuring range of the fluorometer is given [9]. The available resolution of the measuring device (0.1µg/cm²) and the measuring range (0-15µg/cm²) chlorophyll-a will be able to detect the development of the algae biofilm and provide non-biologists with immediate interpretable results. Moist component surfaces can be regarded as temporary aquatic systems, so that the use of the measuring principle should be adequately possible like on wet stones of the benthos.

2.2. Bioadsorption as the initial step in the process of algal colonisation of building materials

At the beginning there is a first generation of already existing airborne algae cells that arrive on a new building material surface. The more algae are accumulated at the beginning, the higher the probability of a permanent presence. The attractiveness of a surface in this phase is determined by its adsorptive properties. It is of interest to know the stimulating factors that influence the adsorption behaviour of algae calls on façade coatings by magnesium-based fillers. To investigate the adsorption behaviour of algae on building material surfaces, a new suspension test was developed to determine the area-related biomass, detected by using the BenthoTorch® fluorescence spectrometer. It is known from the industrial harvesting process of green algae cultures that they can be precipitated by calcium- and magnesium-compounds at certain pH-values [10]. Transferring the principle of algae harvesting to building material surfaces can provide a deeper understanding about the initial contact and the following intensified colonization process.

2.3. Magnesium-containing fillers increase the formation of algal biofilms on façade coatings

In the search for alternative sources of algae-prone factors within the final coatings - the focus is on fillers. Mineral fillers fulfil numbers of important technological functions and reduce manufacturing costs [11]. When looking through various recipes of façade paints, regularly magnesium-containing fillers like dolomite and talc will be found [11]. Natural carbonate rock is also colonized by numerous microorganisms and thus contributes to its weathering and dissolution and underpins the meaning of the chemical composition [12]. Calcium carbonate (lime) is the most important filler and, depending on its geological origin and quality, contains significant amounts of magnesium-based accessory minerals [13]. The chemical composition of the carbonate-based fillers ideally meets the requirements of phototrophic microorganisms as they are mainly obtained from natural mining resources that are the result of primeval marine organism activities [13]. This common past of algae and fillers will meet again on modern façades today and prompts the author to investigate further, because there is no photosynthesis without the magnesium core-ion of chlorophyll-a.

2.4. Efficacy of an algae defence strategy by water-activated functional filler

Equipping surfaces with Lewis’s acids to achieve antimicrobial properties is a well-known technology. The natural acid mantle of human skin works in a similar way [14]. The mechanism is based on the in-situ release of protons through interaction with water. While pathogenic bacteria and viruses can be effectively combated in this way, the aim of this work is to investigate whether this effect is also applicable against aero-terrestrial algae in outdoor exposure of building material samples. Manipulating the pH-level by in-situ generated protons via zinc molybdate is known as an active technology against bacteria and viruses [15][16]. Research reports on the use of zinc molybdate against algae on weathered façades are not to be found and will be examined by the present work. To avoid condensation effects on façades, complex measures and methods are being developed. Instead of elaborately avoiding the dew water, this will become the subject of a control strategy without toxic intervention in the algae's biology.

3. State of the scientific and technological knowledge

3.1. Photosynthesis and basic growth conditions of algae

In nature, algae are found in a wide variety of bodies of water and therefore also occur in temporary aquatic areas like wet building material surfaces (Fig.1). Their presence extends to locations with unusual, rather extreme living conditions, such as deserts, rocks, polar ice, and thermal springs and depending on the light intensity, algae grow in caves, in the soil and deep marine zones [17]. As they are microscopically small, they only become recognizable by their colour pigments once they have reached a certain cell density. Airborne algae are widely distributed through their permanent stages and contribute to the conquest of new biotopes with suitable living conditions. The high reproduction rate of microorganisms also makes them highly adaptable. Ecological factors determine the presence of certain algae species. Essentially, water availability, light conditions, CO_2 concentration, temperature, pH-value, and mineral nutrients determine the permanent presence of an algae culture. Wherever the availability of these elements is guaranteed, algae can be found.

Figure 1: ETICS-Facade in urban area

In addition to the natural light source of the sun, there are artificial light sources (street lighting, building lamps), especially in urban areas. The day/night cycle of light availability is altered, and additional photosynthetically active radiation (PAR) is also available to phototrophic organisms at night. Modern LED lighting in urban areas achieves between 80-100% PAR [18].

Not only modern façades are affected, but historical buildings can also develop biofilms due to changes in façade coatings. The art historian and chronicler Friedrich Schlie describes the Church of Görslow/Germany in 1898 as a plastered brick building with a lime coating [144]. An oil painting from 1850 shows the white building standing free on the shore of Lake Schwerin, while today it is surrounded by tall lime trees. In 2001, the lime-cement plaster was renovated, and the façade was painted with a polymer-modified yellowish silicate paint. From this point onwards, microbial colonisation began (Fig.2).

Figure 2: Görslow Church, built in 1844 anno 2020 [photo: author]

Even to strong fluctuations of growth factors, the autotrophic microorganisms are adapted [19]. Recognizable algae colonization manifests itself depending on the species by the green-yellow to red-orange discoloration of the façade (Fig.3). Chlorophyll-a is at the centre of these phototrophic metabolic processes. The initial ignition of photosynthesis as a biochemical reaction takes place in the chlorophyll molecule through the element magnesium, where the first charge separation takes place and light energy will be converted into chemical energy [20].

Figure 3: Biofilm detection with BenthoTorch® at Görslow Church 2020

Metal ions play a major role in many biological processes [21] and in the context of microbial colonization of façade coatings by algae, the focus is on magnesium. The green pigment chlorophyll-a (Fig.4) acquires its specific colour through the interaction of the organic porphyrin structures and the bivalent magnesium ion. The alkaline earth metal magnesium accounts for 1.94% of the structure of the earth's shell and is therefore one of the top 10 most common elements [22]. We encounter it as a component of water hardness, and it is contained in seawater at more than 1 kg per cubic meter [22]. Of all known metal porphyrins, the magnesium complex has the most favourable redox behaviour in water at -1.7 Volts and is therefore predestined to release electrons and convert water into protons in photosynthesis using sunlight [20]. The amount of light that can be processed in the chlorophyll molecule is not arbitrarily high. To protect against light stress, part of the absorbed energy can be emitted in the form of thermal (Infrared) or fluorescent radiation (685 nm) [23].

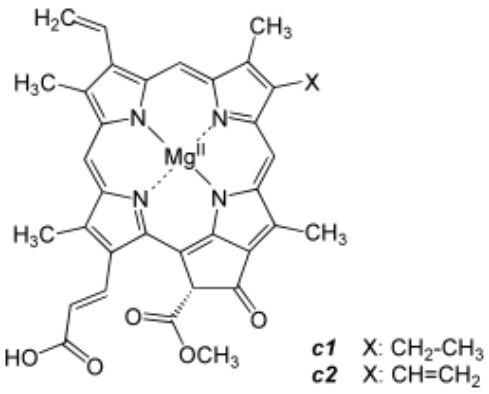

Figure 4: Structure of Chlorophyll a molecule with substituent c1, Chlorophyll b with substituent c2 [20].

The magnesium content of chlorophyll-a is 2.72% [w/w] while the chlorophyll content of algae dry matter in *Chlorella spp*. is up to 4% [24]. In 1828, Carl Sprengel formulated the minimum law, according to which growth is limited by the scarcest resource. Applied to the façade habitat and the phototrophic settlement organism algae found there, magnesium is an important minimum factor. A comparison of the magnesium supply for the long-term development of a possible algae population on façades makes clear what a huge potential is hidden in the coating material itself. Special influences in the splash water zone of the façade are not the focus of this study, but rather the systematic reasons for large-scale colonization of component surfaces. In the period from 1995 to 2015, energy-related particulate matter emissions (PM10 fraction) from households, trade, commerce, services, transport, and the energy industry fell from 150,000 tons to 70,000 tons [25]. The measured values of seven Federal Environment Agency monitoring stations in Germany showed a decreasing development of particulate matter (PM10) from 50 to less than 20 µg/m³ for the period from 1970 to 2010 [25]. The declining particulate matter loads are therefore less and less available as a nutrient source for microbiological growth on façades. Magnesium is part of the eleven macro nutrient elements and does not enter the cells of microorganisms in mineral form. It must be converted in the presence of water into magnesium ions. Only in dissolved state, the cell walls can be passed. In symbiotic collaboration with fungi, algae can open a colonized substrate by secreting organic acids [26]. Carbonates, as salts of the weak carbonic acid, offer an easy attack surface here, as in the case of dolomite

$CaMg(CO_3)_2$. A mutualistic relationship between algae and fungi in the form of lichens, in which each symbiotic partner contributes its strengths to the relationship develops [27]. An investigation of bio-deteriorated granite found a selectively enhanced dissolution of calcium, sodium, magnesium, and manganese [28]. Green algae and fungi have a common interest in the supply of mineral nutrients, especially magnesium and manganese. Microorganisms are extremely adaptable and algae in particular impress with their opportunistic behaviour. A comparison of the advancing knowledge on the metabolism of algae with the ash content of other lower plants according to Fig.5 [29] shows that algae must have a more diverse set of bio-tools. The function of these tools results from the mineral-cationic co-factors. Even in the dark, the green alga *Chlamydomonas reinhardtii*, for example, continues its metabolism by switching to hetero- or mixotrophic mode. The corresponding bio-tool for this is flavodiiron, an iron-containing protein for oxygen recycling [30]. In photosystem II of algal photosynthesis, water is split with the help of sunlight. The bio-tool for this is a Mn_4O_xCa cluster, who's now clarified molecular formula reveals which mineral co-factors are active [31]. The growth-promoting effects of magnesium and manganese salts on deficiency cultures of various algae species were extensively investigated by PIRSON et al. in the 1950s [32].

Species	Ash content [%]	Species [n]
Algae	17,3	7
Bacteria	8,9	5
Ferns	7,7	6
Mushrooms	5,7	10
Moose	3,3	8

Figure 5: Average ash content of low plants [29]

Due to their high pH value, fresh mineral coatings have a sufficient buffering capacity against acid attacks and possibly an initial growth retarding effect. Magnesium ions are bound as hydroxide at pH values > 10. The carbonation of surfaces with CO_2 from air decreases the pH value below this threshold and thus increases the bioavailability of the magnesium-ion while weathering.

3.2. Bioavailability of mineral nutrients in building materials

Any material supply to the algae cells takes place through their cell wall. Liquid water takes over the transport function of the nutrients and carbon dioxide dissolved in it. The basic prerequisite for the permanent presence of algae is liquid water and a minimum solubility of important nutrients. It is assumed that nutrients reach the façade through atmospheric dust in the same way as the algae [33]. An evaluation of the air quality annual reports of the state of Mecklenburg-Western Pomerania, Germany shows a declining development of the mineral nutrient content of the air in the last decade (Tab.1). Magnesium decreased by 65% in the period analysed [34].

Table 1: Anion- and cation content of PM10 in [µg/m³], own summary from [34]

Year	PM10 min	PM10 max	SO4	NO3	Cl	NH4	Na	K	Ca	Mg
2011	18	33	2,51	3,6	0,86	1,61	0,72	0,12	0,23	0,09
2012	15	26	2,47	4,5	0,68	1,79	0,68	0,12	0,21	0,07
2013	14	26	1,94	2,59	0,43	1,24	0,42	0,09	0,23	0,07
2014	18	28	2,22	3,65	0,46	1,51	0,42	0,22	0,25	0,07
2015	16	24	1,79	3,48	0,56	1,19	0,57	0,12	0,29	0,08
2016	15	23	1,57	3,59	0,76	1,34	0,6	0,15	0,25	0,06
2017	15	22	2,10	3,30	0,20	1,50	0,20	0,20	0,10	0,03
2018	17	24	1,56	2,22	0,12	1,15	0,16	0,15	0,04	0,01
2019	15	23	1,21	1,92	0,15	1,01	0,2	0,15	0,04	0,01
2020	12	19	1,74	1,64	0,15	0,72	0,28	0,17	0,11	0,04

The present investigations were carried out in the geographical area of this air quality reports. Building materials have different material properties, depending on whether they are of natural origin (sediments, volcanic rock) or man-made (plastics, bricks, plaster) or how they are processed (firing temperature). From a material point of view, high firing temperatures (>1200°C) lead to sintering effects in mineral mixtures. During the firing process, a temperature limit is exceeded at which the crystal structures are lost, and the material mixture melts together amorphous glass-like. As a result, the porosity is decreased, and the cohesion of the components is increased. The water solubility of the sintered structure is significantly lower than that of the individual starting materials. As a result, these building material surfaces represent a barrier to the bioavailability of essential ions for algal interaction or supply.

Fig. 6 shows an example of only colonized mortar joints between the bricks after 18 years of weathering, while the clinker bricks are totally free of any detectable algal growth (total cell number = 0). The average total cell number of the 12 joints is 15,086 cells/mm² (s=3,472).

Figure 6: Biofilm formation on 13-clinker brine bank (detail picture)

Fig. 7 and Fig.8 provide an overview of the cell counts measured in the individual joints and the total sum concentration of chlorophyll-a.

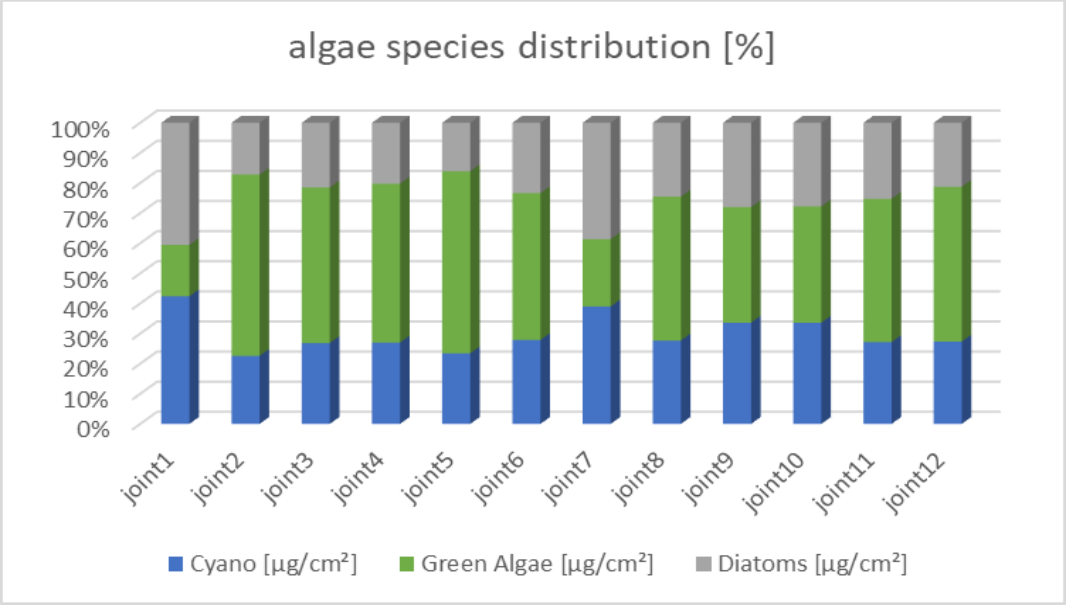

Figure 7: Biofilm composition of joints of Fig. 3

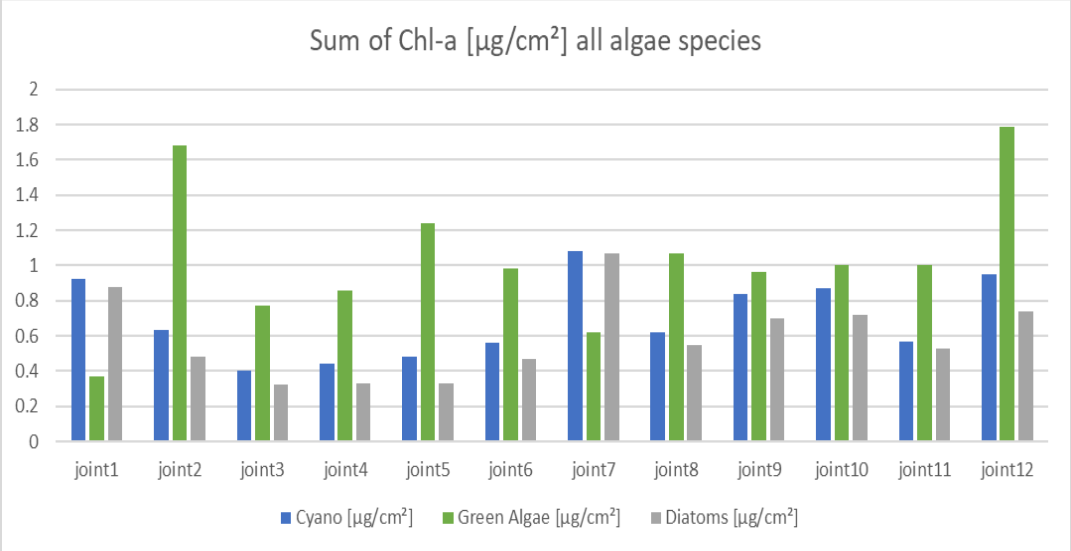

Figure 8: Chlorophyll-a content of each joint of Fig. 3

3.3. Transport mechanisms to the façade

Starting with a first generation of existing airborne algae cells that arrive on a building material surface. If many cells are transported to this surface per unit of time and area, there is a high infection load, for example from nearby sources of vegetation or water bodies. Whether there is permanent contact between the algae cell and the building material, or the cell simply bounces off, has been largely investigated. In the simplest case, the dry algae cell bounces off the smooth, dry surface of the building material. In the second case, the dry, smooth building material surface is polymer-modified and electrostatically charged, and the algae are electrostatically bound together with other dust fractions [3]. In the third case, there is a weather-depending film or drops of moisture on the surface that binds the algae [35]. Under these conditions, the algae cell is also moistened and can be excellently attached with its hydrophilic cell surface. A rough texture of the building material surface supports the yield of accumulated algae cells in all cases [36]. Water films on polymer-modified hydrophobic building material surfaces (with a contact angle > 90°) can achieve an average film thickness of 50 µm [35]. The production volume of a 1-liter photobioreactor is thus equivalent to an effective building material surface of 20 m².

Airborne algae mainly get onto vertical façade surfaces by wind and wet deposition [3]. Once there, the vegetative production of biomass in long-term requires sufficient essential mineral substances. Regardless of the declining quantities of particulate matter, the path to the facade is not automatic. The transfer of an aerosol particle from the air to a surface is size-dependent [3]. Two aspects are limiting the yield of this transport route. The falling direction of the rain is mainly parallel to the façade surface and the washing out of dust fractions will never be quantitative. This means that only a small part of the fine dust reaches the building envelope. In the water balance of a façade, the daily condensation events (morning and evening) outweigh the time-to-time events of rain [37], an additional limiting aspect of the nutrient yield of particulate matter. Dew water is a locally limited condensation process in the vicinity of the façade with minimal range for the transport of airborne particles, but a constant water source.

3.4. Functional fillers and pigments in coating recipes

In normative terms, the following applies to a filler in accordance with DIN 55943 and ISO 3262 Part 1: "*A substance consisting of particles that is practically insoluble in the application medium. Practically insoluble substance which is used to increase the volume to achieve or improve technical properties and/or to influence optical properties*" [38].

The required practical insolubility in a paint formulation leads to so-called dispersion paints. Fillers are predominantly of mineral origin and are present in the form of carbonates, silicates, sulphates, sulphides, oxides and possibly mixtures of these [39]. At 42%, fillers make up the largest proportion in paint and varnish formulations and are dominated in Europe by carbonates with a share of over 85% [39]. Magnesium is involved in the formation of dolomite, talc, montmorillonite, and bentonite, among others. Talc is a widely used filler, which is characterized by a high oil number, low shrinkage, low cracking tendency and a favourable critical pigment volume concentration in paint formulations [39]. The magnesium content of talc $Mg_3[Si_4O_{10}(OH)_2]$ is 19.2%. With a normal surface application of 150-180 ml/m² of a façade paint according to the manufacturer's application volume, the presence of talcum results at magnesium values of 2.7 g/m². The average magnesium content in particulate matter fine dust (PM10) is on average 0.053 µg/m³ of air (Tab.1). To deliver the same amount of magnesium by airborne PM10, 50.9 million cubic meters of air would be required and must be completely washed out by rain and transferred to 1 m² of the vertical façade surface. This comparison clearly reveals the great potential of mineral nutrients hidden in the coating formulations themselves.

The main white pigment, titanium dioxide was previously considered to be possibly cancer-causing, even after a court decision. The substance was labelled as potentially carcinogenic when inhaled with particle sizes up to 10 µm according to the 14th amendment of the CLP Regulation. This classification and any additional EU phrases for mixtures containing titanium dioxide were set to take effect from October 1, 2021 [40]. However, some manufacturers challenged this classification at the European Court of Justice. In a ruling on November 23,

2022, it was deemed unlawful by the European Court of Justice that titanium dioxide be classified as "probably carcinogenic by inhalation" and have an additional labelling requirement for mixtures containing it under the EU's implementation of the 14th ATP [40]. Rising prices and the impending ban on the use of the white pigment titanium dioxide in coatings can technologically force manufacturers to adjust their formulations. The use of fillers containing magnesium was already evident before the restrictions on titanium dioxide. Own EDX-analyses in 2017 of 9 façade products available at the region Wismar market showed that 5 products contained an average magnesium content of 3.6% ± 0.8%. The investigations were extended to 16 existing buildings with refurbished facades in the Wismar area. The visually assessed algae infestation showed a strong correlation (R^2=0.82) with the magnesium content of the weathered façades [41] - a first indication for triggering the algal growth.

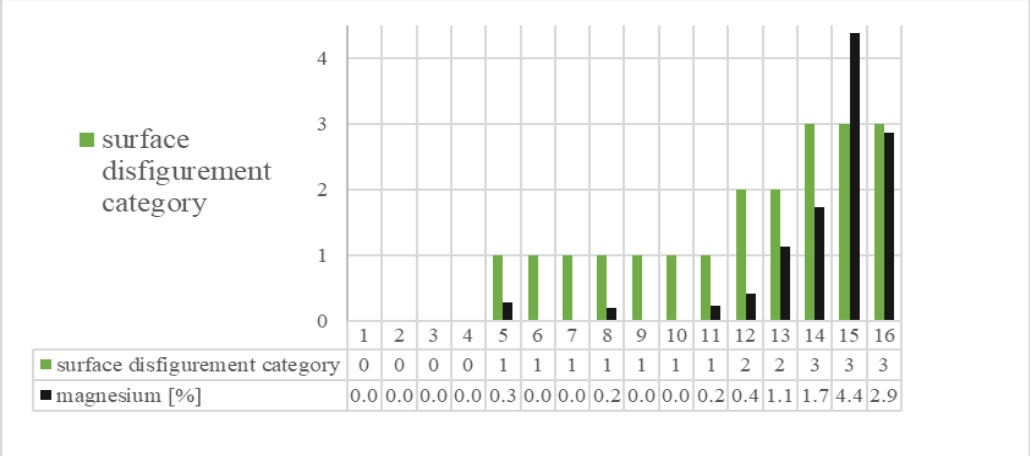

	1	2	3	4	5	6	7	8	9	10	11	12	13	14	15	16
surface disfigurement category	0	0	0	0	1	1	1	1	1	1	1	2	2	3	3	3
magnesium [%]	0.0	0.0	0.0	0.0	0.3	0.0	0.0	0.2	0.0	0.0	0.2	0.4	1.1	1.7	4.4	2.9

Figure 9: EDX analysis of 16 façade samples with visual algal evaluation [41]

3.4.1. Multi-functional filler Zincmolybdate – ZnMoO4

In the present work, powdered zinc molybdate from Carl Roth, Germany with a purity of 99.0% was used. The practically water-insoluble, white powder with the molecular formula $ZnMoO_4$ (CAS No. 13767-32-3) has a molar mass of 225.3 g/mol. With the density of 4.3 g/cm³ and a melting point >700°C [42], the pure white zinc molybdate meets the basic requirements of fillers [43]. Molybdenum compounds have been mentioned as a corrosion inhibitor more than 50 years ago [44] and is also known for its flame-retardant properties [45]. In addition,

molybdenum compounds are described in various publications as additives with antimicrobial properties [46-53]. From a chemical point of view, the transition metal is attributed proton-releasing properties in combination with water or humidity to reduce the pH value to such an extent that pathogenic germs can be combated [15][16]. The release of protons in combination with water prompted the author of this work to investigate whether the active principle can be transferred to the control of early algae biofilm formation in the context of outdoor weathering of façade coatings (Thesis 4). Research assumes that it is not possible to achieve permanent pH values on external surfaces that are suitable for preventing biofilm development by microorganisms [54]. This application should clarify whether the zincmolybdate filler can overcome the buffering effects of the weathered surface and the algal reduction effect occurs.

3.5. Detection and assessment methods of algal biomass

3.5.1. Visual evaluation according EN 16492:2014

The applied standards for evaluating optical changes caused by microbial growth on coating surfaces are based on visual methods DIN EN 16492:2014 [55]. The degree of growth is determined on selected partial areas of a façade. In case of doubt, a microscope is used to differentiate between dust, algae, or fungi. Annex A of the standard describes the assessment according to EN ISO 4628-1. The results are expressed in the form of evaluation numbers and are 0-1 for the intensity of visible fouling, 0-5 for the number of spots with visual change and 0-4 for the percentage of area. The assessment is therefore depending to subjective influence and the biological expertise and experience of the assessor. The visual assessment by a person could be replaced using the BenthoTorch®, as in addition to the detection of the biofilm, the reflectivity is also determined as a possible sum parameter of a surface change.

3.5.2. Efficacy of film preservatives according to DIN EN 15458:2007

The standard describes the procedure for the evaluation of film preservatives for building coatings regarding the biocidal active substances they contain [56]. The results are used for classification in accordance with the Biocidal Products Regulation (BPR Regulation EU 528/2012) [7]. In this work, the incubation method was adapted for comparative testing of algae growth on various building material samples. The building material samples served as the sole culture medium; the visual evaluation was replaced by the fluorescence measurement of the BTo. The previous normative disinfection using gamma radiation was replaced by thermal treatment (1h, 120°C) of the samples.

3.5.3. Digital evaluation via image area percentage method

Replacing the human eye with a digital camera leads to simple image analysis. The use of digital cameras for image analysis, particularly in the context of area under the curve (AUC) determination, has been explored in various studies [57] [58]. Image thresholding is used to extract quantitative data from images. The area to be evaluated is photographed and converted into an 8-bit grayscale image. Using various available image analysis tools (Fig.10), the area percentage of defined grey levels under the curve between histogram thresholds is determined [58].

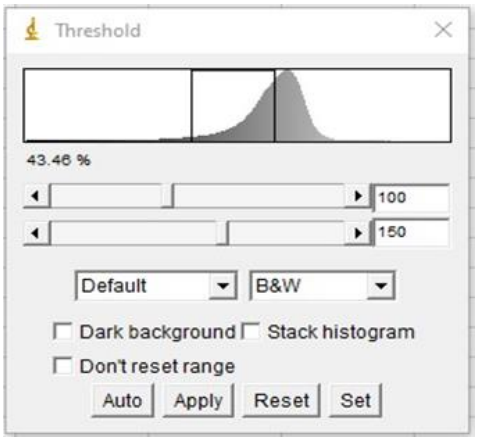

Figure 10: Application window ImageJ for adjustment of histogram threshold [59]

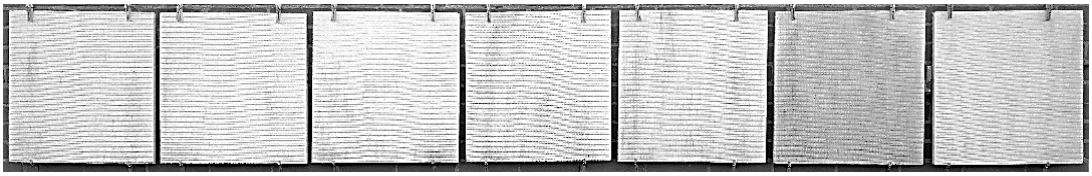

Figure 11: 8-bit greyscale picture after 730 days of weathering

In addition to the first two visual evaluation methods, each test specimen was recorded photographically (Fig. 11). After conversion into 8-bit grayscale images, the analysis was carried out using ImageJ processing and analysis software [59]. The optical influence of the mounting brackets was eliminated by using a central square section of 95% image area fraction. Subtracting a fix offset for the structural-borne shadows, the percentage area of the algal biomass was calculated with histogram threshold between 100-150 (Tab.2).

Table 2: Covered area of samples within histogram thresholds

Sample	ImageJ area [%]
PK00	7.52
PK01	13.75
PK02	16.26
PK03	23.98
PK04	22.19
PK05	38.46
PK06	4.95

3.5.4. Spectroscopical evaluation via PAM fluorometry

Pulse amplitude modulated fluorometry (PAM) is a more complex procedure compared with BTo and has been introduced in 1985 by joint development between U. Schreiber and H. Walz [60]. PAM fluorometry provides information on the photosynthetic activity of plants and algae. Using the intensity and duration of light flashes of specific wavelengths, electron transport rates between the different photosynthetic systems can be determined. The quantification of chlorophyll-a is also possible but is not the focus of this enhanced measurement principle. This method determines the algae biomass by fluorescence quantum yield as there is a correlation to chlorophyll-a concentration [61][62].

The area to be tested must be subjected to prior dark adaptation, which involves considerable effort. Measurements in complex installation situations are therefore more difficult and its use is more practical for laboratory purposes. There is a need for a practical measurement method that does not require time-consuming sample preparation and enables also non-destructive detection of algal biomass directly at the object. The measurement result should be immediately interpretable and have a reference to the measurement surface without the need for in-depth microbiological expertise. Building diagnostics research groups have many years of experience in the use of PAM fluorometry for the detection of algal biofilms [62][63].

In this process, previously dark-adapted test specimens are stimulated with modulated light signals and the fluorescence response of the algal pigment chlorophyll-a is detected. The fluorescence quantum yield provides information on the algal mass, its vitality and visual detectability for the classification of colonization susceptibility [64]. In this method, fluorescence excitation is performed at a single wavelength of 470 nm and does not allow assignment of fluorescence responses to the different algae species. More detailed information on the composition of biofilms could provide further insights. There is a need for measurement methods that provide such information in a single measurement process.

Pulse Amplitude Modulation (PAM) fluorometry has been used in various studies to evaluate the resistance of building materials to algal growth. Tab. 9 presents an overview of the publications that have dealt with the investigation of building materials since the introduction of commercial PAM fluorometers. The last 25 years were dominated by investigations via PAM devices. The BenthoTorch® related publications of measurements of building materials are available since 2017; the papers on this topic are summarized in Fig. 12.

Year	Author	PAM-related topic	Ref.
1998	E. Brechet	Novel blue LED-based handheld fluorometer for detection of terrestrial algae on solid surfaces	[109]
2006	N. Häubner	Quantification of algal biofilms colonising building materials: chlorophyll a measured by PAM-fluorometry as a biomass parameter	[110]
2007	Y. Tang	en Autofluorescence in Dinoflagellates, Diatoms, and Other Microalgae and Its Implications for Vital Staining and Morphological Studies	[111]
2008	H. Venzmer	Algal defacement of façade materials—results of long term natural weathering tests obtained by new diagnostic tools	[112]
2009	L. Gustavs	In vivo growth fluorometry: accuracy and limits of microalgal growth rate measurements in ecophysiological investigations	[113]
2010	N. Konkol	Fluorometric detection and estimation of fungal biomass on cultural heritage materials.	[114]
2011	S. Johansson	Pilot study of activity of photosynthetic organisms growing on render measured with Imaging-PAM	[115]
2011	M. Gazulla	Relationship between certain ceramic roofing tile characteristics and biodeterioration	[116]
2011	F. Gladis	Influence of material properties and photocatalysis on phototrophic growth in multi-year roof weathering	[117]
2012	A. Maury-Ramirez	Titanium dioxide based strategies to prevent algal fouling on cementitious materials	[118]
2013	J. v. Werder	The potential of pulse amplitude modulation fluorometry for evaluating the resistance of building materials to algal growth	[119]
2014	S. M. Blanco	Bioreceptivity optimisation of concrete substratum to stimulate biological colonisation	[120]
2014	S. Manso	Bioreceptivity evaluation of cementitious materials designed to stimulate biological growth	[121]
2015	C. Ferrari	REVIEW ON THE INFLUENCE OF BIOLOGICAL DETERIORATION ON THE SURFACE PROPERTIES OF BUILDING MATERIALS: ORGANISMS, MATERIALS, AND METHODS	[122]
2016	S. Eyssautier	Chlorophyll fluorescence and colorimetric analysis for monitoring the algal development on biocide-treated stone	[123]
2017	H. Vojtkova	Algae and their biodegradation effects on building materials in the Ostrava industrial agglomeration	[124]
2018	D. Vazquez-Nion	Bioreceptivity index for granitic rocks used as construction material	[125]
2018	Yun-Wang Choi	A Study on the Fundamental Quality of Magnesia-Phosphate-Formed Mortar Composites Using Superabsorbent Polymer for Development of Concrete for Biological Panel	[125]
2019	B. Prieto	Functional properties and biodeterioration behavior of new formulations of lime technical mortars.	[127]
2020	P. Sanmartin	Impact of colour on the bioreceptivity of granite to the green alga Apatococcus lobatus: Laboratory and field testing	[128]
2021	A. Stefanova	Photosynthetic textile biocomposites: Using laboratory testing and digital fabrication to develop flexible living building materials	[129]
2021	E. Fuentes	A laboratory approach on the combined effects of granite bioreceptivity and parameters modified by climate change on the development of subaerial biofilms	[130]
2022	U. Karsten	Apatococcus lobatus (trebuxiophyceae) dominates green algal biofilms on roof tiles in Northern Germany	[131]
2022	A. Crawford	Clay 3D printing as a bio-design research tool: development of photosynthetic living building components	[132]
2023	L. Stohl	Bioreceptivity of concrete: A review	[133]

Figure 12: Literature review of PAM-related research papers regarding the evaluation of building materials

3.5.5. Spectroscopical evaluation via BenthoTorch®

The bbe-Moldaenke BenthoTorch® (BTo) utilizes chlorophyll fluorescence in living organisms to measure the types of algae and total algal mass present in underwater and benthic environments. It can distinguish between three groups of algae - cyanobacteria, green algae, and diatoms by analysing the unique fluorescence patterns of their photosynthetic pigments (Fig.13). Cyanobacteria contain phycocyanin, diatoms contain fucoxanthin, and green algae have a specific combination of chlorophyll-a and -b. Chlorophyll-a, which is found in all photosynthetic organisms [65], is commonly used as an indicator for algal biomass. The BTo provides data on total algal biomass as chlorophyll-a concentration per unit area and community composition as chlorophyll [µg/cm²] or cells/mm². This makes it a potentially more practical alternative to current complex and time-consuming methods (PAM) for characterizing supramural algal communities. A comparison between extractive laboratory methods and the BenthoTorch® showed good agreement if the chlorophyll a content was below 4 µg/cm² [9]. All measured values of the outdoor weathering were clearly below this limit in the linear measuring range.

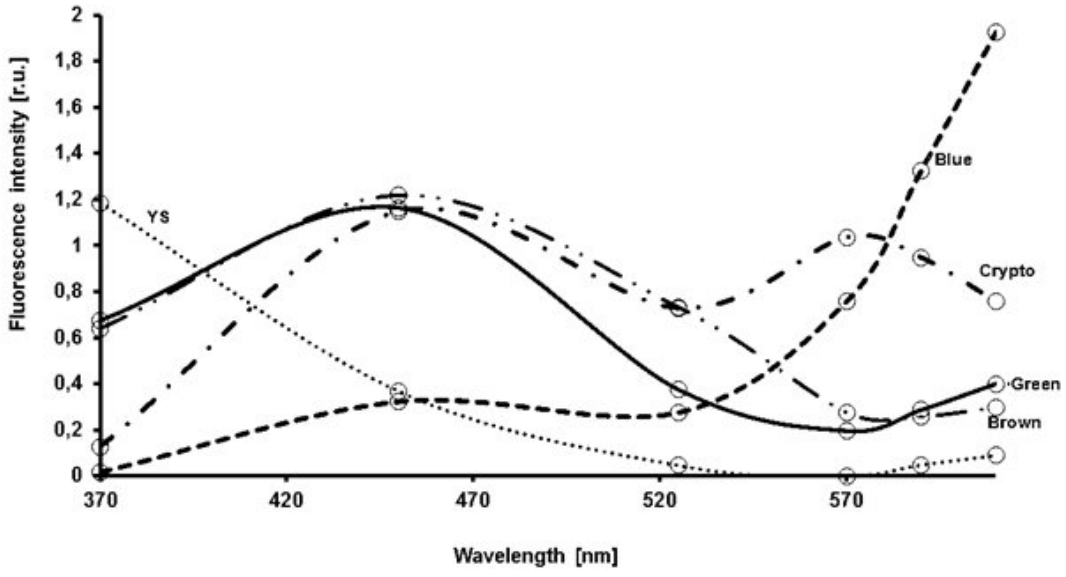

Figure 13: algae-specific fluorescence response signals after excitation [66]

A special feature of the BTo is the use of three different excitation wavelengths. These address the species-specific photopigments and allow conclusions to be drawn about the composition of the biomass. With the PAM method, only a sum signal is obtained, as only one wavelength is used for excitation. It is of scientific interest to be able to differentiate between algae and cyanobacteria, as these have different effects on the colonization and corrosion processes of building materials. The development of bio-receptive component surfaces can be much more targeted with this extended information about possible symbiotic microorganisms. The calibration protocols while using the device during this work are attached in the appendix (Fig.116 and 117).

Figure 14: bbe moldaenke BenthoTorch [8]

Publications are now available that deal with the application of the BenthoTorch for the detection of biofilms on building materials (Fig.16).

Figure 15: Application of BenthoTorch at building facade in Wismar/Germany

Year	Author	BTo-related topic	Ref.
2017	V. Hoff	Variation in benthic colonization on tile and in leaf degradation-results from a flume experiment in Norway	[134]
2018	V. Morin	Concrete with improved bioreceptivity	[135]
2019	H. Heinrich	Multifunctional detection method for the differentiated in-situ analysis of supramural biofilms during renovation measures on component surfaces	[136]
2021	M. Romani	Diversity and activities of pioneer bacteria, algae, and fungi colonizing ceramic roof tiles during the first year of outdoor exposure	[137]
2022	R. Bellopede	Biocorrosion of speleothems driven by lampenflora: preliminary observations in Bossea show cave (NW-Italy)	[138]
2022	V. Morin	Development of laboratory tests to measure the growth kinetic of micro-algae of concrete in marine environment and comparison to in-situ experiments	[139]
2023	P. Reboah	Influence of climatic factors on cyanobacteria and green algae development on building surface	[140]
2023	H. Heinrich	Investigation of façade coatings containing algae-prone fillers	[141]
2023	V. Drakard	Colonisation after disturbance on artificial structures: The influence of timing and grazing	[142]

Figure 16: Overview of BenthoTorch-related research papers regrading biomass detection on building materials

3.6. Adsorption mechanisms and flocculation of algae

Looking for comparable environmental conditions for microalgae on façades, they can be found in the field of industrial algae production. The high and controllable content of fatty acids, proteins and carbohydrates makes green algae an important raw material in the production of biofuels and animal feedstock [67]. The main interest is the complex harvesting process, which can be simplified and optimized using calcium and magnesium compounds [68]. Algae cells are contained in wastewater as an organic component and lead to problems and higher costs in water treatment due to their dispersing properties [10]. Earlier studies have already shown a correlation between a high pH-value and magnesium compounds in the chemical flocculation of algae, which is driven by a complex bonding interaction of cationic metal-ions with the cell-wall-located functional groups where magnesium-compounds have shown high flocculation efficiency over a wide pH-range for *Chlorella spp.* [67][69]. In the study on the biosorption of uranium using the green algae *Chlorella vulgaris*, functional groups were determined on vital and dead cells by potentiometrically determined titration curves that confirmed carboxyl, phosphate, amino and hydroxyl groups [70]. These multifunctional bio-equipment enables the algae to buffer changes in pH and interact with several metal cations, which are widely contained in mineral based building material surfaces. The cell wall structure of algae is more complex than that of fungi and bacteria, so the evolutionary origin of the various algae species must be considered [71]. This is where the importance of a differentiating measurement system becomes particularly clear. On the metal side, the affinity towards biofilms is affected by ionic radius and electronegativity and magnesium plays a special role here [72].

When flocculating algae suspensions, the same chemical additives are used that are also find as fillers in facade paints. At this point, the research question arises as to the expected adsorption effects of algae on building material surfaces (Thesis 2).

3.6.1. Algae cell wall interaction with metals

The morphological structure of the various microalgae such as green algae, cyanobacteria and diatoms will not be discussed in detail here. However, the focus is on the presence of functional groups on the outer surface of these photosynthetically active microorganisms. These functional groups represent reactive points of contact for interaction among each other and other surface components, as they have real charges under certain conditions (Fig.17). The general term of such interactions on the cell surface based on physical adsorption, ion exchange, chelation and complexation with functional groups is bioadsorption. These reactions can take place with living and dead biomass and depends on the pH value, temperature, cation concentrations of the metal and biomass in aqueous solutions [73].

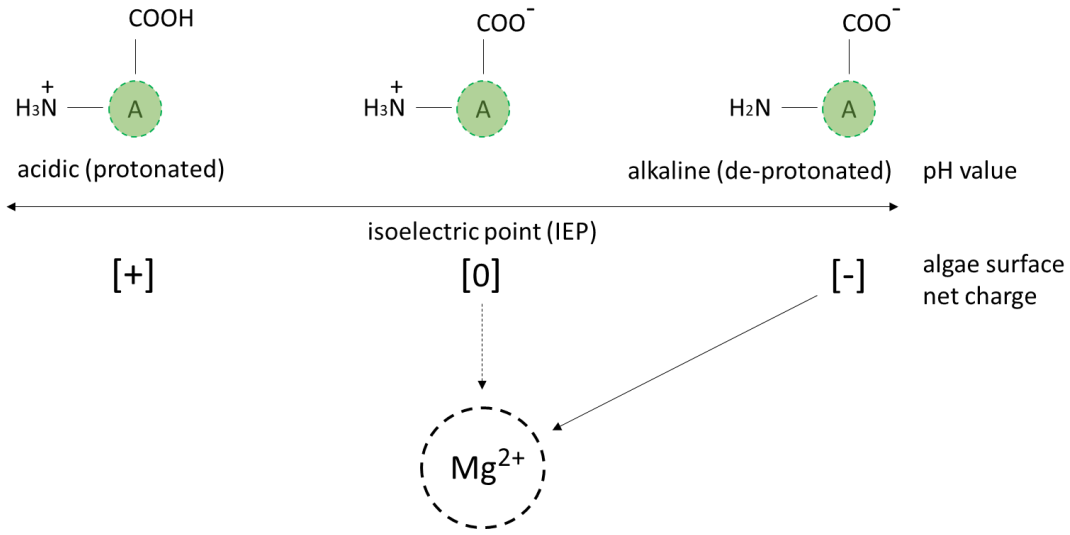

Figure 17: pH-depending charge-configuration of algal (A) functional groups

Chlorella vulgaris is a well-researched algae and consists of polysaccharides and proteins which provide several binding sites for the metals [69]. Representative of the two different charges of these groups, the amino and carboxyl function is shown in Fig. 17. The functional groups, such as carboxyl, hydroxyl, phosphoryl provide a negative or amino groups a positive charge on the cell surface [10]. The simultaneous presence of different functional groups leads to a resulting total charge under certain pH values. The isoelectric point (IEP) is the pH value at which the total charge is zero. At pH values above the IEP, negative charge

excesses result and enable interaction with oppositely charged cations (Fig. 17).

3.6.2. Biofilm as survival strategy

With a proven existence of over 3 billion years, the biofilm represents the prototype of a multicellular organism and are not only the oldest, but also the most resistant form of life [74]. The high degree of protection against harmful environmental influences, such as temperature, lack of nutrients, biocides, UV light and pH value, make biofilms an evolutionary success model for bacteria, algae, and fungi. The main ingredients to form a biofilm are available at the most modern building facades: a surface, nutrients, and water.

Biofilms are defined as a sessile population of microorganisms at interfaces, and they are formed when microorganisms attach to phase interfaces of substances in different aggregate states and multiply there [75]. The cohesion of microorganisms of different genera is achieved by means of an extracellular polymeric substance (EPS), which is produced and excreted by the consortium itself and consists of 95% water, as well as polysaccharides, lipids, and proteins [76]. The highly viscous EPS matrix acts as a binding agent between the cells and for the transport of substances. The individual capabilities of all microbial participants can be combined in this common matrix. Incorporation of water is favoured by their hydrophilic components, which form a kind of hydrogel and is also the reason for the greatly delayed desiccation of biofilms [76]. The adhesion mechanism of a biofilm is divided into three phases: Initial adhesion to a surface, germination phase and maturation phase with synthesis of EPS [77]. Microorganisms on component surfaces colonize a wide variety of inorganic and organic materials. The adhesion to the interface is strengthened by a combinatorial effect of organic acids that perforate the substrate. The biofilm matrix can thus penetrate deeper and deeper into the substrate and expand the form-fit bond [78].

3.7. Technologies to prevent algal growth on façade surfaces

With the legal classification as an optical defect [79], algal biofilms on façades are still the subject of product development and research of building materials. Interdisciplinary research teams are working together to improve coating products. Two main objectives are being pursued. On the one hand, the classic approach with active biocides and, on the other, the manipulation of the hygrothermal and constructive properties of surface material physics [80].

3.7.1. Influencing of thermal properties

Hygrothermal approaches focus on building physics to avoid condensation and long-lasting water films [81]. Constructive measures have been known for centuries and are the easiest to implement to keep rain away from the building structure (i.e. roof overhangs). The selection and design of the building material surfaces influences porosity and roughness, which are essential factors that, together with moisture, lead to increased colonization of microorganisms [82]. More sophisticated approaches of the last four decades ended up in hydrophobic additives (lotus effect) [83], infrared absorbing pigments with lower emissivity [84], phase-change-materials (PCM) in plasters [85]. The chemical approaches focus on encapsulated biocides with long-lasting effect [86] and photocatalytic pigments (Anatase TiO2) tried to generate a selective destruction of microorganisms via free radicals [87]. The isolated investigation of individual strategies, partly in the laboratory and partly in the field, led to euphoric product launches. Unfortunately, the deficits only became apparent in real-life applications, while algae growth being delayed at best with PCM or even increased at worst with hydrophobic additives, that promotes the availability of dew on surfaces [88]. All these insufficient technologies in long-term ultimately led to the use of biocides and leaching of toxic substances into the environment still happens.

3.7.2. Direct control of algae cells

The use of biocides is aimed directly at the algae cell and involves the use of organic substances that block physiological processes or destroy the cell structure. Based on available findings, biocidal additives only have a temporary effect [89] and must be critically scrutinized from an ecological point of view. Due to new EU directives, considerable restrictions on the use of organic active substances are to be expected [7]. The active substances are washed out of the coatings by rain and condensation water and thus enter the soil and sewer. When biocides are used, the algae cell is directly attacked. The various active substances disrupt the metabolic processes, the photosynthesis processes, or the integrity of the cell wall. The predominantly organic compounds must come into direct contact with the algae cell. The prerequisite for the absorption of the biocides into the algae cell is their solubility in water [90]. This significantly reduces the durability of the active substances in the coating [86] as it is in contact with water. The type of binder matrix can delay the loss of biocidal functions but cannot prevent it in the long term [91]. In conjunction with UV decomposition from daylight, individual active substances can no longer be detected after just a few months. The high pH value of mineral based building materials can lead to alkaline hydrolysis of the active ingredient and restrict the choice of substances [92]. Since the ban on using pigments containing heavy metals in paints, it has become more difficult to ensure conservation. In addition to colouring, these toxic pigments also fulfilled part of the biocidal function [93].

3.7.3. Antimicrobial effects under real-life conditions

To prove the microbiological effectiveness of hygiene paints, so-called film adhesion tests are used. In the frequently used ISO 22196, the coating material is inoculated with a defined bacterial count of various types of bacterial species (e.g. Staphylococcus aureus, Escherichia coli) [94]. The cell suspension is covered with a sterile polyethylene film and incubated for 24 hours at 35±1°C. After this time, the bacteria surviving on the carrier are determined. A significant antibacterial efficacy is certified if after 24 hours a reduction of two powers of ten (>99%) is observed compared to an untreated sample.

The active ingredients used in antibacterial formulations must reach the cells to develop their effect. For this reason, the standard microbiological procedures described above are always carried out in an aqueous medium, as this is where both the organisms live, and the biocides can act [95] Own investigations and developments have shown that many claimed biocidal product properties are not maintained under real-life conditions [96][97]. The development of antimicrobial active substances and their application in coatings must withstand the conditions of everyday use including the transmission pathways [98]. Testing under the normative warm-humid (35±1°C) conditions is rarely practical and may lead to deceptive certified results. In the present work, a possible antimicrobial effect of zinc molybdate on algae colonization on façade coatings was investigated in a 730-day outdoor weathering test under real-life conditions.

4. Applied analytical procedures

4.1. Field evaluations with fluorescence spectrometer BenthoTorch®

In preparation for the later use of the measuring device, extensive field tests were carried out with different building materials under various conditions. On the one hand, the tests served to improve understanding of how to use the spectrometer and, on the other, to determine possible influencing factors on the subsequent measurement results. To obtain the widest possible range of measured values and installation situations, both long-term weathered component surfaces and fresh samples were used. To validate the measurement routine and as preparatory tests, measurements were carried out on building material samples that were subjected to outdoor weathering for 3 years in the later area of free weathering test. Bricks, sand-limestone, and concrete blocks were stored outside

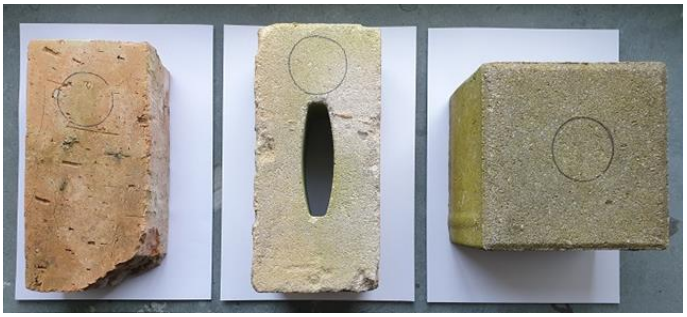

Figure 18: Material samples after 3 years of weathering (brick, lime sandstone, concrete)

in the same habitat under identical conditions. A detectable biofilm was thus able to develop on the samples. For the repetitions, the measuring range on the test specimens was marked with a circle (Fig. 18). All measurements were carried out at 23±1°C room temperature. The quantification of biofilms of phototrophic microorganisms is carried out by determining the chlorophyll content. The function of this photopigment is closely linked to the presence of water. To achieve reproducible measured values, prior moistening of the sample surfaces

is required. Humidification depends on the absorbency of the substrate and should be checked before measurement. The measurement was carried out after a waiting time of 10 minutes. Application using a spray bottle has proven successful for this purpose, as the droplet size can be adjusted and homogeneous application over the entire surface is guaranteed.

The brick sample was first moistened with distilled water (abscissa in Fig. 20 measuring points 0-15) and after 12 hours of drying measurement without humidification (measuring points 25-42), finally with tap water (hardness level 13). The spray water was tempered to 22-23°C in each case to avoid thermal effects. The amount of water applied was determined gravimetrically and amounted to 80 ±5 g/m² for 2 spraying processes from a 30 cm distance. An influence of the water quality relevant to the short series of measurements could not be determined. For the further tests, distilled water was used. The measurement cycles were repeated three times within a week (n=88) and resulted in a chlorophyll-a content of 4.57 ± 0.43 µg/cm² (green algae) and 0.58 ± 0.13 µg/cm² (cyanobacteria) for the masonry brick. The diatoms were not included in the analysis as the concentration was below the detection limit of the device and therefore of no practical relevance.

Figure 19: Tripod construction stand for interval measurements

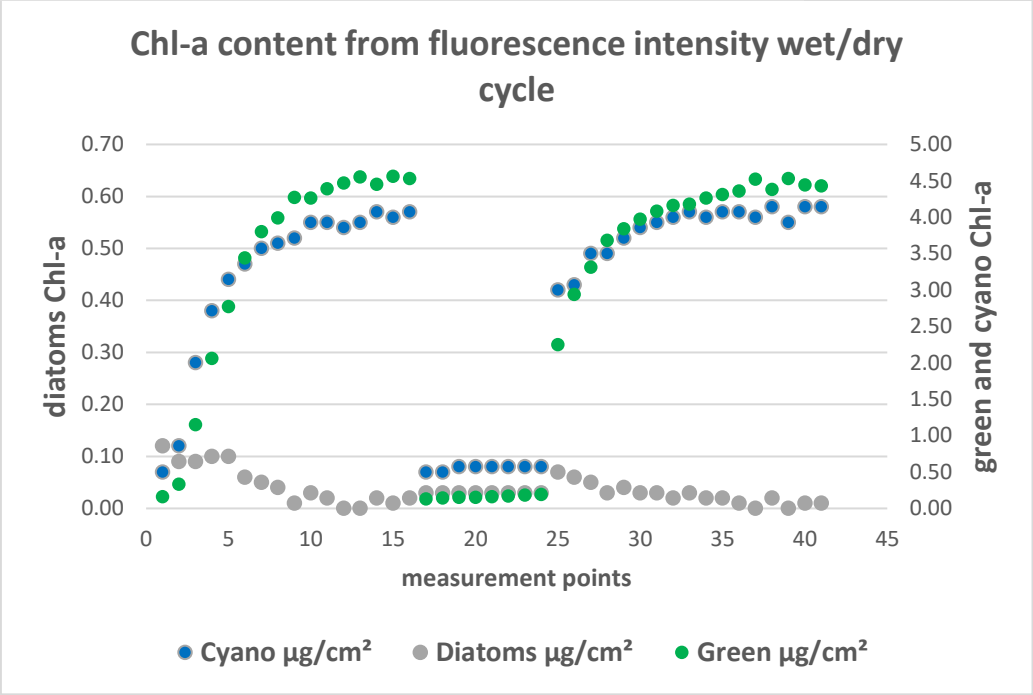

Figure 20: dry/wet-cycle on brick (Fig.18) with development of Chl-a

The repeated dry/moist measurement cycle confirms the influence and the need for the prior humidification on the signal stability for the detection [64]. After drying the test specimens and rewetting, the same signal level of chlorophyll-a content has recovered. The measurement interval was set to 600 seconds (each dot in Fig. 20) and the measurement duration is 10s. The BenthoTorch® has a programmable automatic interval control. A measuring tripod was constructed for better handling (Fig. 19). The tripod ensures a vertical measuring arrangement and enables interval measurements over long periods. The measured values are stored in the internal memory (up to 2000 data sets) and can be transferred to a PC by means of a data connection via USB connection. The supplied software offers several editing options and complements the graphic display (Fig.21).

Figure 21: Digital display - Main menu

The measuring range of 0-15 µg/cm² appears low at first glance but corresponds to 0-150 mg/m² of algal biomass and thus goes far beyond the quantities relevant in practice. The replaceable sponge-like rubber front of the BenthoTorch® enables a shading zone for the time span of measurement. Measurements in the field rarely take place under defined laboratory conditions. Fluorescence measurements on biogenic analytes are temperature-dependent. The influence of the substrate temperature was determined in the interval from -8.8°C to 39°C using the brick as an example. For this purpose, the test specimen was stored outside in a first series of measurements and subjected to an interval measurement. The temperature of the test specimen was then determined.

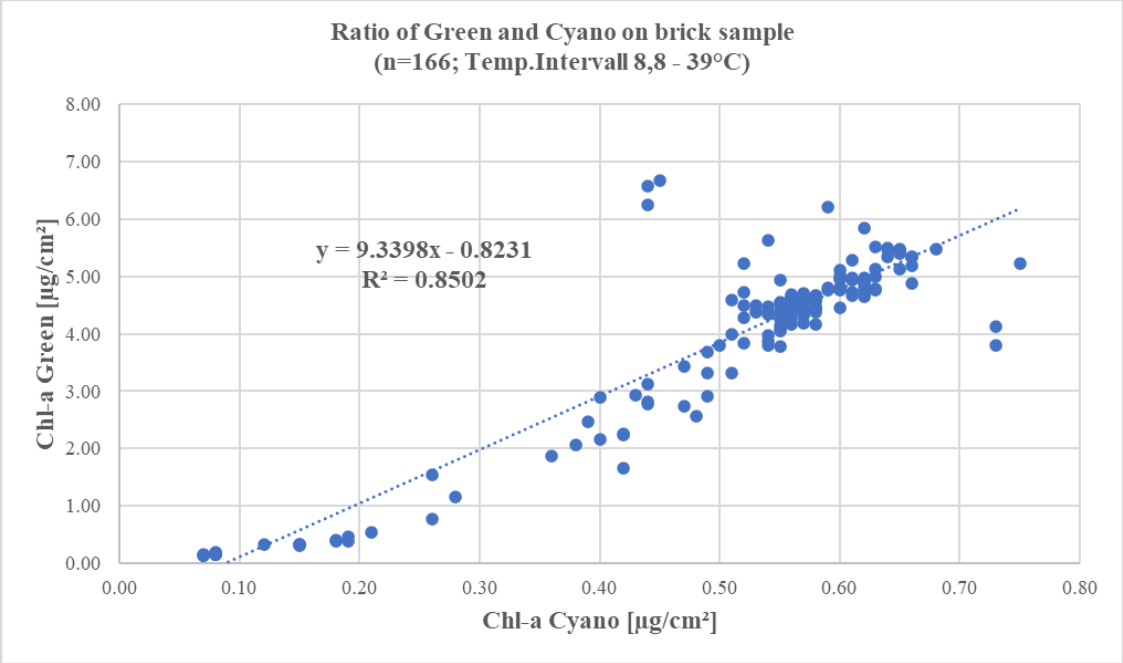

Figure 22: Species ratio of green algae and cyanobacteria in the field

The analysis of the measured data on brick revealed the joint presence of green algae and cyanobacteria in a stable ratio (Fig. 22, n=166, R^2=0.85). The measured values confirm the common presence of various microorganisms, which has already been approved [54]. Algae only occur as a monoculture in laboratory tests, while different species act together in biofilms in outdoor areas as a survival strategy against extreme living conditions [71].

4.2. Light reflectance value and sample brightness

The thermal load of façade coatings due to solar radiation poses a considerable risk. According to DIN 55699:2017, when using dark colours on external thermal insulation composite systems (ETICS), their TSR value (Total Solar Reflectance) must be considered [99]. The brightness value (HBW, Hellbezugswert) and the TSR value (Total Solar Reflectance) set minimum requirements for the reflectance behaviour of final coatings to avoid thermal stress. The light-protective pigments of microorganisms (carotenoids, melanin and scytonemine) are extremely UV-light-stable [100][101] and remain on the facades even after the organisms have died. The reflection behaviour decreases and the thermal load due to long-wave irradiation increases. The evaluation according to brightness reference value is usually carried out by means of grey scale colour fans (Fig. 24) in which the brightness values (L* values Cielab colour space) are mapped with the brightness reference values Y* [102].

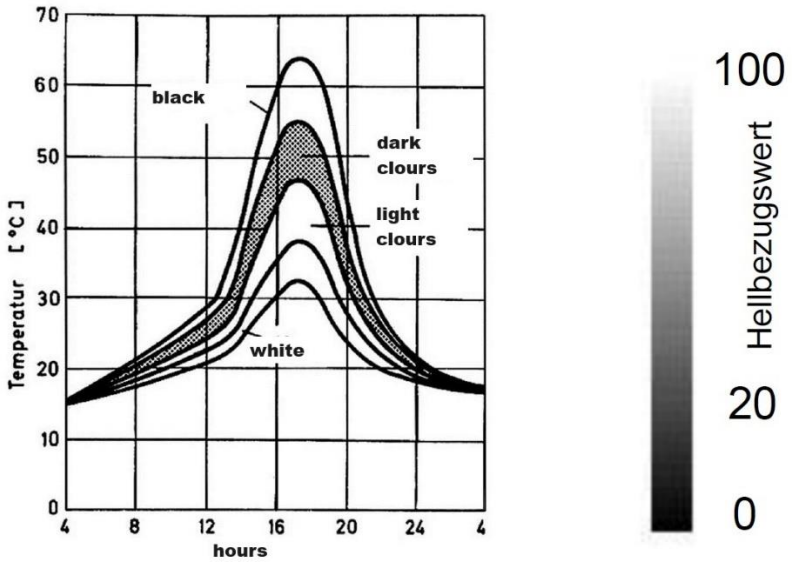

Figure 23: Surface temperature with different colour tones [103]

The lightness value expresses the brightness of a colour tone for the human eye in comparison to pure white (HBW100) or deep black (HBW0).

The brightness reference values, and the brightness values are functionally related to each other. The reflectance measurement of the BenthoTorch® is performed in the near-infrared range at 700nm. The colour fan was measured in triplicate with the BenthoTorch® to determine a correlation.

Figure 24: Grey scale colour fan as template [104]

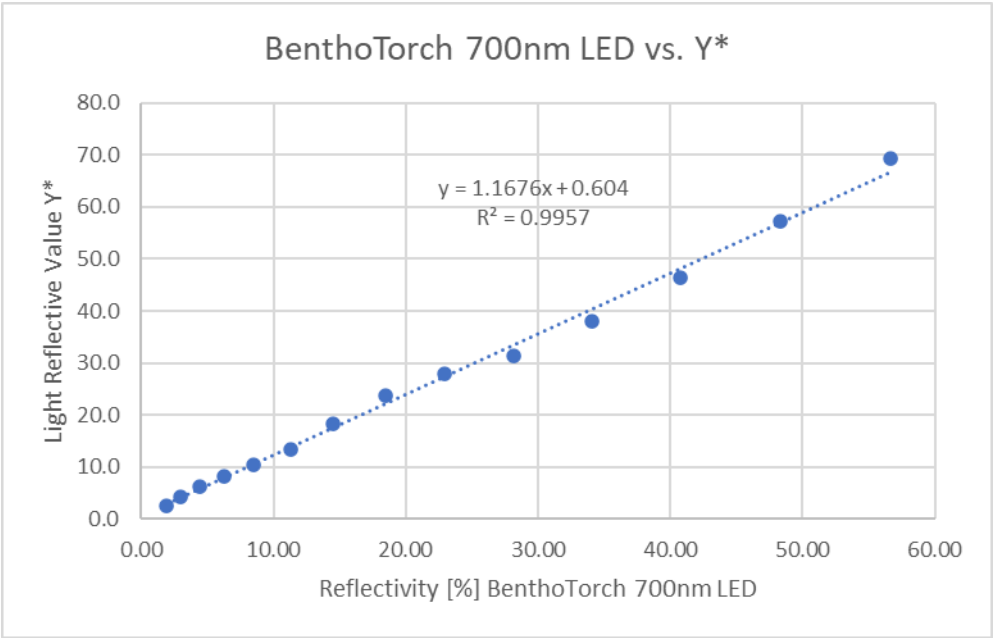

Figure 25: Relation of measured reflectivity at 700 nm vs. light reflectance value Y* [5]

As a result, the integrated reflectivity measurement of the BenthoTorch® can be used to determine the brightness reference value. The reflectivity value of the BenthoTorch® at 700nm is divided by 0.8 to obtain the brightness reference value (Fig.25). For external thermal insulation composite systems, a HBW >20 is recommended [99]. The permanent compliance with this limit value could be co-determined in parallel with the monitoring of microbial activities and thus reduces the potential of thermally induced stress cracks in the coating.

The visual change in façade surfaces due to colonization with microorganisms was determined by measuring reflectivity at the façade of the Swedish Provianthaus in Wismar, Germany and provides an ideal measuring surface with gradual progression of colonization. The optical impairment in relation to the chlorophyll-a concentration was determined on the facade of an extension to the building from the 17th century (Fig. 26). Due to the gradual course of the colonization area, the object is a good example of the visual warning limit of colonized building component surfaces.

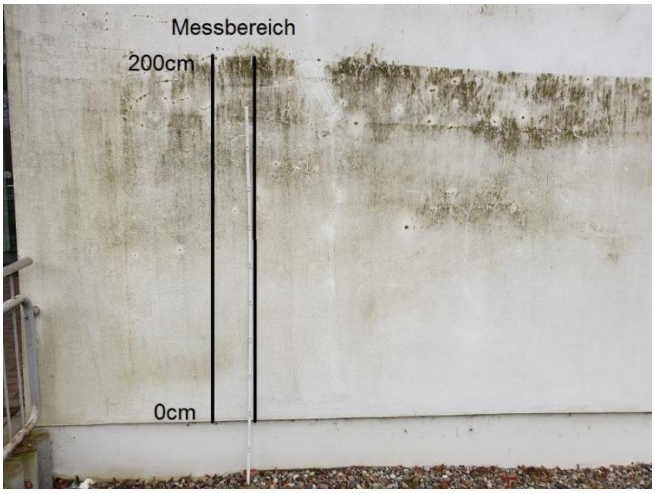

Figure 26: Measurement area at the facade of Provianthaus Wismar/Germany

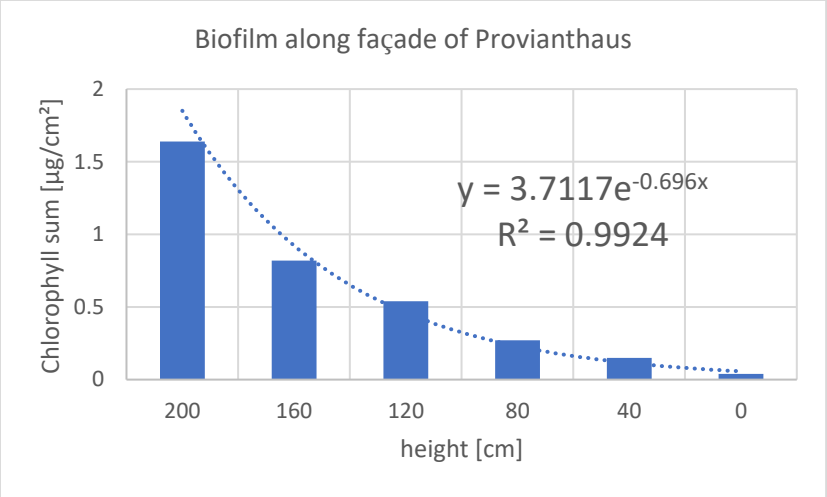

Figure 27: Chlorophyll-a concentration all species along façade in Fig. 26

The reflectance behaviour of the coating drops considerably due to the biogenic growth, the brightness reference value is reduced by 71%. The base area of the extension was subsequently painted, and the colonization density reflects the layer thickness of the paint application. The paint was applied from top to bottom, creating a gradient of properties within the area that is followed by the algal colonization.

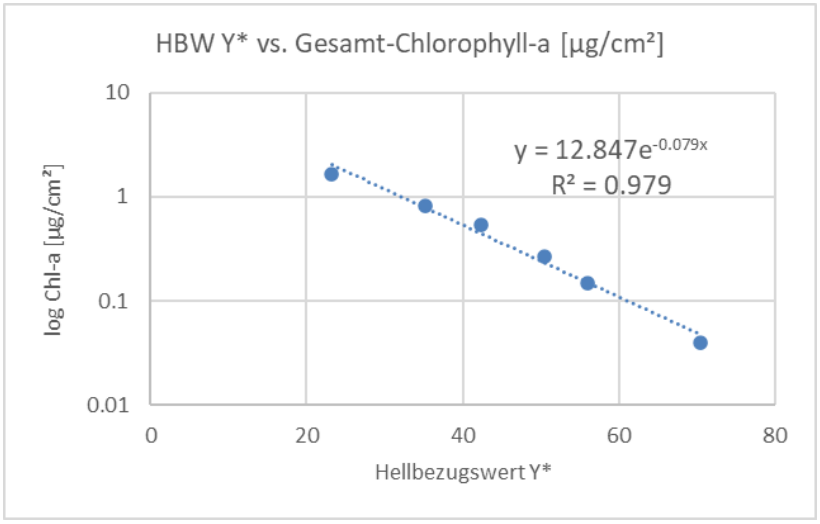

Figure 28: Light reflectance value (HBW, Y*) depending on chlorophyll content

4.3. Algae incubation test with different building materials

Standard EN 15458:2014 describes a laboratory method for testing coatings containing preservatives against algae [56]. A modified incubation test of various building materials was carried out based on this standard. The process of initial contact of the microorganisms with the building material surfaces was investigated. Brick, marble, concrete, and sand-limestone as typical masonry building materials were first thermally disinfected (1h/120°C) and subjected to a 35-days wet incubation test at 23°C/75% RH to determine their tendency to colonize algal biofilms.

Figure 29: Material samples (from left to right: brick, concrete, marble fine, marble grey, marble coarse, lime-sandstone)

A day-night-cycle of 16h/8h was applied by using a cultivation-lamp. The algae cultures for inoculation were collected over a period of 14 days at the outdoor weathering site, cultivated and microscopically examined. The building material samples, 50x50x5 mm in triplicate, were both the substrate and the sole source of nutrients after inoculation. After 0, 7, 14, 21, 28 and 35 days at 23°C and a relative humidity of 75% [data trend appendix Fig.118], the total cell count, and chlorophyll-a content were analysed using a BenthoTorch® fluorescence spectrometer. The humidity in the climate chamber was adjusted using a saturated sodium chloride solution (Fig. 30).

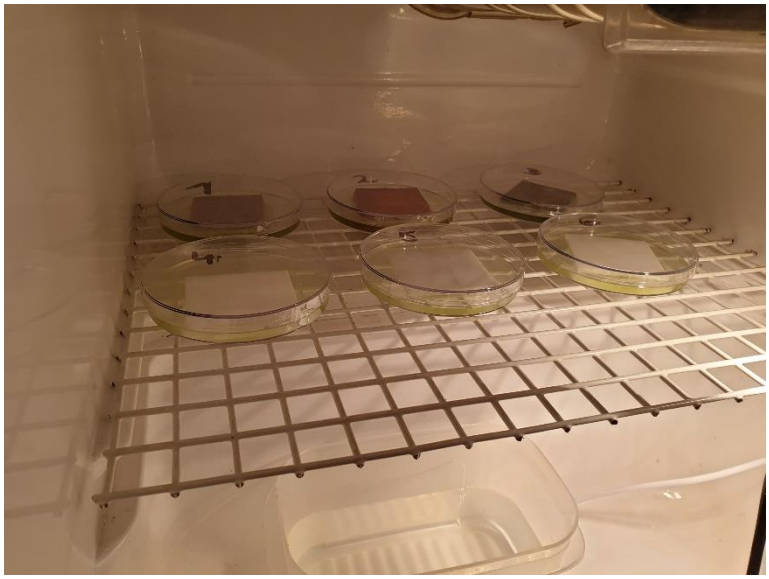

Figure 30: Incubation chamber with cultivation lamp and samples

After every 7 days, the samples were measured using the BenthoTorch fluorescence spectrometer and the chlorophyll-a content and total cell count were determined. A normative visual evaluation was dispensed with, as the fluorescence measurement responds clearly and selectively to the three types of algae. For this reason, initial disinfection with gamma rays was also dispensed with. Only the rubber sleeve of the BenthoTorch® was changed before each measurement to avoid the transfer of algae cells between the test specimens.

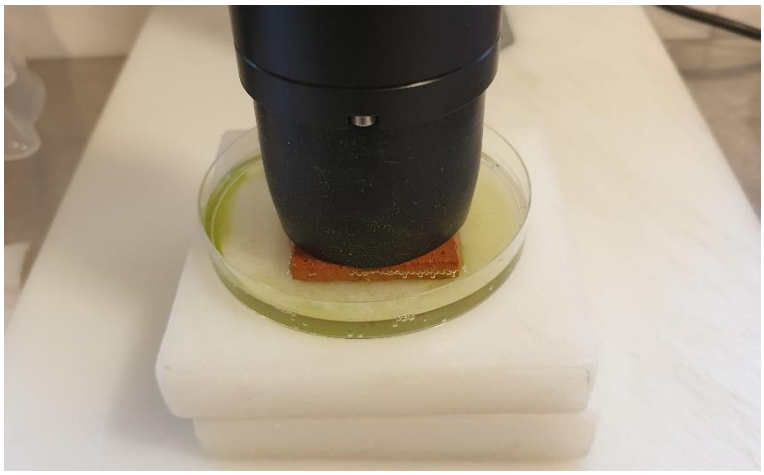

Figure 31: Weekly measurement with BenthoTorch

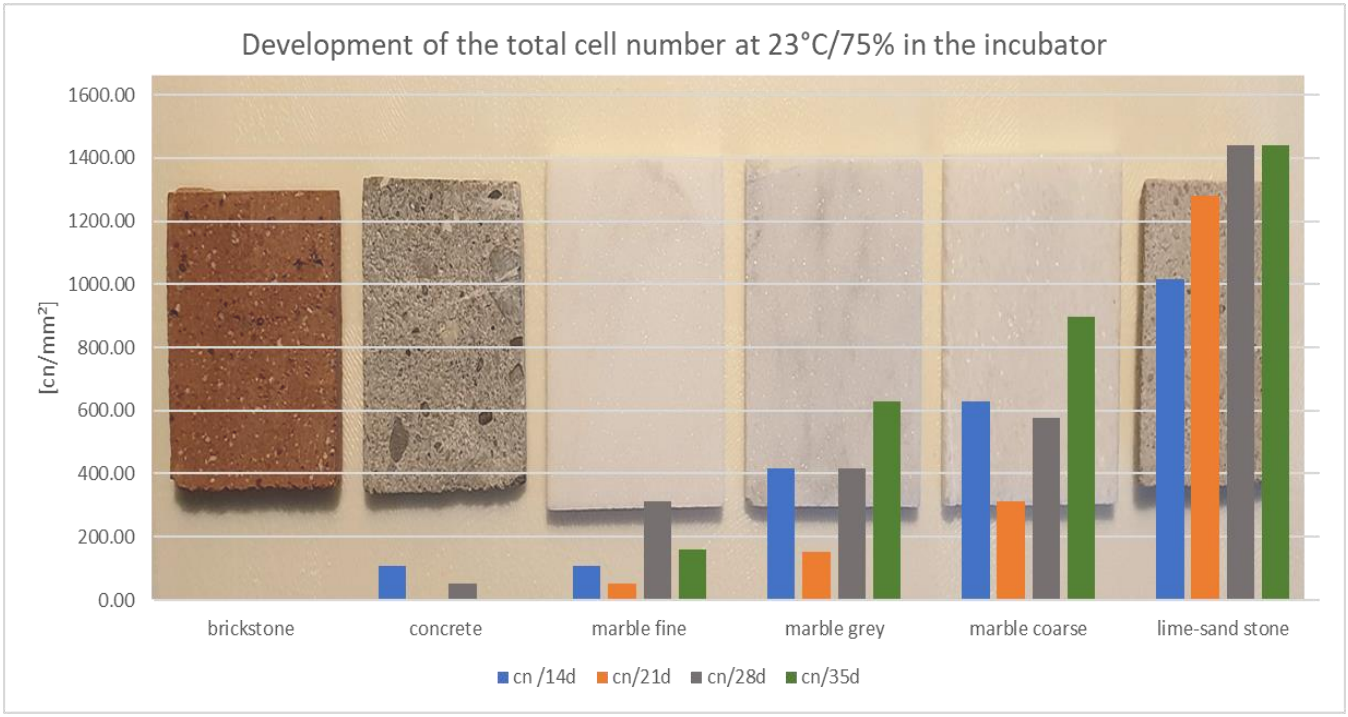

Figure 32: Total cell-numbers all species (cells/mm²) trend while incubation test

The elemental composition of the material samples was analysed in triplicate by Scanning Electron Microscopy, FEI Quanta 250 with Noran System 7 EDX detector in the laboratory of the Faculty of Civil Engineering at the University of Wismar, Germany (Fig.33).

Element	Calcium		Magnesium		Aluminium	
Sample	EDX* [%]	ICP-AES* [%]	EDX [%]	ICP-AES [%]	EDX [%]	ICP-AES [%]
brick	0	0.07	0.21	0.01	8.37	0.09
limesandstone	13.1	12.20	0	0.13	1.16	0.43
concrete	17.8	13.00	0	0.05	2.28	1.02
marble fine	29.8	24.80	10.2	12.60	0	0.01
marble coarse	42.9	43.20	1	0.24	0	0.01
marble grey	50.2	43.30	0	0.04	0	0.01
***measurement uncertainty: EDX <5% and ICP-AES <0.5%, all results mass%**						

Figure 33: Energy-Dispersive-Xray (EDX) and Inductively Coupled Plasma-Atomic Emission Spectrometry (ICP-AES) analysis of material samples for incubation test

Validating the EDX values, the samples were additionally analysed by Inductively Coupled Plasma Atomic Emission Spectroscopy (ICP-AES) in a certified external environmental laboratory [105] with an R^2=0.97 for calcium (Fig.38).

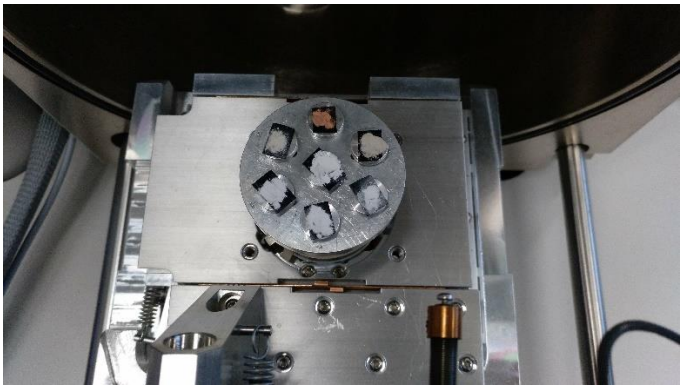

Figure 34: Sample positioning for EDX analytics (Picture: Dr. T. Barfels, Wismar)

Only one EDX spectra (marble fine) is shown here as an example for all samples that can be found in the appendix [Fig. 89-115].

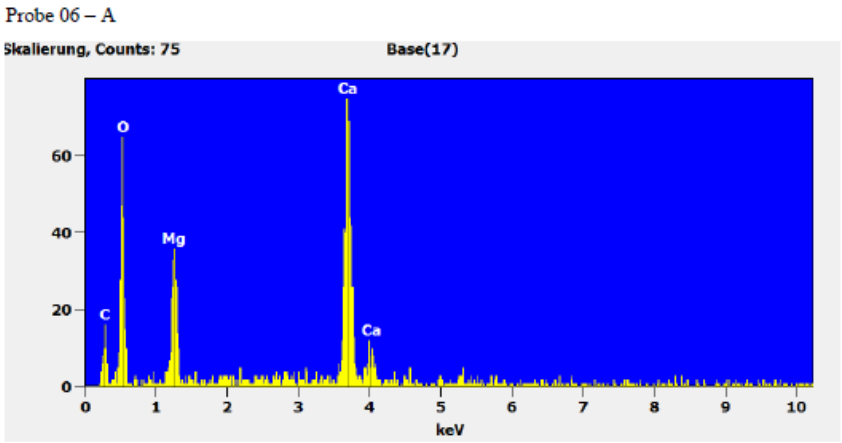

Linie	Gew.-%	Atom-%
C K	9.72	16.41
O K	45.95	58.20
Mg K	9.10	7.59
Ca K	35.22	17.81

Figure 35: Screenshot of sample 06_A (marble fine first)

Probe 06 – B

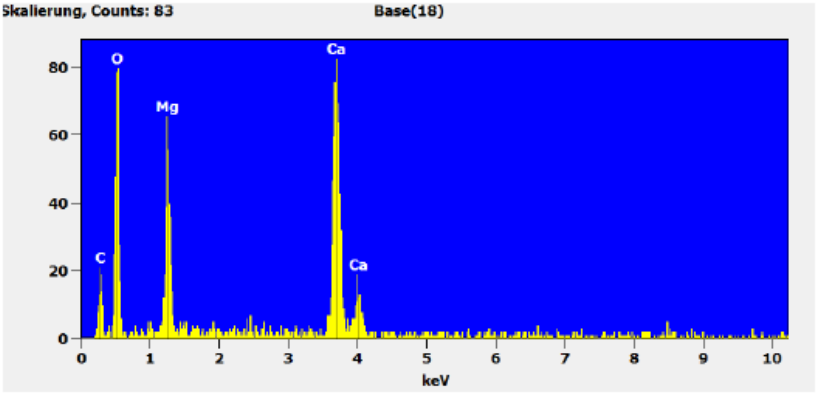

Linie	Gew.-%	Atom-%
C K	10.51	17.32
O K	47.41	58.66
Mg K	10.07	8.20
Ca K	32.01	15.81

Figure 36: Screenshot of sample 06-B (marble fine second)

Probe 06 – C

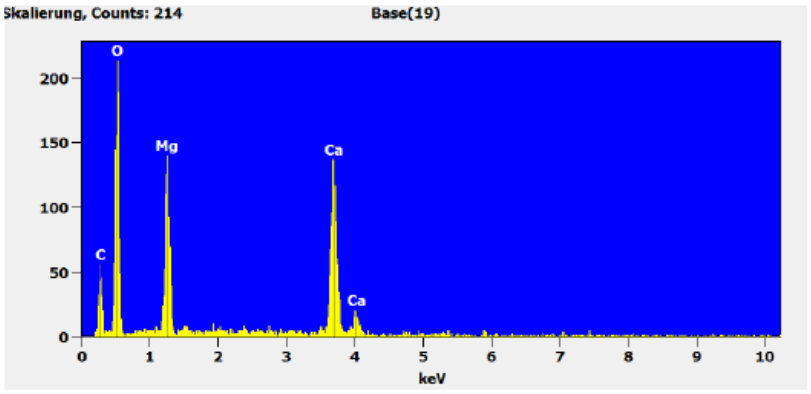

Linie	Gew.-%	Atom-%
C K	13.67	20.86
O K	52.75	60.43
Mg K	11.32	8.53
Ca K	22.27	10.18

Figure 37: Screenshot of sample 06-C (marble fine third)

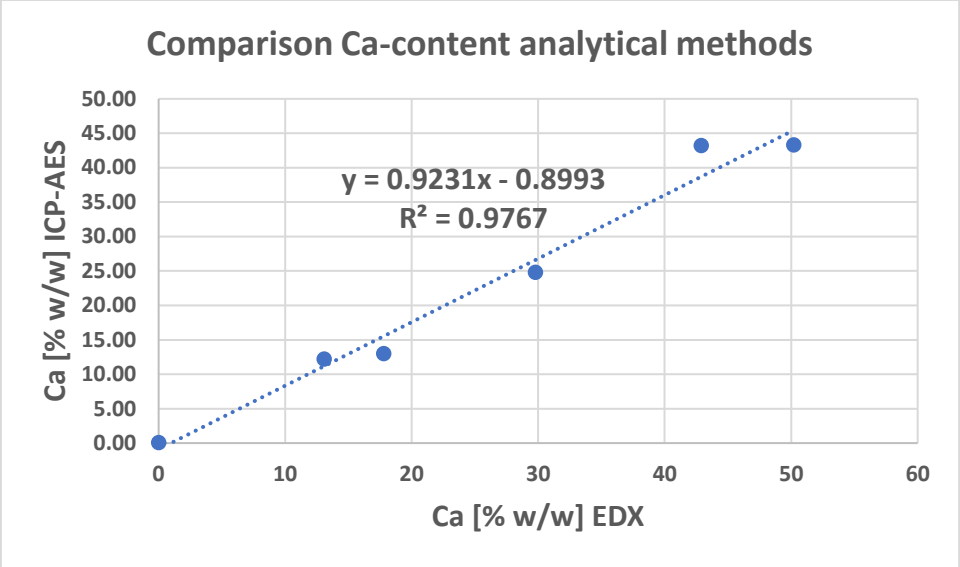

Figure 38: Regression for calcium between EDX and ICP-AES as cross-check

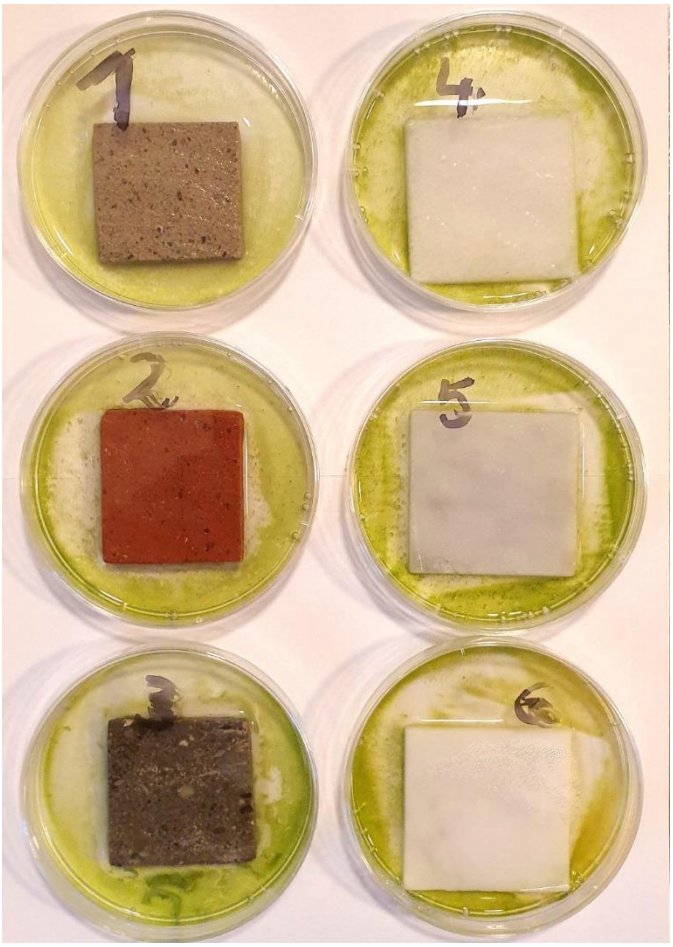

Figure 39: Biofilm formation after 35 days of incubation

4.4. Area-specific algae adsorption test

For realizing the area-specific adsorption test (algae cells/cm²), the prior thermal disinfected (1h/120°C) building material samples (50x50x5mm) were subjected in triplicate to a newly developed algae suspension test. The algae culture from incubation test was diluted with tap water using a 1l-pot of black opaque polypropylene equipped with magnetic stirrer, pH-electrode, and BenthoTorch® fluorescence spectrometer (Fig.40). The cell number per volume of the suspension was set according to Tab. 3 before each measurement by dropwise adding the algal culture. The temperature of the suspension was 10±1°C in each run. A few drops of 5% aqueous ammonia solution were used to adjust the pH-value.

Figure 40: Experimental setup for algae suspension test

Table 3: start conditions of algae suspensions measured at 10°C

sample	pH1	pH2	Cells/ml
brick	7.0	10.8	20,000
sand-limestone	7.0	10.8	20,000
marble coarse	7.0	10.8	20,000

After thermal disinfection, the samples were first cooled to room temperature and then saturated in water of 10°C (expected mean temp. of outdoor exposure). Water saturation cools down to 10°C and compensates for capillary suction effects due to the different porosity and roughness of the specimens, which influence adsorption of material samples [36]. The adsorption of the algae cells should therefore be almost completely determined by the chemical substrate surface. Algae suspension is stirred gently, and the cell count is read on the display. Once a stable cell count has been established, the respective test specimen is completely immersed in the algae suspension. The cell counts were read and recorded at 2-minute intervals until there is no more change.

Figure 41: Clamp as immersing tool for suspension test

The BTo display shows the cell number in the unit cell number/mm². Calibration is performed using a calibration disk, which is included in the scope of delivery. It measures 100µl of the algae suspension on a sample area of 1.0 cm² and achieves a very low layer thickness. This allows the area-related cell-count to be converted to a volume-related cell count. In the suspension test, however, the cell-count per material area is to be determined, so the measured values can be taken over and interpreted directly. The conversion from cells/mm² to cells/ml is achieved by multiplying by 10. The difference between start value of cell numbers and end value will give the adsorbed number of algae cells.

Figure 42: Calibration disk with 100µl algae suspension for cross-check

For the algae suspension test, three building materials were selected from the incubation test, which showed clear differences in colonization behaviour. Brick without colonization, sand-limestone with the strongest colonization and marble coarse with medium algal colonization. This allows a greater differentiation of the samples and the expected results in the following suspension test. Marble was selected because it is used as a coarse grain for structuring in plaster preparations. Our own observations have shown that algae colonization starts around the marble grains.

Figure 43: ETICS with algae infestation starting around marble grains

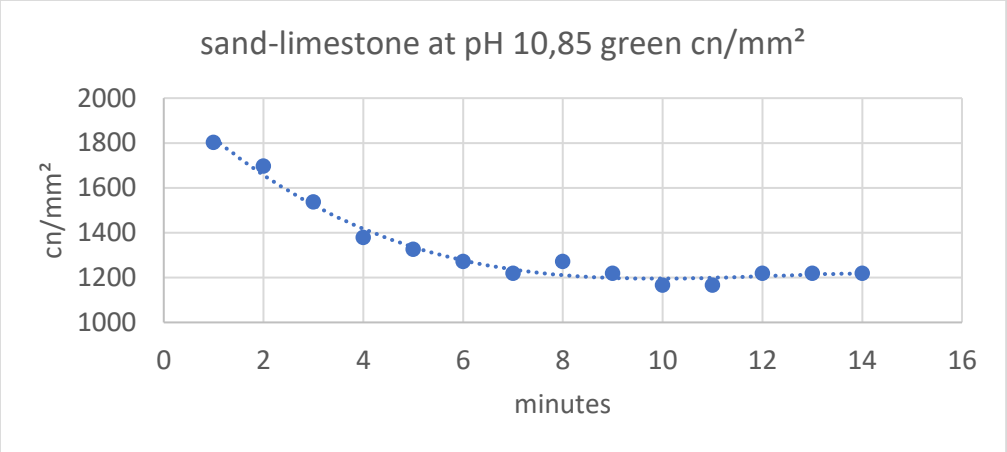

Figure 44: Trend of total cell number algae in suspension at 10°C

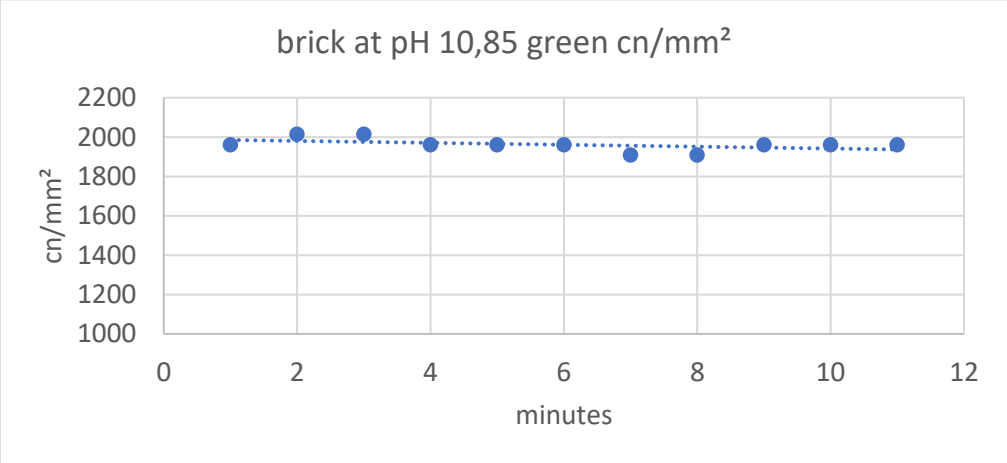

Figure 45: Trend of total cell number algae in suspension at 10°C

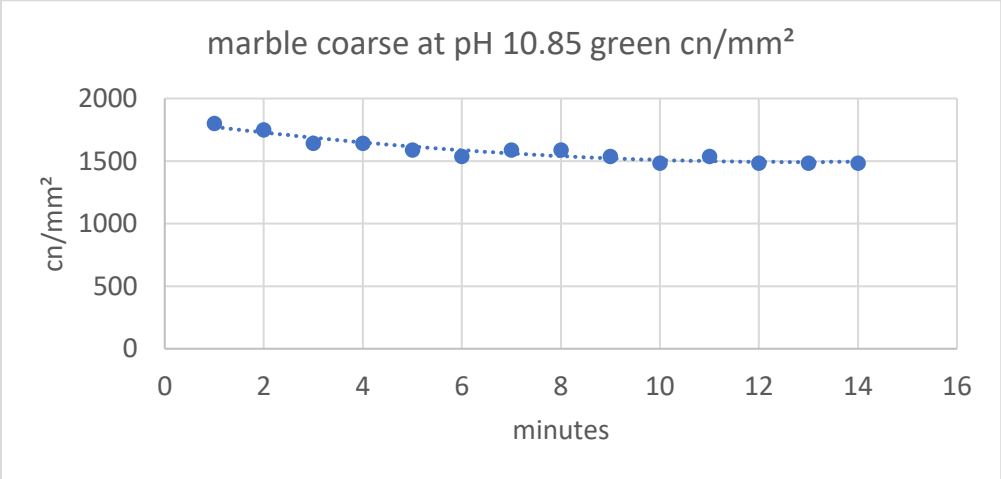

Figure 46: Trend of total cell number algae in suspension at 10°C

The absorption test was repeated with fresh material samples at a pH value of 7.0 and no measurable decrease in cell numbers was observed.

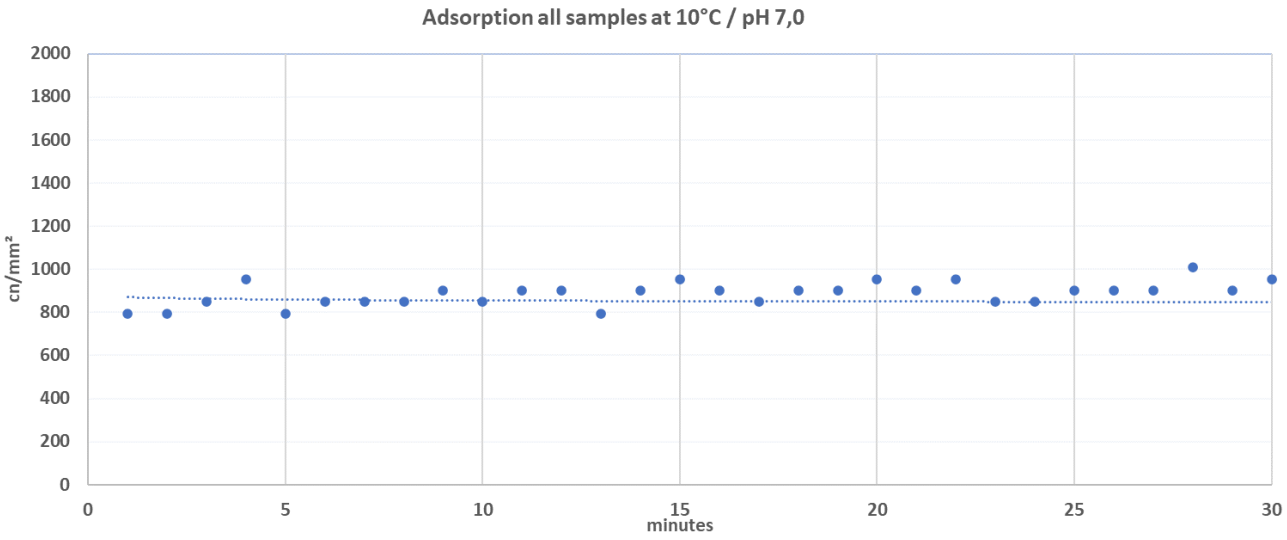

Figure 47: Trend of cell numbers brick (0-10), lime-sandstone (10-20) and marble coarse (20-30)

The test was carried out with a lower concentration of algae cells in the suspension to be more sensitive, but no cells reduction could be detected. Fig. 44-46 shows the course of reduction of the free-floating algae cells in suspension after immersion of the sample. The mean value of the cell counts result from three tests per material sample and are listed in Tab.4. The cell counts are converted by multiplying the display reading by 10 to obtain the total cell count in 1000 ml of suspension and the cell count adsorbed by the test specimen.

Table 4: Calculation of relative and absolute adsorbed algae cells per sample

sample	start [cn/ml]	end [cn/ml]	adsorption [cn]	% adsorption
lime-sand stone	19470	13190	6.28xE06	32.2
marble coarse	18020	14840	3.18xE06	17.6
brick stone	19610	19610	0	0
cn/mm² x 10 = cn/ml, 1000 ml suspension, average of triplicate with error < 5%				

4.5. Free-weathering test of coating recipes

The present investigation was carried out in the geographical area of the air quality reports. In the search for alternative sources of nutrients within the final coatings - the focus is on fillers. Mineral fillers fulfil numbers of important technological functions and reduce manufacturing costs and when looking through various recipes of façade paints, regularly magnesium-containing fillers like dolomite and talc will be found [11]. Calcium carbonate is the most important filler and, depending on its geological origin and quality, contains significant amounts of magnesium-based accessory minerals [106]. The chemical composition of the fillers ideally meets the requirements of phototrophic microorganisms as they are obtained from natural mining resources that are the result of primeval marine organism activities. This common past of algae and fillers will meet again on modern façades today and prompts the author to investigate further, because there is no photosynthesis without the magnesium core-ion of chlorophyll-a.

4.5.1. Test location and conditions

The aim of the weathering test was to compare the algal susceptibility of acrylic-dispersion paints containing different types and amounts of magnesium-containing fillers. The outdoor exposure lasted from December 2019 until December 2021 and included 7 painted panels. The panels were mounted vertically on the north gable of a brick house at an angle of 5 degrees. The test site is situated in a rural area with dense vegetation and agricultural use (Fig.48). The direct distance to the Baltic Sea is 4.5 km in a North-Western direction. The A24 motorway runs 2 km southern of the site.

Figure 48: Weathering location rural area near Wismar, Germany (Source: Google Earth for Chrome, Goldebee 53°89'44''N 11°60'08''E, © GeoBasis-DE/BKG 2009, URL: http://google.com/earth.

Air temperature ranged from -11.5 °C to 36.6 °C with a mean of 10.6 °C and relative humidity ranged from 36.9% to 100% with a mean of 81.3% (Fig.50, n=36,372). Data collection was proceeded using Datalogger UNI-T UT330C for humidity, temperature, and air pressure with an interval of 30 minutes. The dew-point was calculated via intern algorithm of the datalogger (Fig.49).

Figure 49: Position of data recorder at the test panel

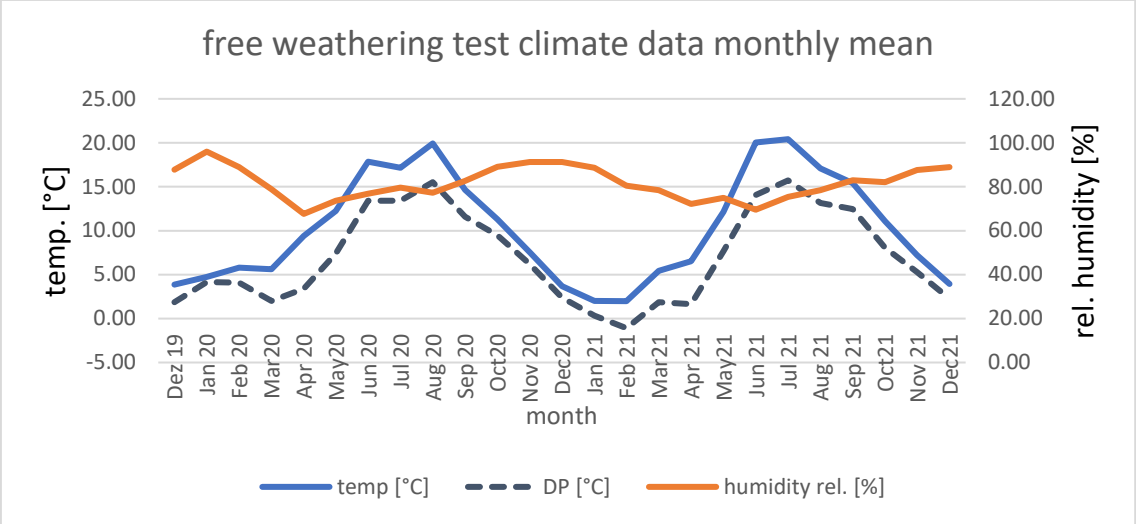

Figure 50: Monthly averaged climate data collected by data logger (n=36,372)

4.5.2. Sample preparation

The materials to be tested were seven laboratory-made acrylic dispersion façade paintings containing different amounts and types of magnesium-containing fillers (Tab.5). The binder base is the non-ionic pure acrylate resin K498 with a pH value of 9.0. This formulation is well compatible with metal cations and has a solids content of 50% w/w. According to the manufacturer, this acrylate is used to produce weather-resistant facade paints and contained an in-can anti-bacterial preservative due to the manufacturing process. The amount of cross-wise roller-applicated wet paint was 250 g/m² for each panel (Fig. 51). Pigment volume concentration was set by varying the amount of acrylate binder, the solid content was adjusted by adding water. Additional biocides were not used. Further technical data can be found in the appendix (Fig.119). The pigment volume concentration (PVC) for each sample kept constant at the level of 50% and set intentionally more critical to simulate an accelerated aging process and having the filler particles more present to the surface. High-quality, wash-resistant façade paints are usually adjusted in the PVC range of 0-45% when using pure acrylates [11]. In principle, PVC describes the mathematical ratio of the volume of pigments and fillers to the total volume of the dry coating and a critical PVC is reached, if there is just enough binder left to cover all pigment and filler particles.

Sample PK06 contains 5% (calculated on non-volatiles) zinc molybdate (Carl Roth GmbH & Co KG, Karlsruhe, Article No. 0874.4) to evaluate an approach as defence-strategy against algal growth. The solids content of the colour formulations was uniformly set to 61%.

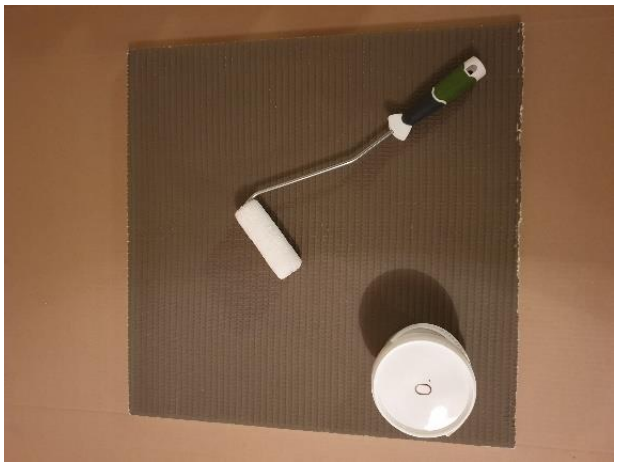

Figure 51: Preparation of coating via roller application

Close to the test area, samples of airborne algae were collected over a period of 14 days and a microscopic evaluation of some main algae species revealed *Scenedesmus spp., Kirchneriella spp.* and *Chlorella spp*. (Fig. 52).

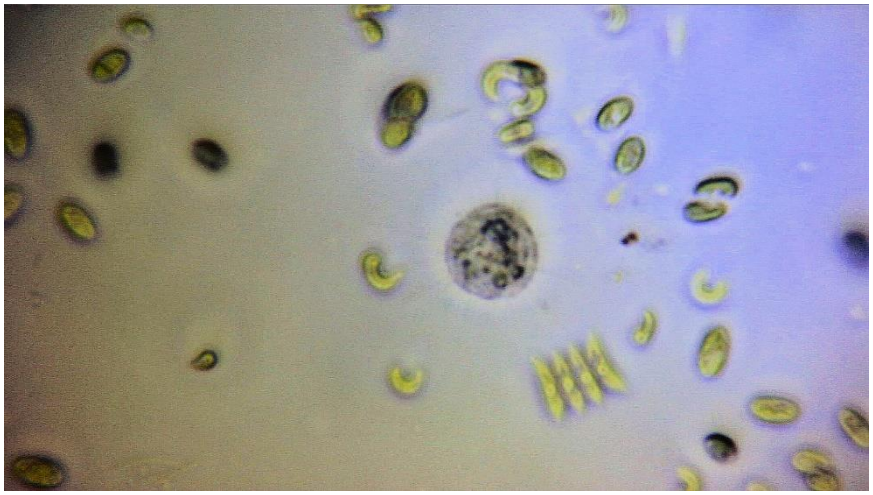

Figure 52: Microscopical evaluation of algae suspension (magnitude Bresser 400x)

After one week of drying, the finished test specimens were mounted at the north gable of the building at an angle of 5° using wall hooks and plastic clips to make them windproof. The panels have no direct contact with the building, and heat flow through the double-skin brick wall with air layer is not possible. The low angle was intended to reduce the influence of rain events and to ensure humidification mainly via condensation water. The main wind direction in the test area was west.

Figure 53: Mounting and fixing of samples at the brick wall north gable

The weather data were recorded via data logger for air temperature, relative humidity, air pressure and dew point temperature in a 30-minute-interval (n=36,372 data sets). This configuration resulted in a comparable specific heat capacity of the surfaces to avoid different condensation loads [35]. The coatings were applied on expanded-polystyrene-based, lightweight Ultrament® building boards (Ultrament GmbH & Co. KG, Bottrop, Germany, annex Fig.88) with dimensions of 20 x 600 x 600 mm each. The concrete-slurry-coated surface, reinforced by a 10 x 6 mm plastic mesh, delivered a well-defined structure for every sample surface (Fig.54) to avoid structural effects on the biofilm distribution between samples.

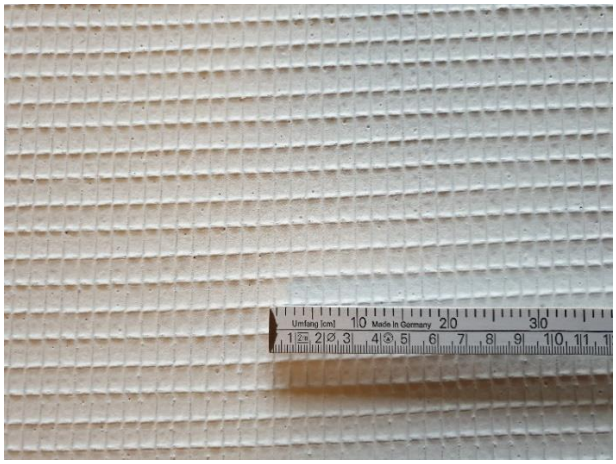

Figure 54: Ultrament® construction board with surface texture

Table 5: Composition of coating recipes of free weathering test

Components [g]	**PK00**	**PK01**	**PK02**	**PK03**	**PK04**	**PK05**	**PK06**
Titanium dioxide	7.5	7.5	7.5	7.5	7.5	7.5	7.5
Calcium carbonate	112.5	112.5	112.5	112.5	112.5	112.5	112.5
Quartz powder	4.5	4.5	4.5	4.5	4.5	4.5	4.5
Dolomite	-	21.0	45.0	77.0	76.0	75.0	-
Talcum	-	-	-	-	26.0	-	-
Mg-Hydroxycarbonate	-	-	-	-	-	70.0	-
Zinc molybdate	-	-	-	-	-	0	9.4
Pure Acrylic Disp. 50%	105.0	125.0	140.0	170.0	190.0	250.0	110.0
Water	60.0	70.0	80.0	95.0	110.0	125.0	65.0
Total [g]	289.5	340.5	389.5	466.5	526.5	644.5	308.8
Pigment vol. conc. [%]	50.0	50.0	50.0	50.0	50.0	50.0	50.0
Non volatiles [g]	177.0	208.0	240.0	287.0	322.0	395.0	189.0
Solid content [%]	61.0	61.0	61.0	61.0	61.0	61.0	61.0

4.5.3. Detection of algal biomass after outdoor exposure

The algal biomass was quantified using the BenthoTorch® fluorometer (from German company bbe moldaenke GmbH, 24,222 Schwentinental [8], referred to as BTo for short in the following. While sampling was not necessary the destruction of microorganisms and components could be avoided. The panels were humidified in a controlled manner by using a water spray bottle 15 min before measurement. Using a 13-dot template, each test panel was measured 13 times between December 2019 and December 2021 (n =169). The single mode measuring process took 20 s (including 10 s diode initialization) and covered an area of 1 cm². Previous 24-hour dark adaptation was omitted and limited to the initialization phase of the diodes before the measurement process started. The sponge attachment of the measuring optics was changed each time the test specimen was changed to avoid contamination between the samples. Due to the surface texture of the carrier plates, contact with the back of the measuring template was negligible. In addition, the back of the template was cleaned with a damp paper towel before each change

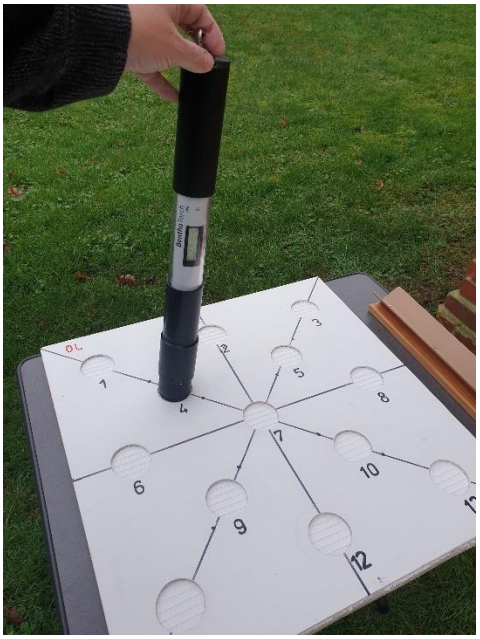

Figure 55: 13-dot template for fluorescence measurement

4.5.3.1. Development of algal biomass via BenthoTorch®

During weathering, the coatings showed a strong fluctuating stock of algal biomass. The first signals of green algae were detected after 44 (PK04) and 89 days (PK03) but disappeared again in the further course and were below the visual threshold. Above exposure time of 327 days permanent signals of green algae appeared (PK03, PK04, PK05). Sample PK05 was continuously and visibly colonized from day 327(Fig. 63). Fig. 57 depicts the mean value of the total cell numbers of all algae species after 730 days. The corresponding chlorophyll-a contents were between 0.01 and 0.60 mg cm². The mean value of fluorescence detected algal biomass was composed of 92.3% green algae, 6.3% cyanobacteria, and 1.4% diatoms.

Figure 56: Biofilm visual impression of weathered samples after 730 days

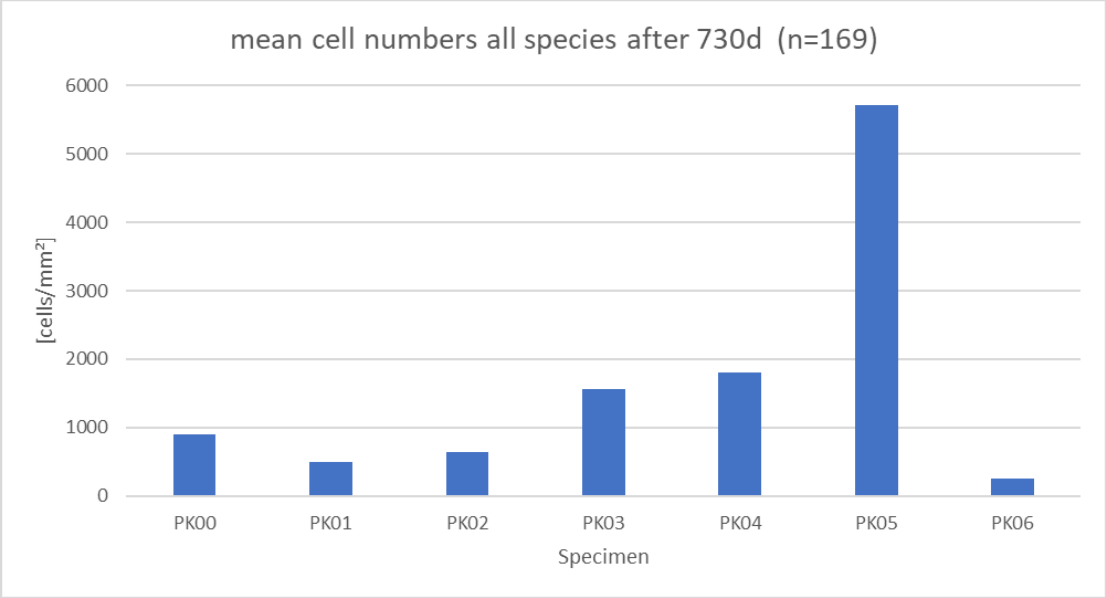

Figure 57: Biofilm total cell number after 730-day weathering

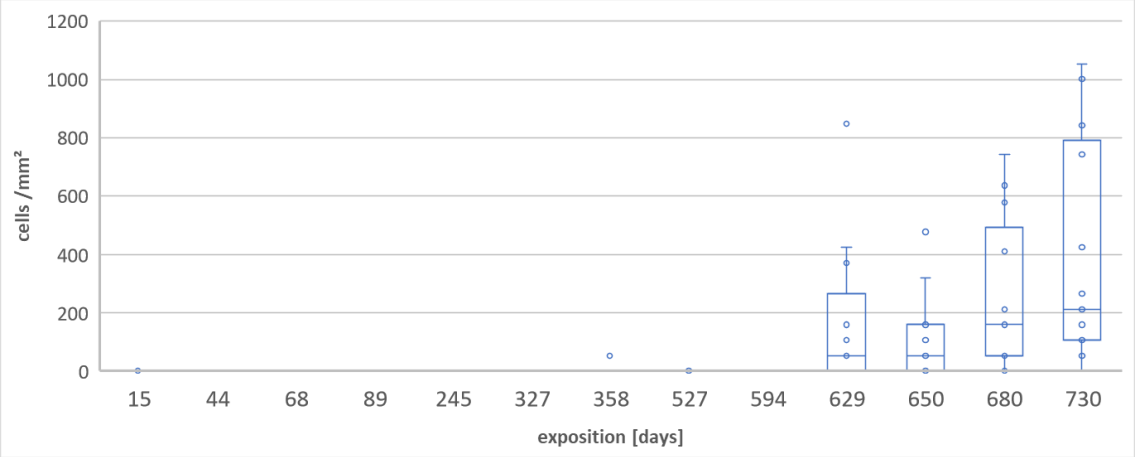

Figure 58: Boxplot of total cell numbers PK00 (reference without added Mg-based fillers)

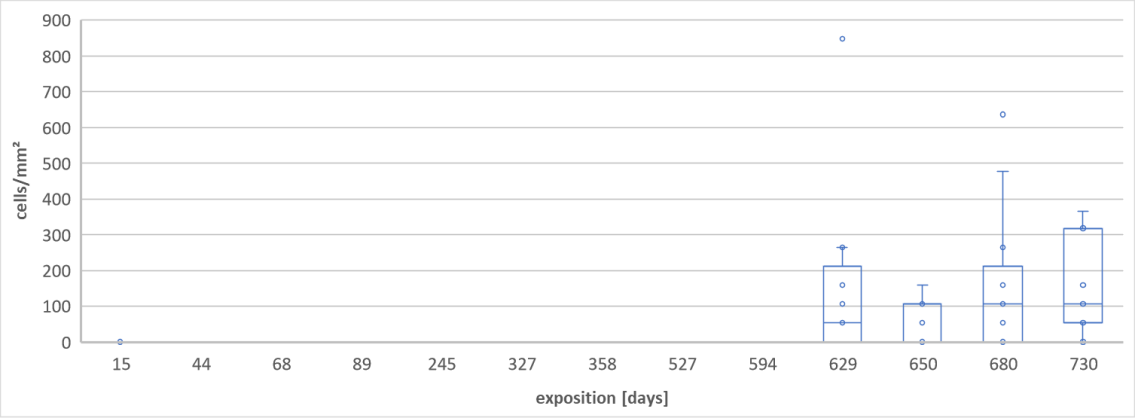

Figure 59: Boxplot of total cell numbers PK01

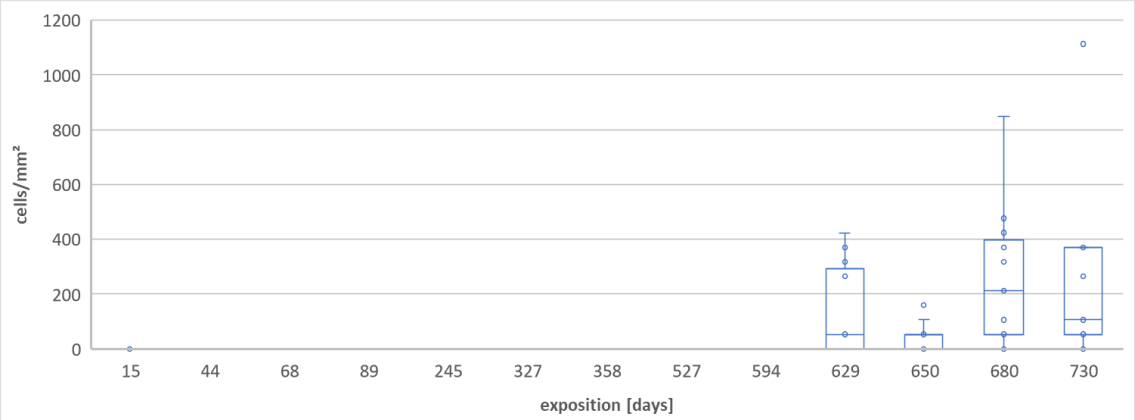

Figure 60: Boxplot of total cell numbers PK02

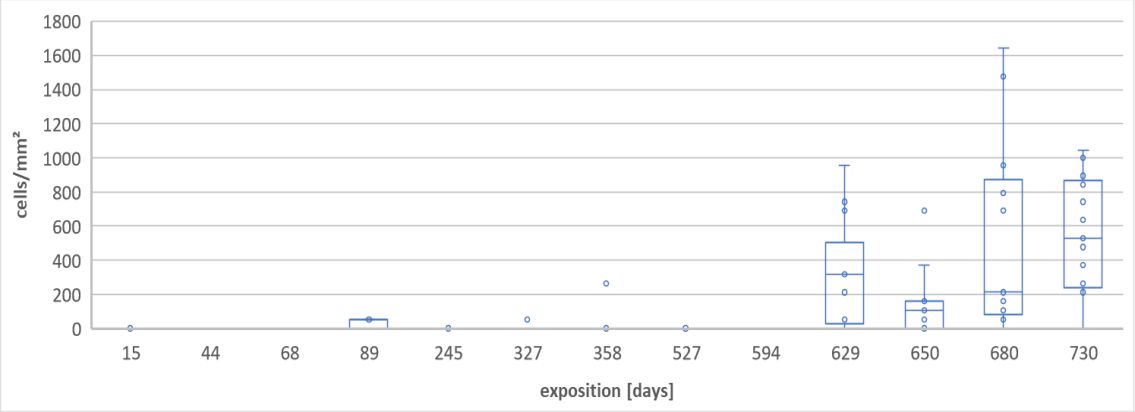

Figure 61: Boxplot of total cell numbers PK03

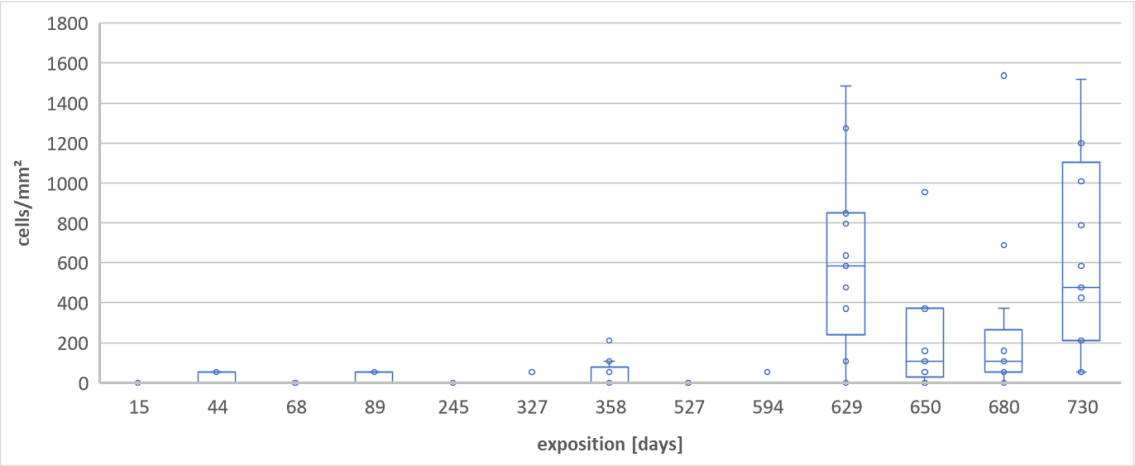

Figure 62: Boxplot of total cell numbers PK04

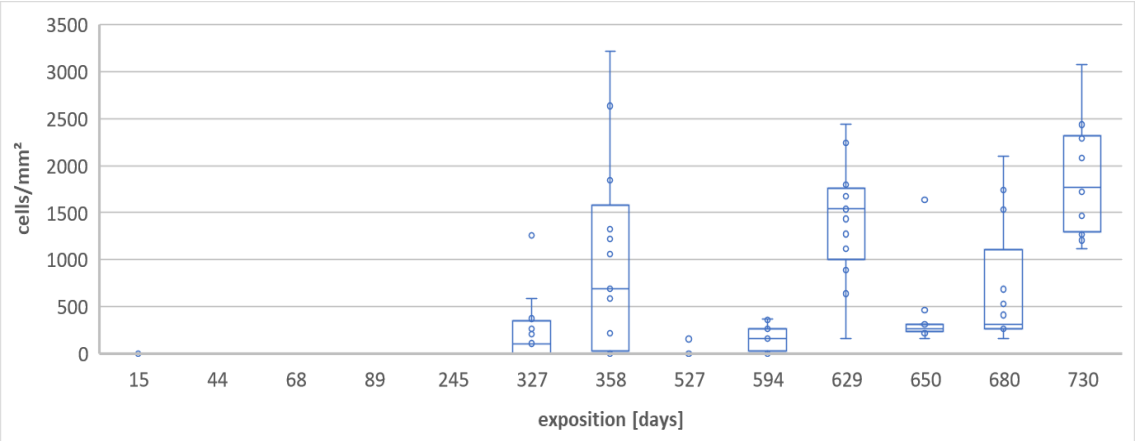

Figure 63: Boxplot of total cell numbers PK05 (highest content of Mg-based filler)

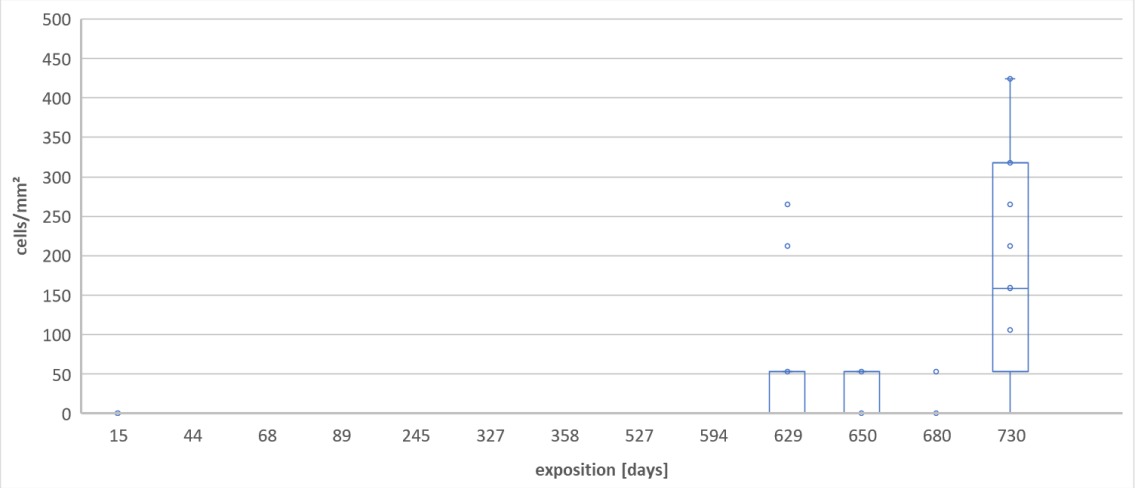

Figure 64: Boxplot of total cell numbers PK06 (with functional filler $ZnMoO_4$)

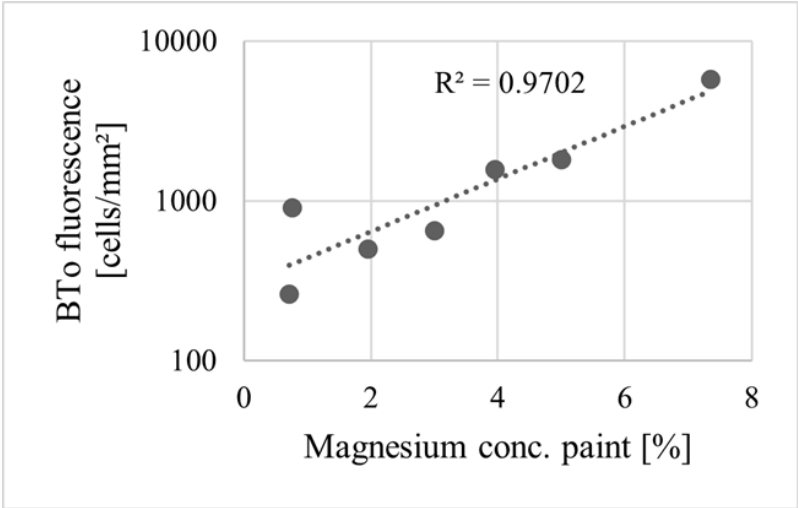

Figure 65: Regression of cell number BTo vs. Mg-concentration coating

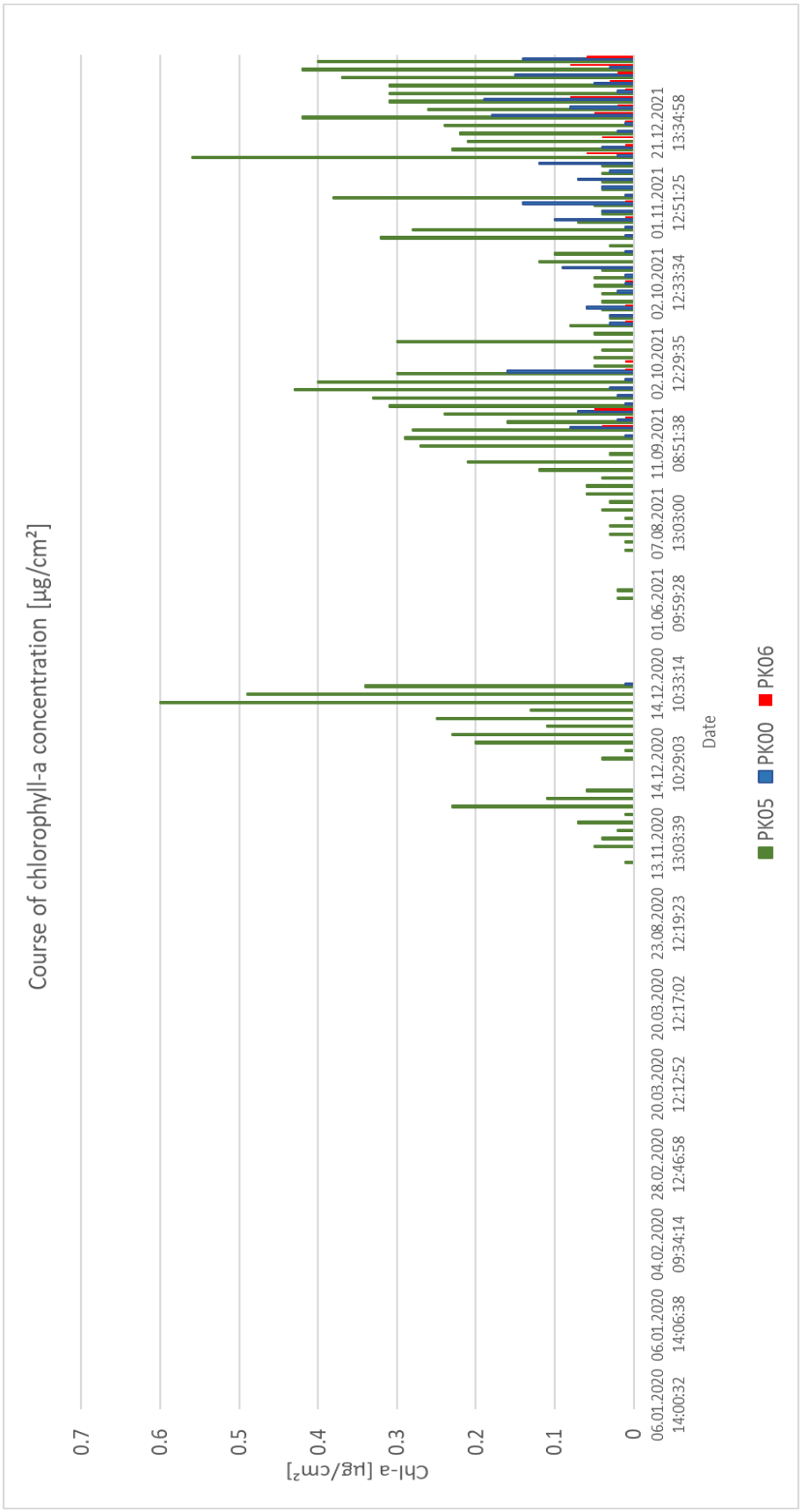

Figure 66: Course of high (PK05) and low (PK06) chlorophyll-a [µg/cm²] with reference (PK00) over total outdoor exposure of 730 days

4.5.3.2. Evaluation of algal biomass according EN 16492:2014

According to the German Standard DIN EN 16492:2014 the evaluation of the surface disfigurement was conducted visually and expressed to the criteria of intensity, quantity, and area proportion [55].

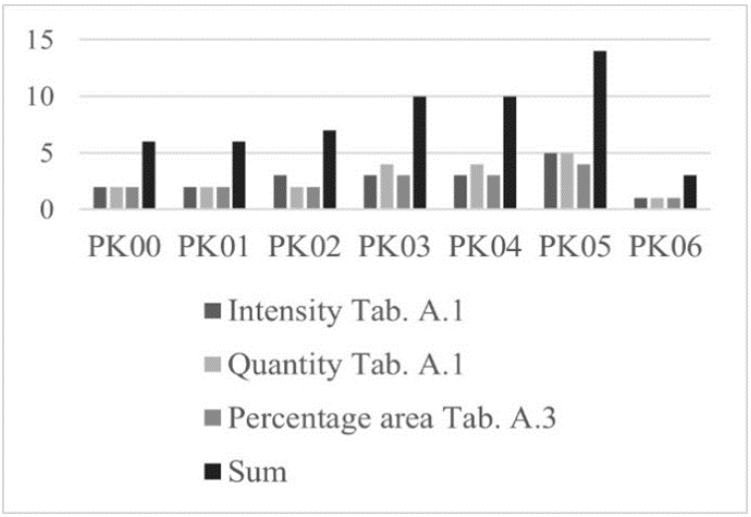

Figure 67: Evaluation based on criteria of annex A EN ISO 4628-1

To enhance the effect of microbial colonization, the sum of all criteria was calculated in deviation from the standard (Fig.67).

Sample	ImageJ area [%]	BTo [cells/mm²]	EN16492 sum	Mg [%]
PK00	7.52	906	6	0.76
PK01	13.75	497	6	1.96
PK02	16.26	648	7	3.00
PK03	23.98	1563	10	3.96
PK04	22.19	1806	10	5.00
PK05	38.46	5712	14	7.35
PK06	4.95	261	3	0.71

Table 6: Data sets for correlation of results between all methods

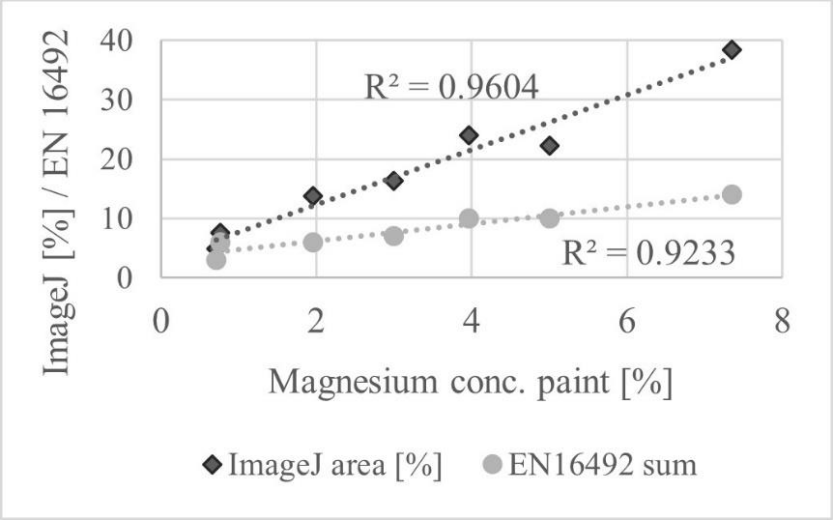

Figure 68: Cross-check of visual and digital evaluation of weathered samples

4.5.3.3. Sample surface gallery after outdoor exposure

To complete the surface evaluation, the following microscopic images (magnitude 200x) of the most relevant test specimens (reference/high/low biofilm formation) after finished outdoor exposure of 730 days are shown. In addition to the cell counts determined, PK05 is particularly species-rich with a carpet of green algae and various lichens (Fig.71-74). At Sample PK06, cracks are recognizable that no other sample shows (Fig. 75-76).

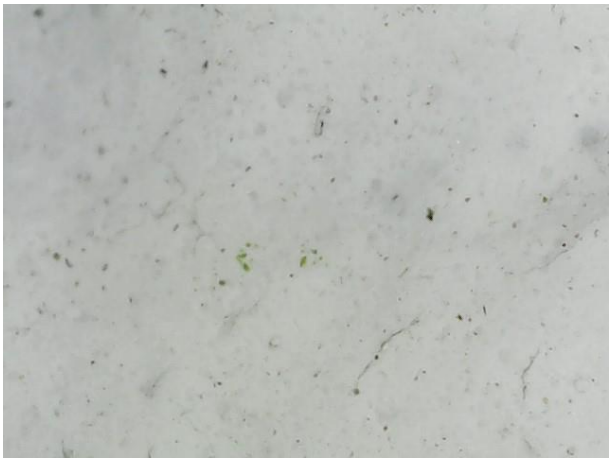

Figure 69: PK00_01 (reference)

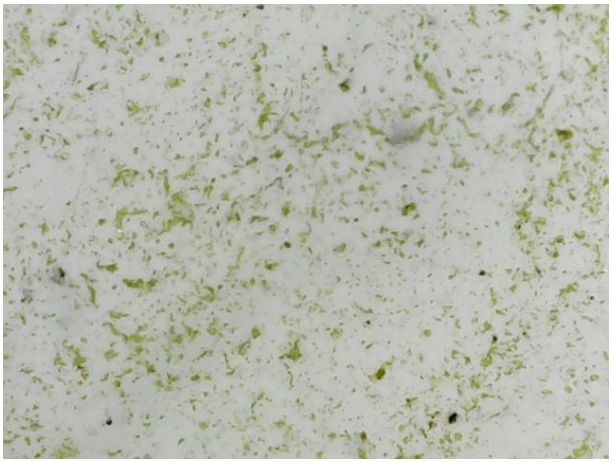

Figure 70: PK00_02 (reference)

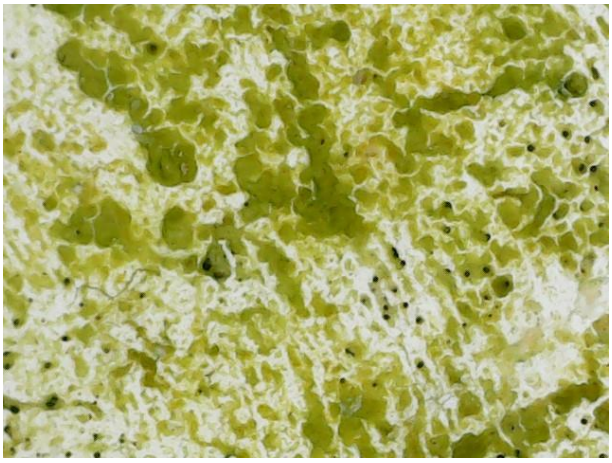

Figure 71: PK05_01

Figure 72: PK05_02

Figure 73: PK05_03

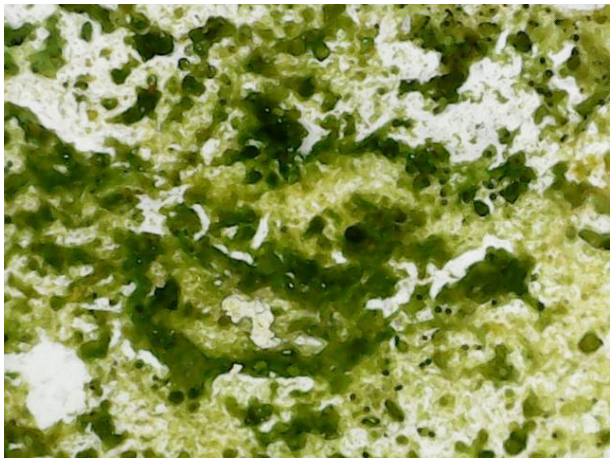

Figure 74: PK05_04

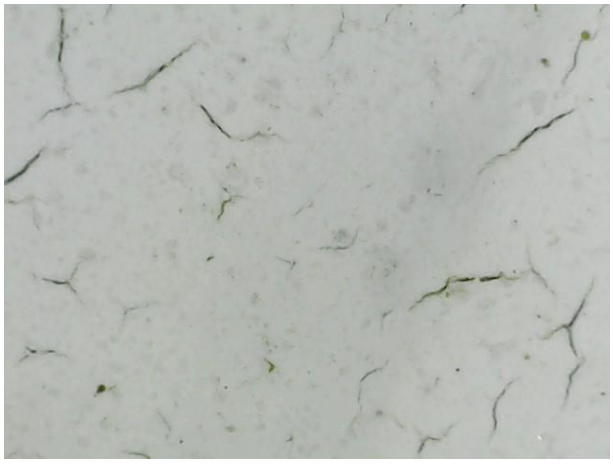

Figure 75: PK06_01 (with $ZnMoO_4$)

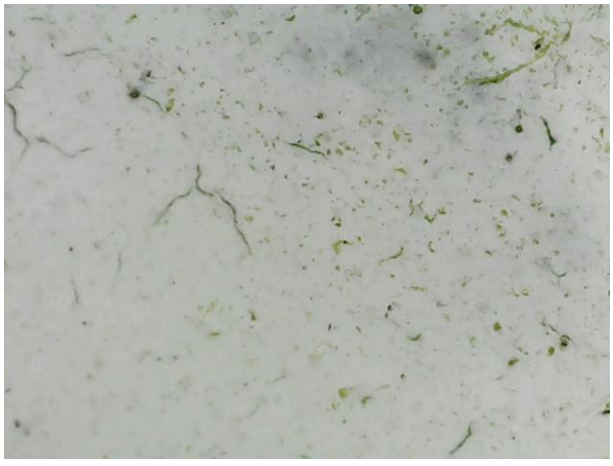

Figure 76:PK06_02 (with $ZnMoO_4$)

4.5.4. Development of surface pH

The first determination of the surface pH value was carried out on the test specimens before installation. The ELMETRON EPX-3 surface electrode was used in conjunction with the PCE 228 pH meter. The electrode was adjusted by means of three-point calibration using buffer solutions with a pH value of 4/7/10. In the further course of the outdoor weathering, the pH value was determined at a defined middle located measuring point 06 of each test specimen (Fig. 77). After applying 1 ml of distilled water to the test point and waiting for 1 minute, the electrode was placed on the drop of water. When the display reached a stable measured value, this was read off and noted. The external PT100 was placed in the water supply for temperature compensation.

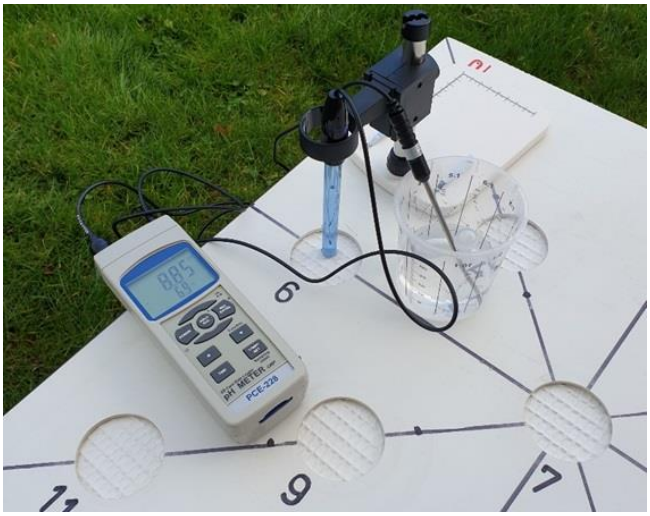

Figure 77: Sessile water drop at point PKXX06 at the template

Unfortunately, the electrode had a defect and could not be replaced due to supply difficulties during the coronavirus pandemic. The measurements were then discontinued. However, the first 19 months could be tracked, and the results are shown in Fig. 78.

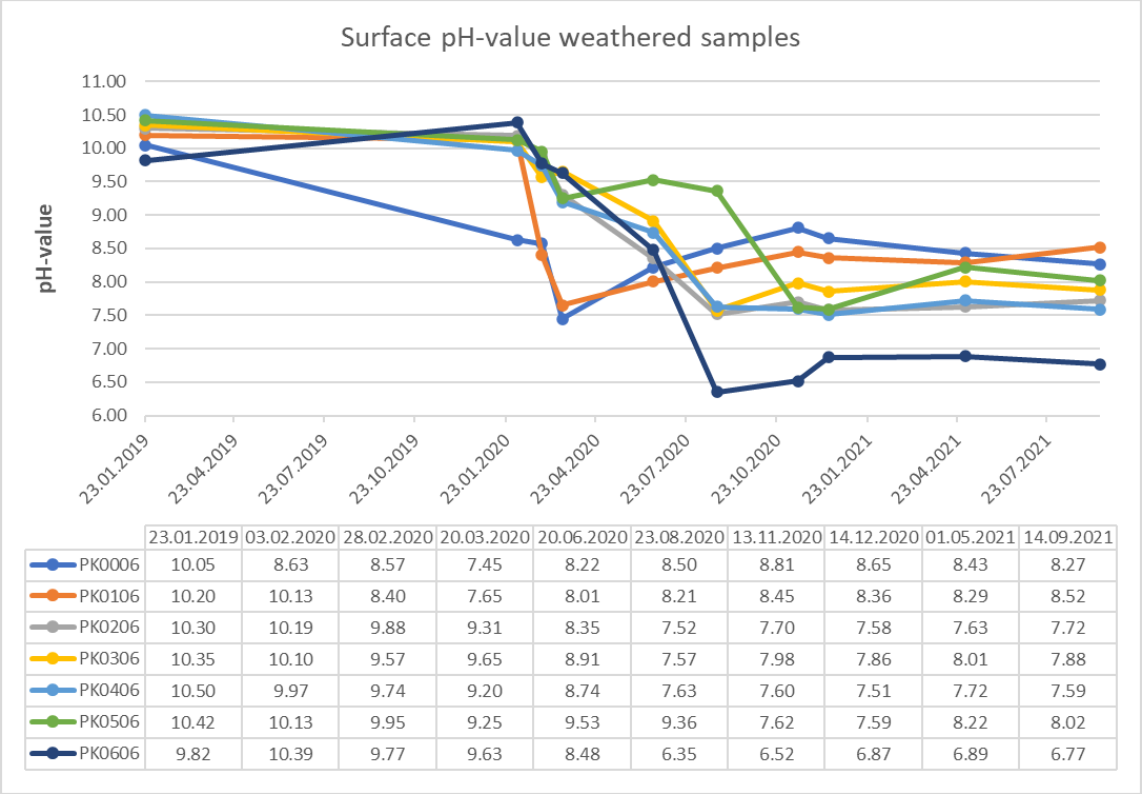

	23.01.2019	03.02.2020	28.02.2020	20.03.2020	20.06.2020	23.08.2020	13.11.2020	14.12.2020	01.05.2021	14.09.2021
PK0006	10.05	8.63	8.57	7.45	8.22	8.50	8.81	8.65	8.43	8.27
PK0106	10.20	10.13	8.40	7.65	8.01	8.21	8.45	8.36	8.29	8.52
PK0206	10.30	10.19	9.88	9.31	8.35	7.52	7.70	7.58	7.63	7.72
PK0306	10.35	10.10	9.57	9.65	8.91	7.57	7.98	7.86	8.01	7.88
PK0406	10.50	9.97	9.74	9.20	8.74	7.63	7.60	7.51	7.72	7.59
PK0506	10.42	10.13	9.95	9.25	9.53	9.36	7.62	7.59	8.22	8.02
PK0606	9.82	10.39	9.77	9.63	8.48	6.35	6.52	6.87	6.89	6.77

Figure 78: Surface pH while outdoor exposition

The initial high pH values are due to the formulation and consistent with the results of existing research [6]. After a start-up phase lasting several months, the measured values decreased to a level between 7.5 and 9.0 and remain there for the rest of the process measured. Only the sample with the functional filler zinc molybdate showed a significantly lower pH level of 6-7 (Fig. 78). Despite the presence of zinc molybdate, PK06 only shows a sharply falling pH value after a start-up period of 13 months. Presumably the filler is only released on the surface after a lead time and develops its proton-releasing effect, as the pH values are all at an alkaline level in the first year.

4.5.5. Reflectivity as sum-parameter

The visual change in component surfaces can be traced back to various factors. In addition to the effects of algae colonization discussed in this paper, dust particles from traffic, industry and agriculture are of particular importance [107]. However, biogenic organisms such as fungi also contribute to the discoloration of facades through their light protection pigments [100]. All these individual factors lead to an overall impression of the surface, which can be evaluated in the form of a sum parameter based on the decreasing reflectivity.

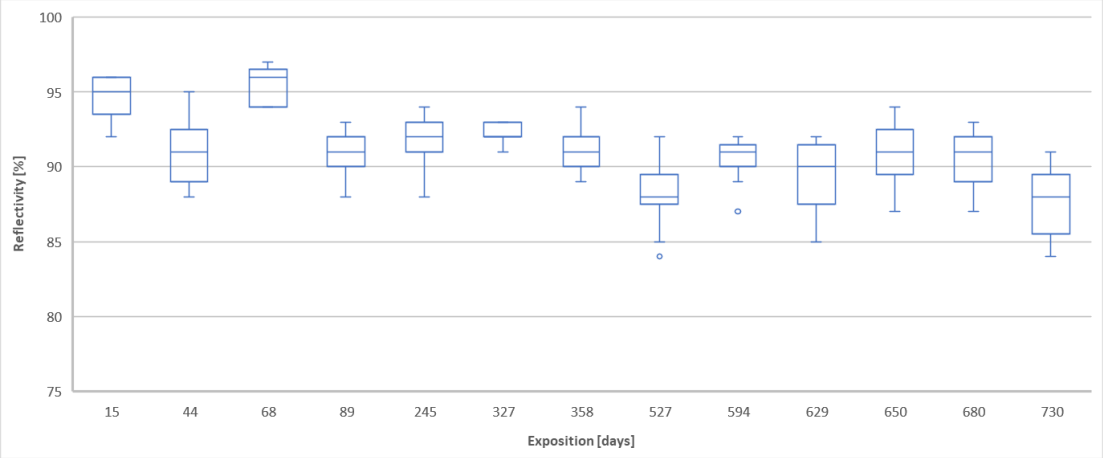

Figure 79: Boxplot reflectivity of PK00 after 730 days of weathering

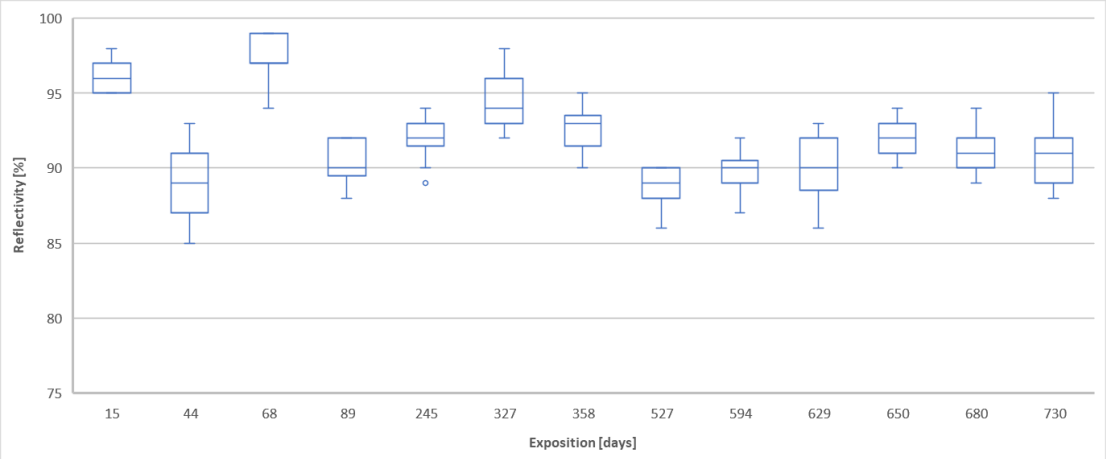

Figure 80: Boxplot reflectivity of PK01

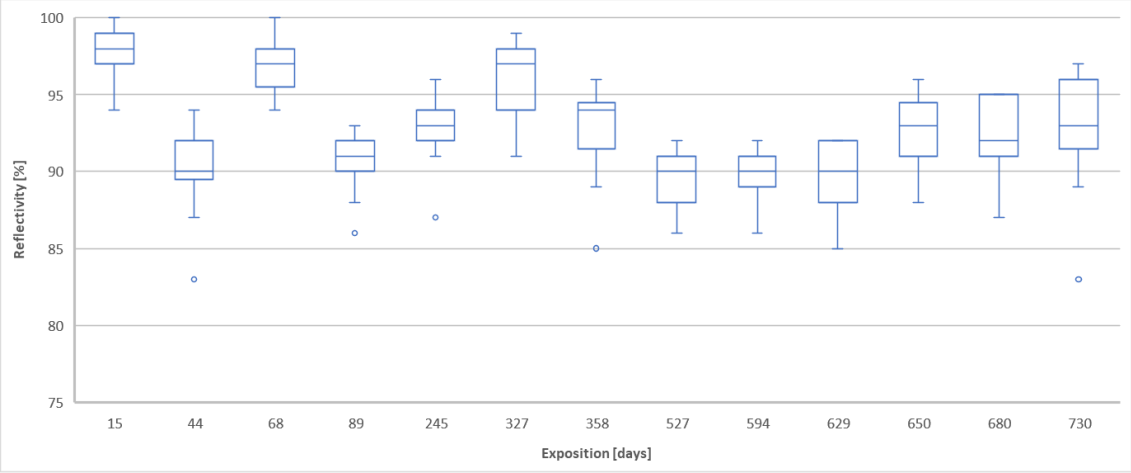

Figure 81: Boxplot reflectivity of PK02

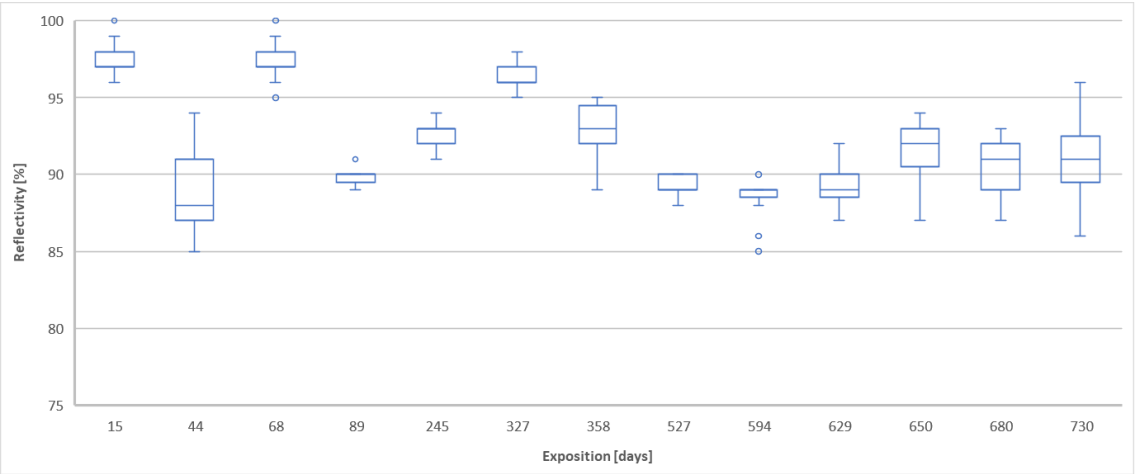

Figure 82: Boxplot reflectivity of PK03

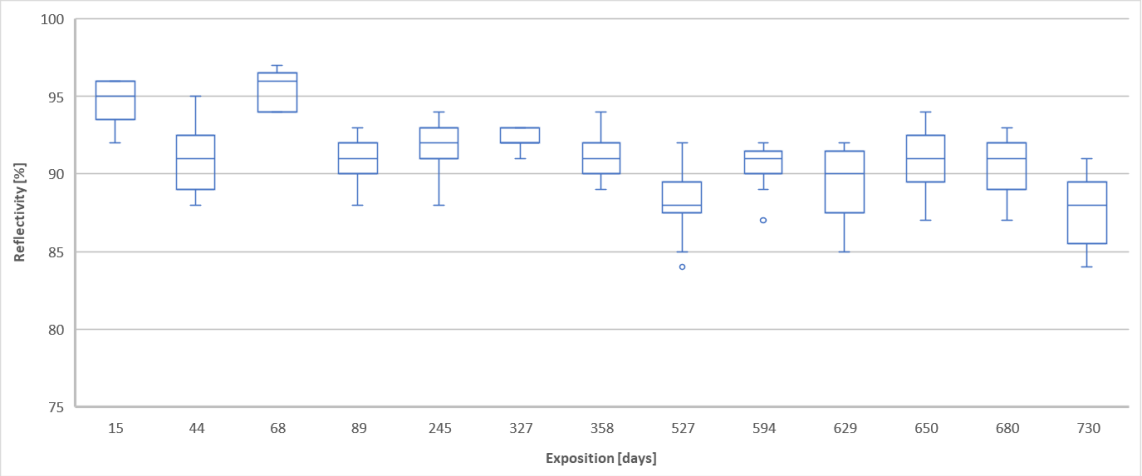

Figure 83: Boxplot reflectivity of PK04

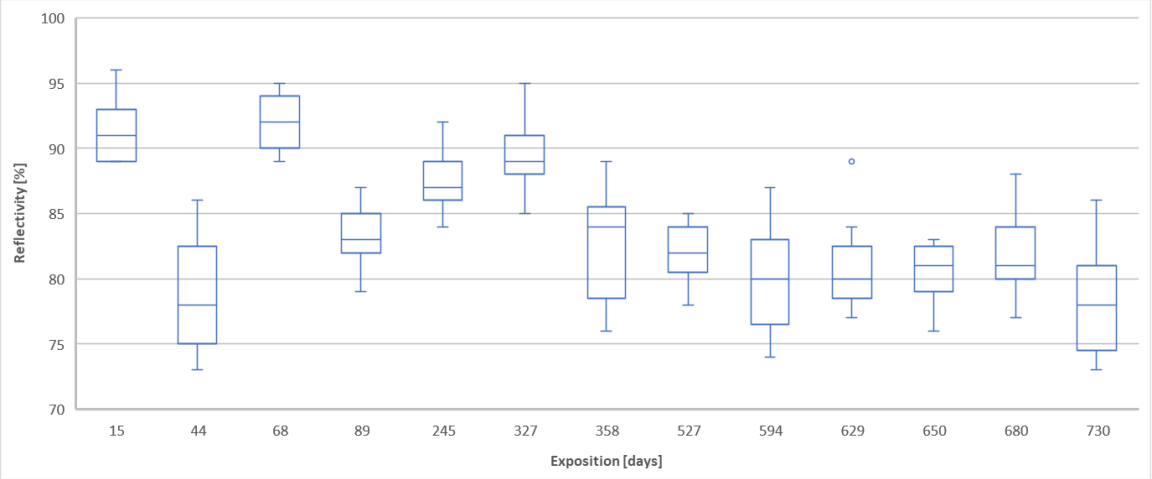

Figure 84: Boxplot reflectivity of PK05 (highest content of Mg-based filler)

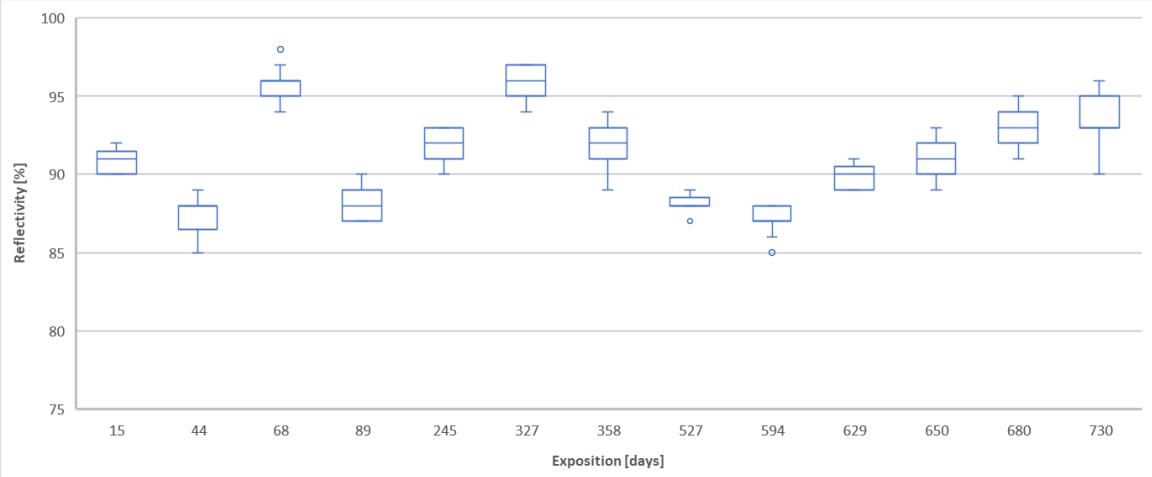

Figure 85: Boxplot reflectivity of PK06 (with functional filler ZnMoO4)

The sample with the highest content of magnesium-containing fillers (PK05) also shows the greatest decrease in reflectivity due to the strongest algae growth (Fig. 84). The sample with the functional filler zinc molybdate shows fluctuating values over time, but after 730 days there is no detectable loss of reflectivity (Fig. 85).

4.5.5.1. Statistical data set analysis – post-hoc Tukey HSD test

Statistical evaluation was carried out according to the Tukey Honestly Significant difference (HSD) test [108]. The p-value corresponding to the F-statistic of one-way-ANOVA is lower than 0.05, suggesting that one or more treatments are significantly different (Tab. 7). The multiple comparison test followed the one-way analysis of variance to determine significant differences between group means. The data set analysed based on total cell numbers measured with BenthoTorch® fluorometer. The post-hoc Tukey test identified 7 out of 21 treatment pairs which are significantly different from each other (Tab. 7).

Table 7: Results of statistical analysis of treatment pairs.

Treatment pair	Tukey HSD Q statistic	Tukey HSD p-value
PK00(A)/PK05(F)	14.1077	<0.01
PK01(B)/PK05(F)	15.3274	<1.01
PK02(C)/PK05(F)	14.8496	<0.01
PK03(D)/PK05(F)	12.0834	<0.01
PK04(E)/PK05(F)	11.2919	<0.01
PK04(E)/PK06(G)	4.7283	<0.05
PK06(G)/PK05(F)	16.0441	<0.01

Descriptive statistics of your k=7 independent treatments:

Treatment →	A	B	C	D	E	F	G	Pooled Total
observations N	169	169	169	169	168	169	169	1182
sum $\sum x_i$	2.1800	1.2100	1.5900	3.7900	4.3800	13.4000	0.6400	27.1900
mean $\bar{x}$	0.0129	0.0072	0.0094	0.0224	0.0261	0.0793	0.0038	0.0230
sum of squares $\sum x_i^2$	0.2298	0.0799	0.1371	0.5395	0.6782	4.0180	0.0310	5.7135
sample variance s^2	0.0012	0.0004	0.0007	0.0027	0.0034	0.0176	0.0002	0.0043
sample std. dev. s	0.0346	0.0206	0.0270	0.0520	0.0581	0.1326	0.0130	0.0656
std. dev. of mean $SE_{\bar{x}}$	0.0027	0.0016	0.0021	0.0040	0.0045	0.0102	0.0010	0.0019

One-way ANOVA of your k=7 independent treatments:

source	sum of squares SS	degrees of freedom ν	mean square MS	F statistic	p-value
treatment	0.6904	6	0.1151	30.7434	1.1102e-16
error	4.3977	1175	0.0037		
total	5.0880	1181			

Figure 86: Results window of statistical analysis software tool [108]

5. Results and discussion

730 days of outdoor exposure revealed a significant difference in the algal susceptibility between the identical constructed samples with different coating recipes. The fluorescence-measured sum of algal biomass [cells/mm²] via BenthoTorch® is positive related (R^2 = 0.97) to the magnesium content of applied paint coatings. The cross-check according to the visual evaluation via Standard DIN EN 16492:2014 (R^2 = 0.92) and the digital image area analysis (R^2 = 0.96) ensured the results. The coefficients of determination between results of evaluation methods (*Table 2*) were BTo [cells/mm²] vs. DIN EN 16492 sum (R^2 = 0.95) and BTo [cells/mm²] vs. ImageJ area [%] (R^2 =0.97). After comparing the test methods, the correlation of the determined algal biomass to the magnesium content of the coatings was performed and reveals the strong relationship between algal biomass and magnesium content of painted samples.

The very first infestation was detected on samples PK03-PK05 after only 9 months but did not persist. The test specimens PK00-PK02 only showed the first fluorescence signals of chlorophyll-a after 24 months and were still below the visual limit. After a start-up period of 12 months, permanent algal growth was observed on the sample with the highest Mg-based filler content (PK05), while the samples with a low filler content were significantly less colonized only after two years. The composition of the biofilm at all samples was identically dominated by green algae (92%) and cyanobacteria (6%), while diatoms (1%) played a subordinate role. The surface pH value of the reference (PK00) and the samples (PK01-PK05) were at a comparable level. The comparison with the magnesium-free reference sample PK00 proved to be difficult in retrospect, as the calcium carbonate used in the formulation contained accessory mineral traces of magnesium compounds. The differences in Mg-concentration and the statistical significance between the test specimens (PK01-PK04) and reference (PK00) were therefore weakened but sufficient.

The water-activated defence-strategy with zinc molybdate (PK06) was significantly able to limit the biomass within the experimental conditions and algal species involved. This sample showed the lowest cell counts during the weathering period of two years and no measurable change in surface reflectivity. Surprisingly, the expected lower pH level due to zinc molybdate was only achieved after the start-up period of 12 months and remained stable until the 19th month. The measurement was then terminated due to a defective electrode.

Current research results confirm the pH-depending bioadsorption of algae, which is determined by the chemical composition of the building material surface. The brick stone showed no measurable algal colonization after 35d-incubation and had an adsorption rate of 0% in the suspension test at pH 10.8/10°C. The sand-limestone showed the strongest algal growth after incubation as well as the highest adsorption rate of 32,2% in the suspension test. The marble specimen shows the second strongest algal growth after incubation and an adsorption rate of 17,6%. The strong differences in algal growth could not be explained by the physical parameters of water uptake as they were compensated by water saturation. Transferring the principle of algae harvesting (tested inoculum) to the tested building material surfaces, the initial settlement of algae can be explained by the presence of necessary mineral components, as well as the alkaline pH-value. Bioadsorption of algae is driven by Ca- and Mg-compounds that interact with the cell wall-located carboxylic groups of algae. All EDX-tested wall materials contained Ca and Mg-compounds, but as known from the literature in various amounts and crystalline modifications. The high firing temperature (>1000°C) of brick may lead to very low surface-availability of Ca and Mg due to sintering effects and no detectable algal colonization in both laboratory tests. The production process of sand-limestone (hot steam at 200°C) maintains the chemical structure of the components and their surface availability.

Algal growth occurs if enough cells are enriched on the component surface. Both play an important role in bioadsorption of algae and are essential nutrients for further growth. Understanding the adsorption process provides important information for the development of biocide-free defence systems and sustainable designed façades.

Construction planner and designer are calculating with a wide variety of load cases. In terms of future façade-projects the assessment of final coatings can be improved based on these results. The simultaneous combination of environmentally hazardous biocides with algae-prone magnesium-based fillers in façade paints is not advisable. Especially since the organic biocides have only a temporary effect and the algae-prone fillers reach the surface during the aging process to develop the effects revealed in this research work. Understanding these interactions provides important information and methods on the reduction of organic biocides in product development. These research results contribute to more sustainable designed true green façades without killing future algal populations and may support the development of bio-receptive building materials.

Availability of water is one of the most important factors for algal colonization on building materials. To avoid condensation effects on façades, complex measures and methods have been developed. Instead of elaborately avoiding the dew water, this should become the subject of a defence strategy. The algal growth was determined by chlorophyll-fluorescence spectrometer over a period of 730 days of free-weathering. In addition, the surface reflection behaviour at 700 nm was determined, which has a strong correlation to the brightness reference value and is also an indicator for the discoloration. Compared with six other coating recipes without defence-strategy, the treated sample showed no detectable algal biomass within the detection limit of 0,15µg/cm² Chlorophyll-a of the measuring device. The averaged reflectivity value (n=130) changed lowermost and no visual recognizable algal colonization could be observed.

The connection between magnesium-containing fillers and microbial colonization of façade coatings is an important result of the present work. On one hand magnesium is an important nutrient for photosynthetic microorganisms (core-ion of Chlorophyll) and on the other hand it is contained in many mineral building materials. Some of these mineral’s origin from prehistoric sediments and, due to the mining of these deposits, reach today's building products. Talc and dolomite are just two examples of such compounds, these two are among the top 10 fillers for façade paints worldwide. Fly ash from coal-fired power plants dominates the

list of possible additives for cement-bound building materials. The mineral composition of all these extenders correspond exactly to the needs of future microorganisms on façades due to its prehistoric vegetable or microbial origin. Water is the basis for all life, even on façades. In combination with the hydrophobic organic binders and its thermal decoupling from the building, an excellent substrate for the development of microorganisms is created. Cyanobacteria, algae, and fungi open these habitats through intelligent cooperation. Without magnesium there is no photosynthesis. The bioavailability of the essential magnesium sources in the building materials depends on their manufacturing conditions. Different materials like concrete, brick and lime sandstones were analysed by non-destructive fluorescence spectroscopy and EDX. For this purpose, a method using a mobile fluorescence spectrometer was developed from water research for use on façades. The device differentiates between green algae, cyanobacteria, and diatoms. Additional information on the microbial colonization of building materials is thus available.

6. Conclusion to the Theses

Thesis 1- Applicability of a benthic detection device for the determination of algal biomass on building material surfaces

Using the mobile BenthoTorch® fluorescence spectrometer, I have quantified phototrophic microorganisms on building material surfaces and differentiated between green algae, cyanobacteria, and diatoms without the need for complex microbiological methods and expertise. I have thus also proven that water films on building materials can be regarded as temporary aquatic habitats, as favoured by benthic biofilms. I have proven through laboratory and field tests that the BenthoTorch® is suitable as a sensor for the non-destructive area-related determination of cell counts and chlorophyll concentrations on moist building material surfaces. I was the first to develop a new algae suspension test using the BenthoTorch® sensor to determine the pH-depending bioadsorption of algae cells on building material surfaces in real time. I have extended the 700 nm LED included in the spectrometer for background compensation to determine the light reference value, which allows the assessment of surface greying independent of biofilm vegetation in one step of the measurement. The results obtained were directly interpretable and I demonstrated that the mobile fluorescence spectrometer is suitable for the measurement requirements. Based on these results, I recommend the assessment of surface disfigurements caused by algae and fungi in accordance with DIN EN 16492:2014 by using BenthoTorch®.

Related publications: [53, 54]

Thesis 2 - Bioadsorption as the initial step in the process of algal colonisation of building materials

To determine the adsorption behaviour of algae cells on building material surfaces, I was the first to develop a real-time suspension test that determines the area-related cell count. Due to the special experimental set-up, I was able to separate the physical deposition from the pure chemical interaction of the functional groups of the algal cells. Using a natural algae culture, I proved that cell adsorption on building materials is dependent on the pH value and can be influenced by targeted manipulation. I have revealed that the measured values of the BenthoTorch® sensor can be used directly in the measurement set-up for the volume- and area-related conversion. After cross-check with 35 days of incubation test, I confirmed that the building materials without measurable cell adsorption in the suspension test also showed no measurable colonisation, while the samples with maximum colonisation also had the highest adsorption values.

Related publications: [55]

Thesis 3 - Magnesium-containing fillers increase the formation of algal biofilms on façade coatings

After two years of outdoor exposure, I revealed a significant difference in the algal susceptibility between identically constructed and mounted samples. Using the BenthoTorch® fluorescence spectrometer, I proved a positive related (R^2=0,97) sum of algal biomass to the magnesium content of the applied coating. Comparing the standard DIN EN 16492:2014 (R^2=0.92), the digital image analysis (R^2=0.96), and statistical HSD analysis, I ensured the results. Based on the experimental set-up, I secured condensation water as the only source of moisture and confirmed that these quantities are sufficient for algae colonisation and can’t be avoided. Based on data analysis of air quality annual reports and coating recipes, I conclude that magnesium-containing fillers are a more important source of essential nutrients for phototrophic microorganisms than airborne dust. From the presence of lichens only on PK06, I conclude that in addition to the triggered accumulation of algae cells due to the highest content of

Mg-based fillers, vegetative reproduction has also taken place. In the outdoor weathering experiment, I demonstrated that Mg-based fillers act as harvesting aids in the short term and as a source of nutrients in the long term. I have demonstrated that the change in the light reflectance value of the test specimens is suitable as a sum parameter for the evaluation of increasing biogenic and non-biogenic pollution.

Related publications: [52, 54]

Thesis 4 - Efficacy of an algae defence strategy by water-activated functional filler

After 730 days of outdoor weathering and statistical HSD analysis, I proved the effectiveness of a dew water-activated functional filler against airborne algal biofilm formation. Equipping an acrylate-based emulsion paint with zinc molybdate, I demonstrated a 73% reduction of algal biofilm compared to the identical reference without functional filler. Using a surface electrode, I proved that the functional filler significantly lowered the pH level by 1.2 units on the logarithmic pH scale. I proved the absence of visible biofilm accumulation by fluorescence detection and non-biogenic disfigurements by 700nm-light-reflectance measurements using the BenthoTorch® spectrometer. Since condensation water was the only source of water, I proved the activation of the functional filler in this way. Instead of elaborately avoiding the dew water, I recommend this non-toxic control strategy without killing future algal populations as contribution to the design of sustainable façades.

Related publications: [54,56]

7. Appendix

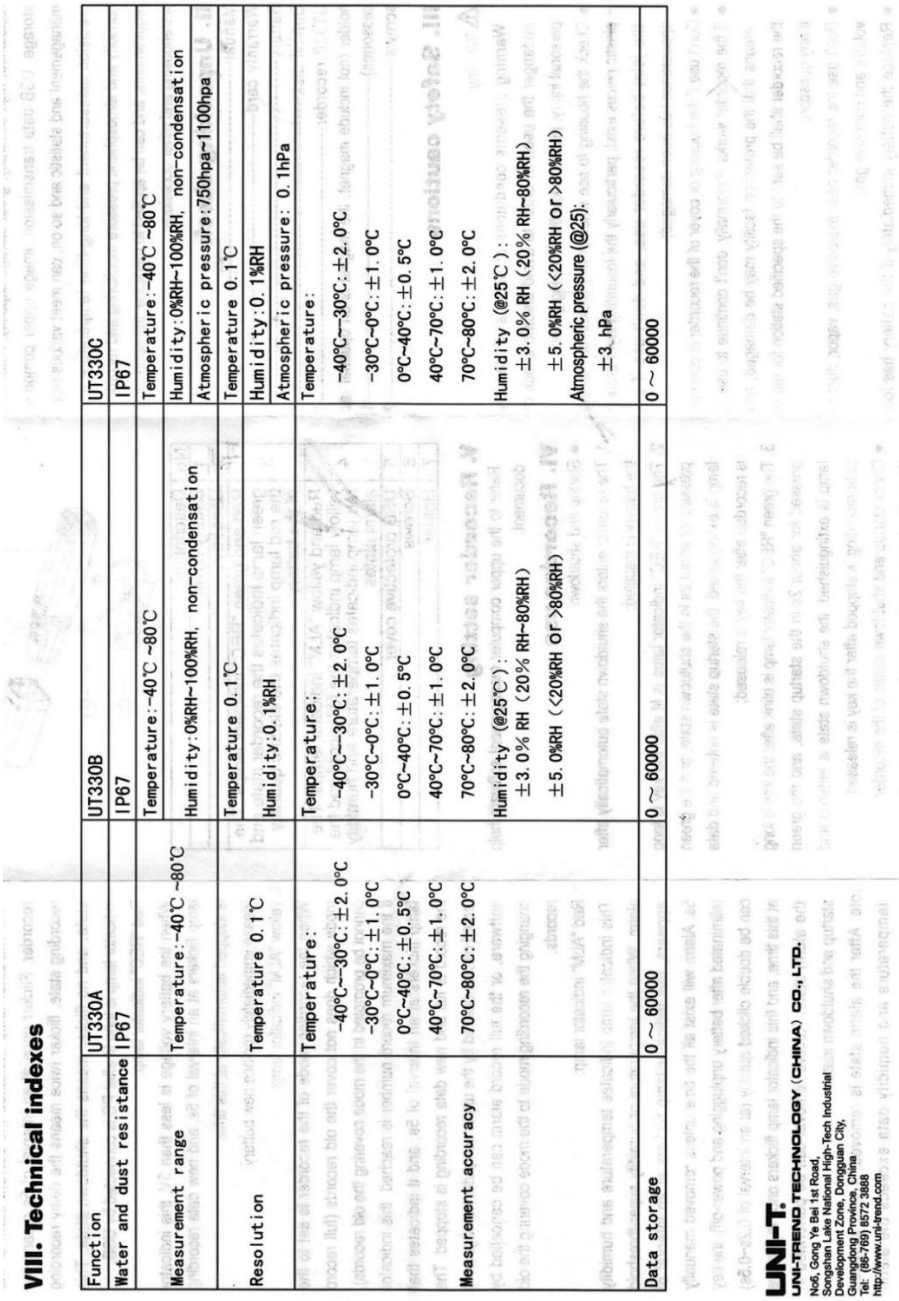

VIII. Technical indexes

Function	UT330A	UT330B	UT330C
Water and dust resistance	IP67	IP67	IP67
Measurement range	Temperature:-40℃ ~80℃	Temperature:-40℃ ~80℃	Temperature:-40℃ ~80℃
		Humidity:0%RH~100%RH, non-condensation	Humidity:0%RH~100%RH, non-condensation
			Atmospheric pressure:750hpa~1100hpa
Resolution	Temperature 0.1℃	Temperature 0.1℃	Temperature 0.1℃
		Humidity:0.1%RH	Humidity:0.1%RH
			Atmospheric pressure: 0.1hPa
Measurement accuracy	Temperature: -40℃~-30℃:±2.0℃ -30℃~0℃:±1.0℃ 0℃~40℃:±0.5℃ 40℃~70℃:±1.0℃ 70℃~80℃:±2.0℃	Temperature: -40℃~-30℃:±2.0℃ -30℃~0℃:±1.0℃ 0℃~40℃:±0.5℃ 40℃~70℃:±1.0℃ 70℃~80℃:±2.0℃ Humidity (@25℃): ±3.0% RH (20% RH~80%RH) ±5.0%RH (<20%RH or >80%RH)	Temperature: -40℃~-30℃:±2.0℃ -30℃~0℃:±1.0℃ 0℃~40℃:±0.5℃ 40℃~70℃:±1.0℃ 70℃~80℃:±2.0℃ Humidity (@25℃): ±3.0% RH (20% RH~80%RH) ±5.0%RH (<20%RH or >80%RH) Atmospheric pressure (@25): ±3 hPa
Data storage	0 ~ 60000	0 ~ 60000	0 ~ 60000

UNI-T.
UNI-TREND TECHNOLOGY (CHINA) CO., LTD.
No6, Gong Ye Bei 1st Road,
Songshan Lake National High-Tech Industrial
Development Zone, Dongguan City,
Guangdong Province, China
Tel: (86-769) 8572 3888
http://www.uni-trend.com

Figure 87: Technical datasheet UNI-T data recorder for free weathering test

Figure 88: Construction board for sample preparation free weathering test

Probe 02 – A

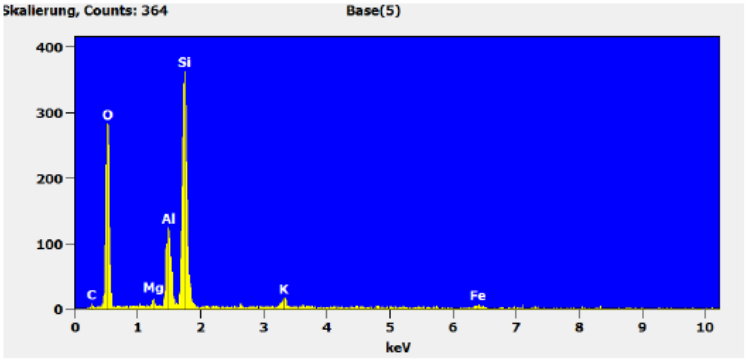

Linie	Gew.-%	Atom-%
C K	3.40	5.61
O K	52.15	64.62
Mg K	0.64	0.52
Al K	8.93	6.56
Si K	28.47	20.10
K K	2.05	1.04
Fe K	4.35	1.55

Figure 89: EDX spectra sample 02-A

Probe 02 – B

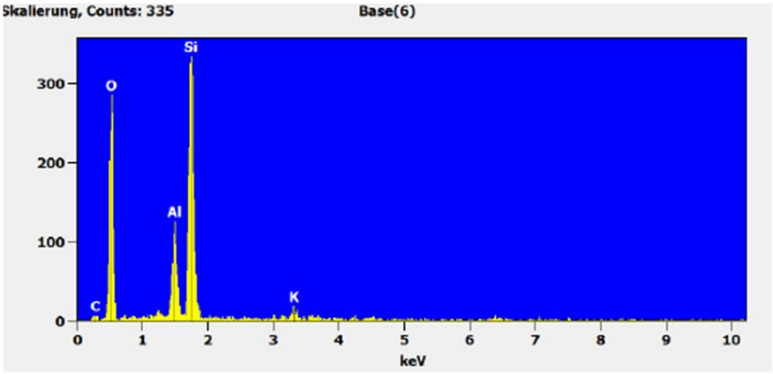

Linie	Gew.-%	Atom-%
C K	4.99	7.89
O K	54.94	65.17
Al K	8.62	6.06
Si K	29.46	19.91
K K	2.00	0.97

Figure 90: EDX spectra sample 02-B

Probe 02 – C

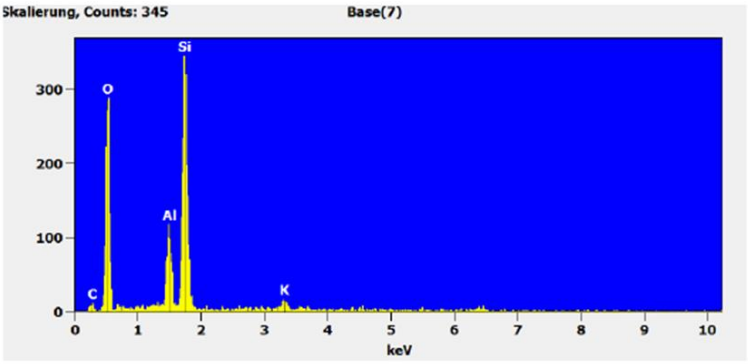

Linie	Gew.-%	Atom-%
C K	6.93	10.68
O K	56.55	65.39
Al K	7.55	5.17
Si K	27.21	17.93
K K	1.76	0.83

Figure 91: EDX spectra sample 02-C

Probe 03 – A

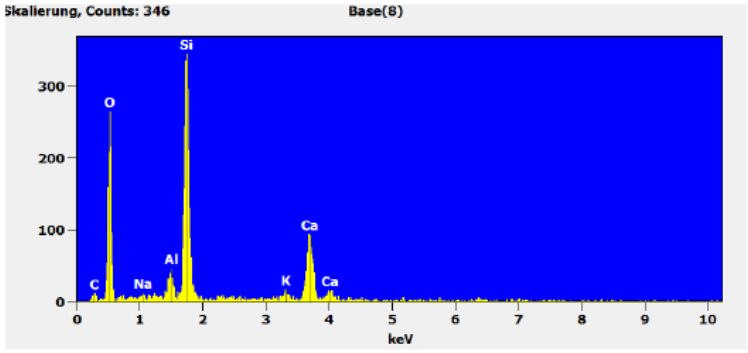

Linie	Gew.-%	Atom-%
C K	5.91	9.79
O K	50.87	63.18
Na K	0.46	0.40
Al K	2.24	1.65
Si K	23.06	16.31
K K	1.44	0.73
Ca K	16.02	7.94

Figure 92: EDX spectra sample 03-A

Probe 03 – B

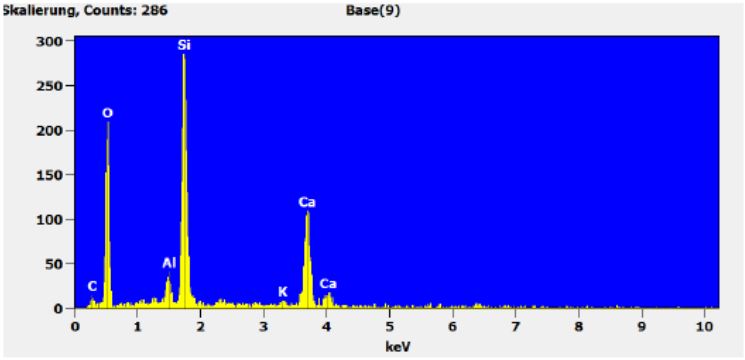

Linie	Gew.-%	Atom-%
C K	6.01	10.00
O K	50.50	63.12
Al K	2.01	1.49
Si K	21.99	15.66
K K	0.66	0.34
Ca K	18.84	9.40

Figure 93: EDX spectra sample 03-B

Probe 03 – C

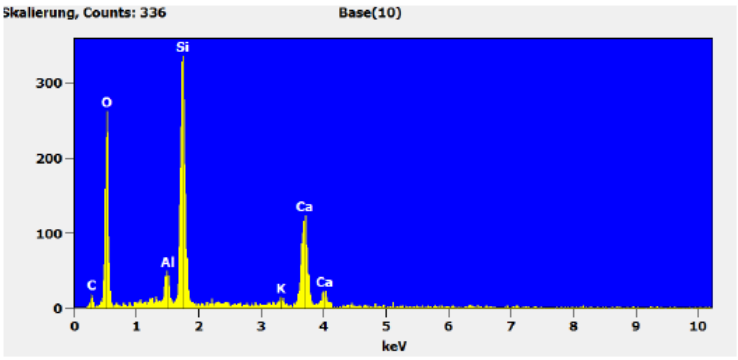

Linie	Gew.-%	Atom-%
C K	6.14	10.21
O K	50.42	62.99
Al K	2.58	1.91
Si K	21.14	15.05
K K	0.92	0.47
Ca K	18.79	9.37

Figure 94: EDX spectra sample 03-C

Probe 04 – A

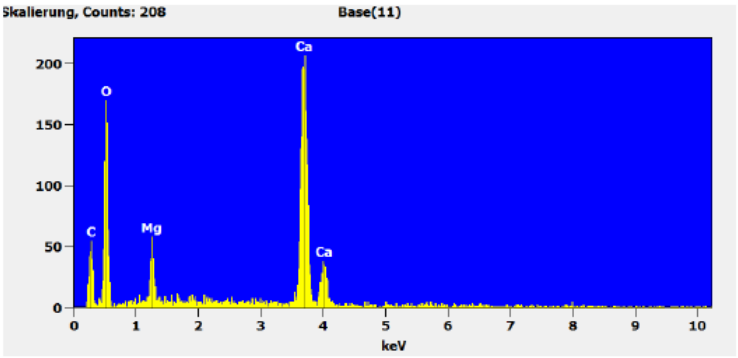

Linie	Gew.-%	Atom-%
C K	11.38	18.97
O K	47.53	59.48
Mg K	3.13	2.58
Ca K	37.96	18.97

Figure 95: EDX spectra sample 04-A

Probe 04 – B

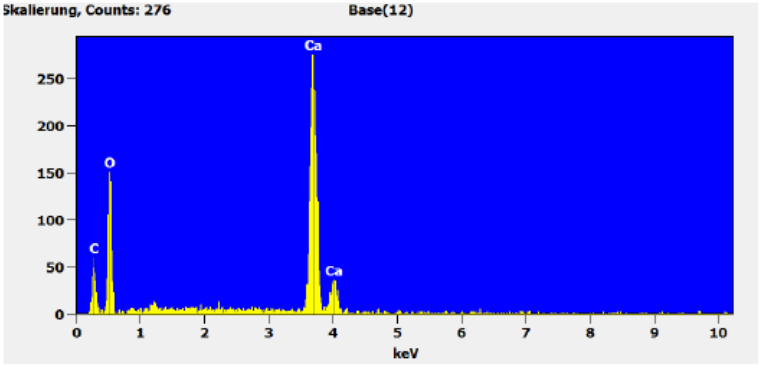

Linie	Gew.-%	Atom-%
C K	9.64	17.02
O K	44.13	58.51
Ca K	46.23	24.47

Figure 96: EDX spectra sample 04-B

Probe 04 – C

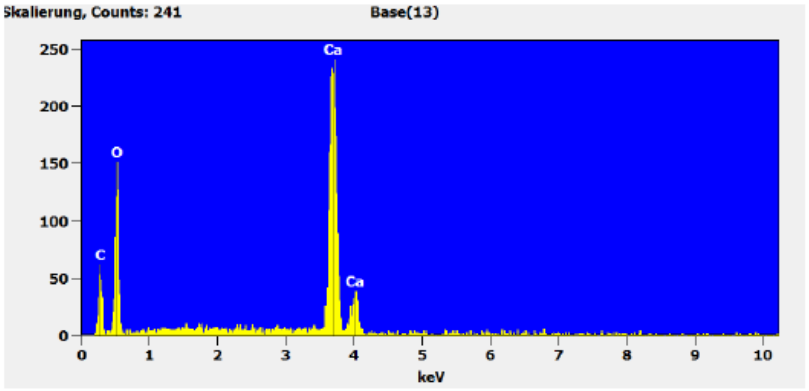

Linie	Gew.-%	Atom-%
C K	10.28	17.87
O K	45.17	58.93
Ca K	44.55	23.20

Figure 97: EDX spectra sample 04-C

Probe 05 – A

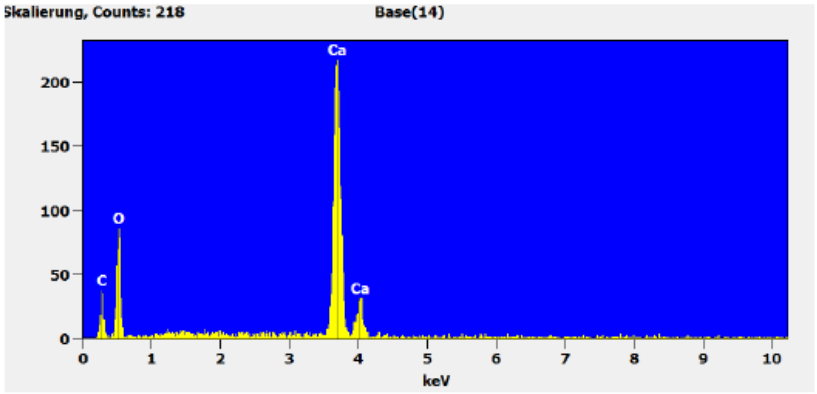

Linie	Gew.-%	Atom-%
C K	7.57	14.11
O K	40.79	57.06
Ca K	51.64	28.83

Figure 98: EDX spectra sample 05-A

Probe 05 – B

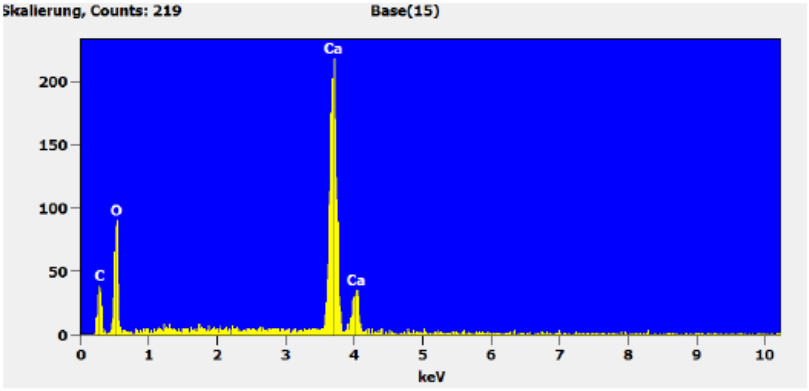

Linie	Gew.-%	Atom-%
C K	9.74	17.16
O K	44.30	58.58
Ca K	45.96	24.26

Figure 99: EDX spectra sample 05-B

Probe 05 – C

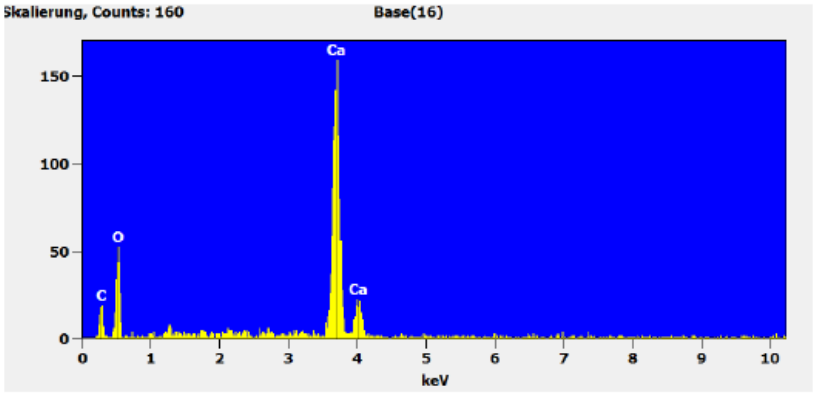

Linie	Gew.-%	Atom-%
C K	7.04	13.31
O K	39.93	56.66
Ca K	53.02	30.03

Figure 100: EDX spectra sample 05-C

Probe 06 – A

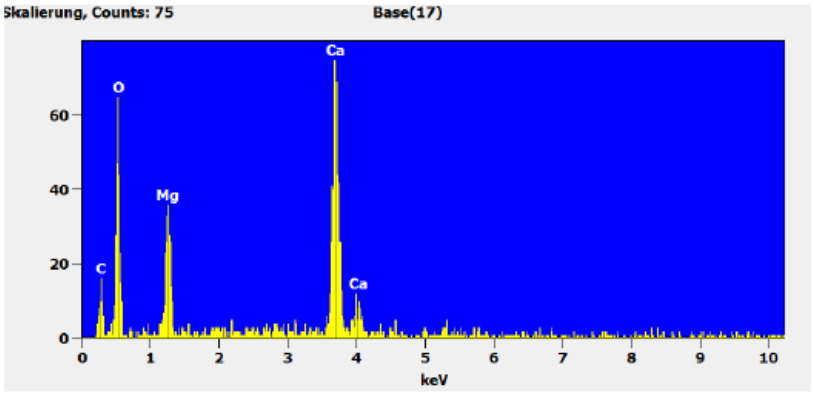

Linie	Gew.-%	Atom-%
C K	9.72	16.41
O K	45.95	58.20
Mg K	9.10	7.59
Ca K	35.22	17.81

Figure 101: EDX spectra sample 06-A

Probe 06 – B

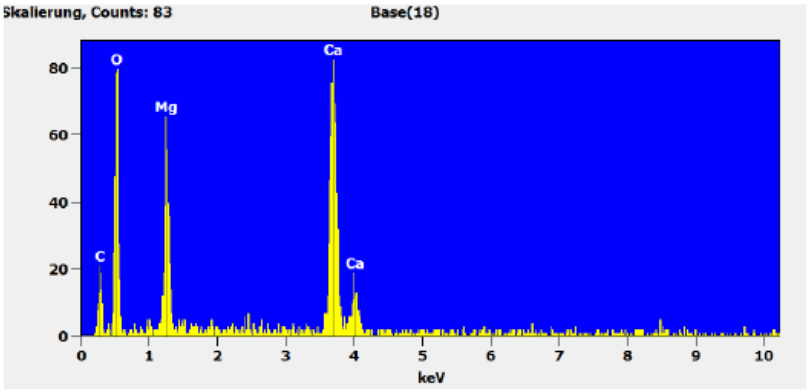

Linie	Gew.-%	Atom-%
C K	10.51	17.32
O K	47.41	58.66
Mg K	10.07	8.20
Ca K	32.01	15.81

Figure 102: EDX spectra sample 06-B

Probe 06 – C

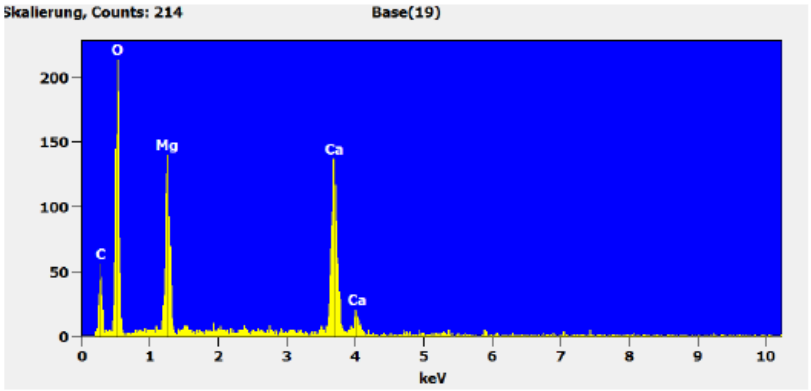

Linie	Gew.-%	Atom-%
C K	13.67	20.86
O K	52.75	60.43
Mg K	11.32	8.53
Ca K	22.27	10.18

Figure 103: EDX spectra sample 06-C

Probe 07 – A

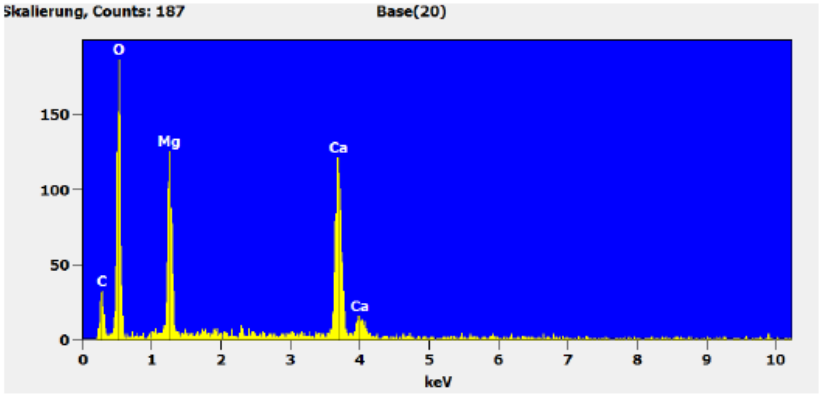

Linie	Gew.-%	Atom-%
C K	6.90	12.07
O K	42.64	56.04
Mg K	15.90	13.76
Ca K	34.56	18.13

Figure 104: EDX spectra sample 07-A

Probe 07 – B

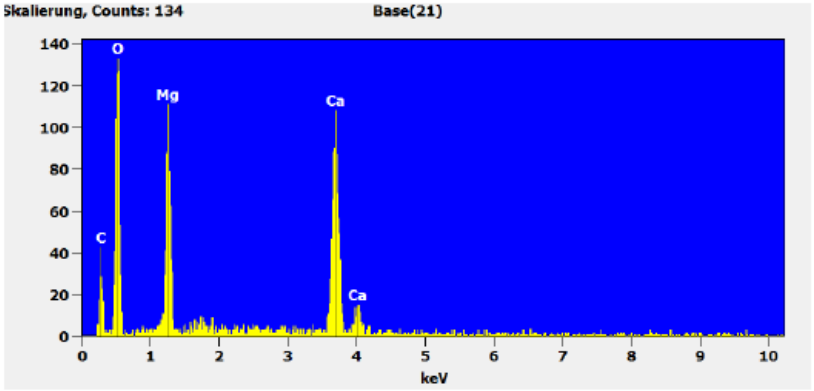

Linie	Gew.-%	Atom-%
C K	12.32	19.37
O K	50.58	59.69
Mg K	11.33	8.80
Ca K	25.77	12.14

Figure 105: EDX spectra sample 07-B

Probe 07 – C

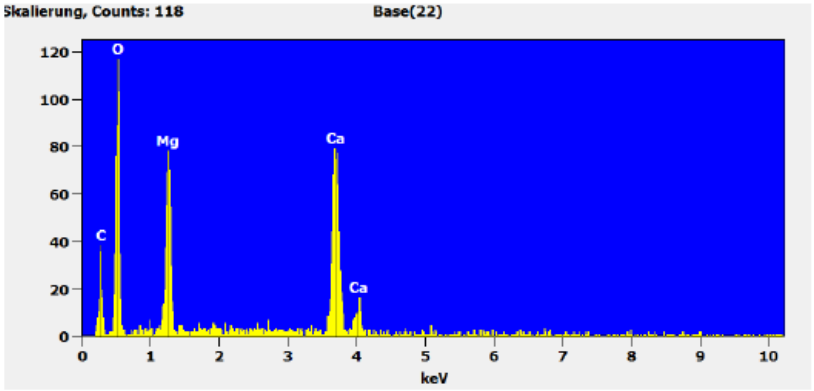

Linie	Gew.-%	Atom-%
C K	12.95	20.13
O K	51.48	60.06
Mg K	10.75	8.26
Ca K	24.82	11.56

Figure 106: EDX spectra sample 07-C

Probe 08 – A

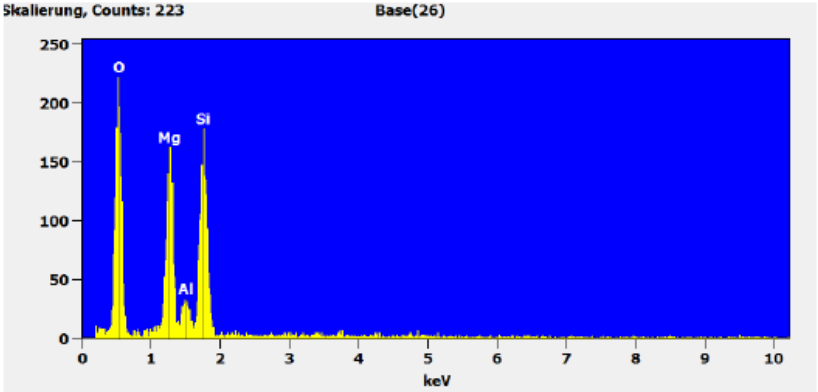

Linie	Gew.-%	Atom-%
O K	48.10	60.43
Mg K	20.62	17.05
Al K	4.48	3.34
Si K	26.80	19.18

Figure 107: EDX spectra sample 08-A

Probe 08 – B

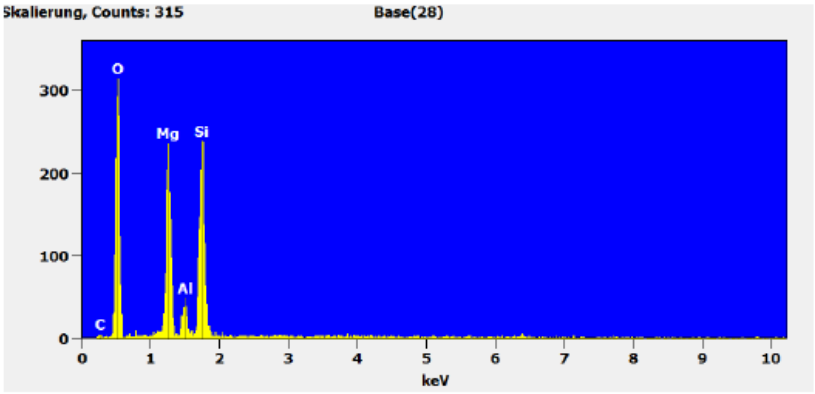

Linie	Gew.-%	Atom-%
C K	3.63	5.79
O K	51.39S	61.53
Mg K	17.93	14.13
Al K	3.65	2.59
Si K	23.41	15.97

Figure 108: EDX spectra sample 08-B

Probe 08 – C

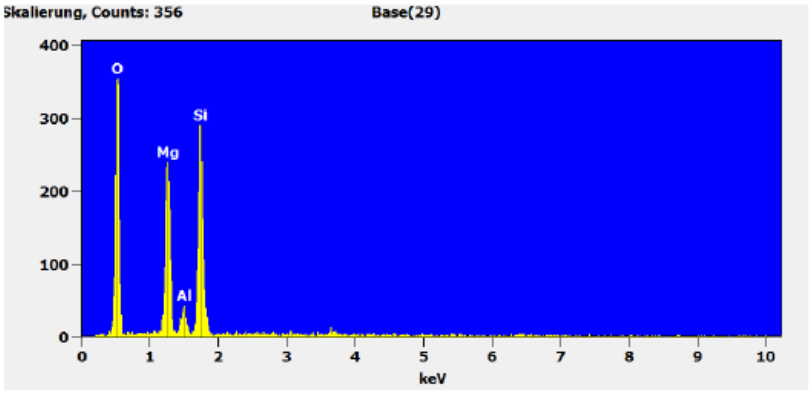

Linie	Gew.-%	Atom-%
O K	48.15	60.48
Mg K	20.73	17.14
Al K	3.84	2.86
Si K	27.29	19.53

Figure 109: EDX spectra sample 08-C

Probe 09 – A

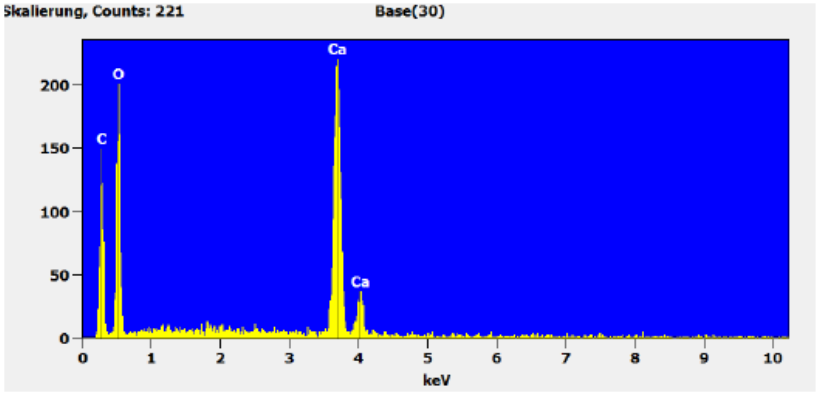

Linie	Gew.-%	Atom-%
C K	16.92	25.24
O K	55.91	62.62
Ca K	27.17	12.15

Figure 110: EDX spectra sample 09-A

Probe 09 – B

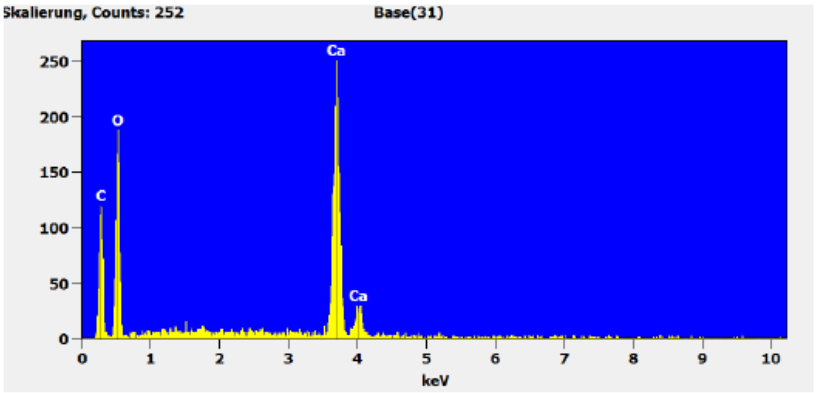

Linie	Gew.-%	Atom-%
C K	16.28	24.62
O K	54.89	62.31
Ca K	28.83	13.07

Figure 111: EDX spectra sample 09-B

Probe 09 – C

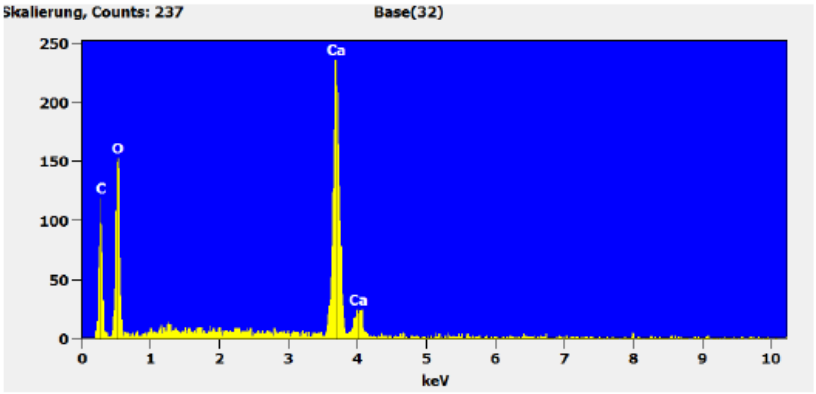

Linie	Gew.-%	Atom-%
C K	15.68	24.03
O K	53.92	62.02
Ca K	30.40	13.96

Figure 112: EDX spectra sample 09-C

Probe 10 – A

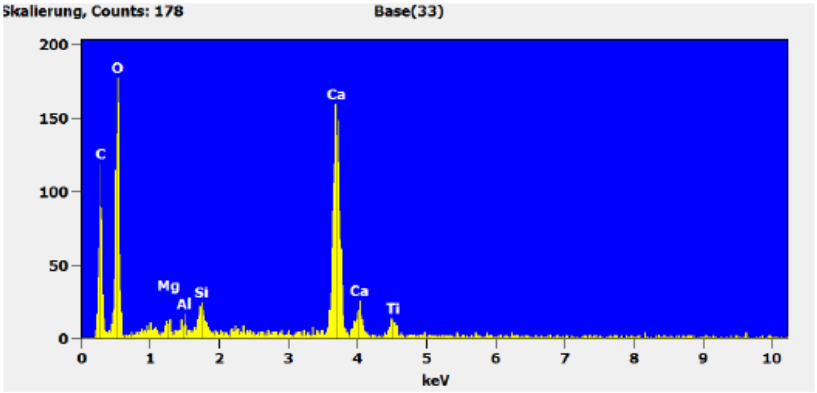

Linie	Gew.-%	Atom-%
C K	16.76	24.77
O K	57.11	63.37
Mg K	0.46	0.33
Al K	0.40	0.26
Si K	1.35	0.86
Ca K	21.28	9.43
Ti K	2.64	0.98

Figure 113: EDX spectra sample 10-A

Probe 10 – B

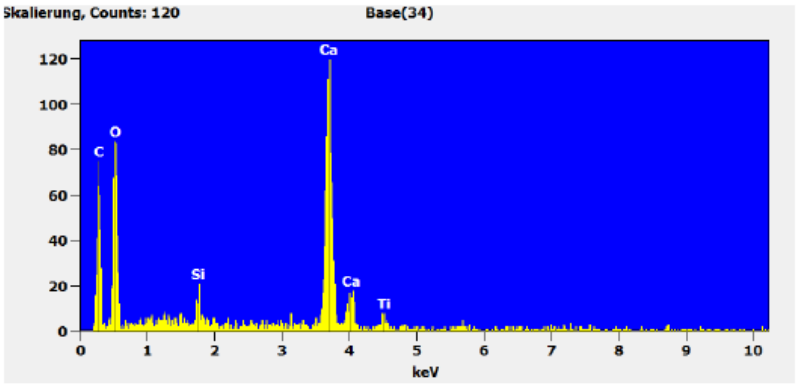

Linie	Gew.-%	Atom-%
C K	16.61	24.78
O K	56.28	63.05
Si K	0.95	0.61
Ca K	24.27	10.85
Ti K	1.90	0.71

Figure 114: EDX spectra sample 10-B

Probe 10 – C

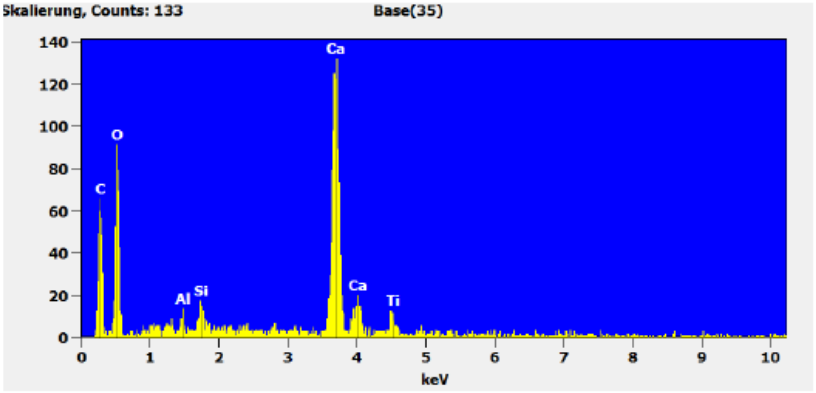

Linie	Gew.-%	Atom-%
C K	15.17	23.28
O K	54.35	62.60
Al K	0.32	0.22
Si K	1.22	0.80
Ca K	26.28	12.08
Ti K	2.66	1.02

Figure 115: EDX spectra sample 10-C

biological · biophysical · engineering

bbe
moldaenke

Preetzer Chaussee 177
D - 24222 Schwentinental

Telefon: +49 (0) 431/380 400
Telefax: +49 (0) 431/380 4010
e-mail: bbe@bbe-moldaenke.de
Internet: http://www.bbe-moldaenke.de

Chlorophyll Calibration Protocol

Operator: B. Franckowiak

Date: 03.12.19
Instrument: BenthoTorch
Serial No.: BTo-08-135
Software vers.: 3.31

Background Offset :

black	OK
grey	OK
white	OK

		Calibration		Check		
		Calibration conc. 1 Chl-a [µg/cm²]	Calibration conc. 2 Chl-a [µg/cm²]	Reference conc. Chl-a [µg/cm²]	Actual value conc. Chl-a [µg/cm²]	Deviation max =5% [%]
Green Algae	*Chlorella vulgaris*	0,61	6,03	0,61	0,60	-1,64
Cyanobacteria	*Microcystis aeruginosa*	0,37	3,87	0,37	0,36	-2,70
Diatoms	*Cyclotella meneghiniana*	0,40	4,09	0,40	0,39	-2,50

Reference instrument Referenz 2 (UV)

Set time and date: OK
Parameter file: BT_8135_04122019

Remarks:

Signature:

Figure 116: Calibration protocol BenthoTorch bbe moldaenke 2019

biological · biophysical · engineering

bbe moldaenke

Preetzer Chaussee 177
D - 24222 Schwentinental

Telefon: +49 (0) 431/380 400
Telefax: +49 (0) 431/380 4010
e-mail: bbe@bbe-moldaenke.de
Internet: http://www.bbe-moldaenke.de

Chlorophyll Calibration Protocol

ISO 9001:2008 CERTIFIED

Operator: B. Franckowiak

Date: 02.03.23
Instrument: BenthoTorch
Serial No.: BTo-08-135
Software vers.: 3.44

Background Offset :

black	OK
grey	OK
white	OK

		Calibration		Check		
		Calibration conc. 1 Chl-a [µg/cm²]	Calibration conc. 2 Chl-a [µg/cm²]	Reference conc. Chl-a [µg/cm²]	Actual value conc. Chl-a [µg/cm²]	Deviation max =5% [%]
Green Algae	*Chlorella vulgaris*	0,83	8,82	0,83	0,81	-2,41
Cyanobacteria	*Microcystis aeruginosa*	0,50	5,69	0,50	0,49	-2,00
Diatoms	*Cyclotella meneghiniana*	0,54	5,73	0,54	0,53	-1,85

Reference instrument Referenz 2 (UV)

Set time and date: OK
Parameter file: BT_8135_07032023

Remarks:

Signature:

Figure 117: Calibration protocol BenthoTorch bbe moldaenke 2023

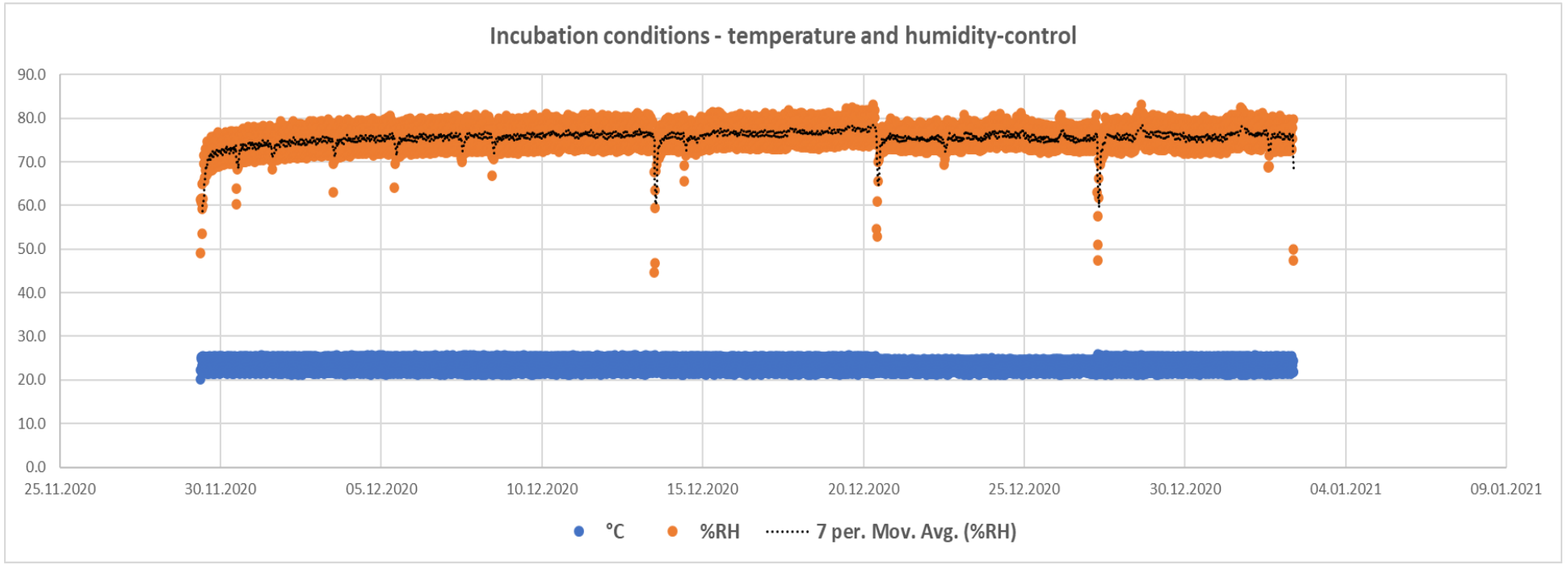

Figure 118: Trend of 35d-incubation conditions

KREMER PIGMENTE

76000 Dispersion K 498

Beschreibung
Wässrige Dispersion eines thermoplastischen Reinacrylharzes.

Lagerung
Gut verschlossen, geschützt vor Frost und starker Wärme 1 Jahr lagerfähig.

Produkteigenschaften

Festkörpergehalt (DIN 53 189)	50 ± 1 %
Aktuelle Viskosität (20°C; Brookfield-Viskosimeter III/6)	3000 – 10000 mPa.s
Ionische Einstellung	nicht ionisch
pH-Wert (DIN 53 785)	9.0 ± 0.5
Dichte	1.05 g/cm^3
Mittlerer Teilchendurchmesser	~ 0.15 µm
Minimale Filmbildungstemperatur (MFT) (DIN 53 787)	~ 5°C

Allgemeine Hinweise
Filmeigenschaften (nach Lufttrocknung unpigmentiert)
Zugversuch (DIN 53 455)

(Abzugsgeschwindigkeit: 100 mm/min)

Reißfestigkeit	σ_R	~ 4 N/mm^2
Rei0dehnung	ε_R	~ 400%

Torsionsschwingungsversuch (DIN 53445) (Frequenz: 1 Hz)

Temperatur im Dämpfungsmaximum	$T\Lambda_{max}$	~ 26°C
Schubmodel	$G_{20°C}$	100 N/mm^2

Anwendungsgebiete
Bindemittel für die Herstellung von vergilbungsfreien, wetterbeständigen Fassadenfarben, Kunstharzputzen, Betondachsteinbeschichtungen, Gasbetonbeschichtungen, Voll- und Abtönfarben, Grundierungen, Isolieranstrichen, Spachtel.

Weiterhin eignet sich Dispersion K 498 als Zusatzkomponente zur Herstellung von Organo-Silikatfarben.

Kremer Pigmente GmbH & Co. KG · Hauptstr. 41-47 · DE-88317 Aichstetten · Tel. 0049 7565 914480 · info@kremer-pigmente.com· www.kremer-pigmente.com

Figure 119: Technical data sheet pure acrylic dispersion

8. Declaration of Honour

I hereby confirm on my honour that I personally prepared the present doctoral thesis and carried out myself the activities directly involved with it.

I also confirm that the thesis has not been submitted to any other examination authority and that I have used no resources other than those declared. All formulations and concepts adopted literally or in their essential content from printed, unprinted or Internet sources have been cited according to the rules for academic work.

Holger Heinrich (VAPX00)

Goldebee, 24th April 2024 (Signature)

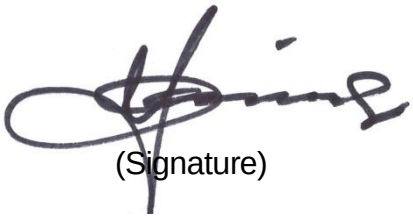

9. Acknowledgements

This dissertation was written as part of the scientific collaboration between the Marcel Breuer Doctoral School at the University of Pécs/Hungary and the Faculty of Engineering at the University of Applied Sciences Wismar/Germany. I would like to take this opportunity to thank all those involved in this cooperation.

I would like to thank in particular ...

... first, to my family - thank you for your understanding and consideration.

... Dr. habil. Adél Len University of Pécs, Faculty of Engineering and Information Technology, Civil Engineering Department, for supervising this thesis

... Prof. em. Dr. Dr. habil. Helmuth Venzmer – for putting me on the path of algae on building materials and supporting me as external tutor of the doctoral program

… Prof. Dr. Ing. Winfried Malorny - for the technical laboratory support in the Faculty of Civil Engineering and constructive discussions along the way

… Dr. Torsten Barfels - for carrying out the measurements on the REM/EDX at the Laboratory of the University of Applied Science Wismar/Germany

… the participants of the Wismar Doctoral College in the circle of the Dahlberg Institut e.V. Wismar for the time spent together.

10. References

[1] Krus M., Sedlbauer K., and Lenz K. (2003) Influence of different measures on the undershooting of the dew point on exterior surfaces (in German), Special Edition 4. Dahlberg-Kolloquium, Wismar, Germany, H. Venzmer, Ed., Berlin: Huss-Medien GmbH, Verlag Bauwesen, 2003, pp. 83–94.

[2] Von Werder J., Kots L., Lesnych N., Messal C., Venzmer H. (2003) Algae colonization of energetically renovated facades, 4. Dahlberg-Kolloquium, Wismar, Germany, H. Venzmer, Ed., Berlin: Huss-Medien GmbH, Verlag Bauwesen, 2003, pp.252-253 (in German)

[3] Rüger C., (2016) Dust binding – Wet adhesion. The Ways of Dust – In Human Environment. Springer Verlag GmbH, Berlin Heidelberg, 2016, (in German)

[4] Stamm, Aia (1980): The influence of sulphite on the growth and CO2 fixation of unicellular green algae, Environmental Pollution Series A, Ecological and Biological Vol. 22, Issue 2, Juni 1980, Pages 91-99, Elsevier (in German)

[5] Heinrich H., Venzmer H. (2020): Multifunctional detection method for the differentiated in-situ analysis of supramural biofilms during renovation measures on building component surfaces, Chapter 3 (eBook), Building Preservation III Detection methods and applications, Edition Bautenschutz, Ingenieur-Kontor Prof. H. Venzmer, Ostseebad Insel Poel, ISBN 978-3-00-066509-7 (in German)

[6] Schwerdt R. (2011) Durability of Biocidal Agents in Architectural Coatings in a Multi-year Field Trial (in German). vol. 8, Research results from building physics, Fraunhofer Verlag, Stuttgart

[7] Biocidal Products Regulation (BPR, Regulation (EU) 528/2012), https://echa.europa.eu/regulations/biocidal-products-regulation/legislation, ECHA European Chemicals Agency, Helsinki Finland (online: 29.12.2023)

[8] bbe moldaenke GmbH, Schwentinental/Germany, Measurement of Phytobenthos Fluorescence (in German), 2022. [Online]. https://www.bbe-moldaenke.de/en/products/chlorophyll/details/benthotorch.html. Accessed: January 2, 2022.

[9] Harris T. D., Graham J. L. (2015): Preliminary evaluation of an in vivo fluorometer to quantify algal periphyton biomass and community composition, Lake and Reservoir Management, 31:2, pp 127-133, DOI: 10.1080/10402381.2015.1025153

[10] Wu Z., Zhu Y., Huang W., Zhang C., Li T., Zhang Y., and Li A. (2012) Evaluation of flocculation induced by pH increase for harvesting microalgae and reuse of flocculated medium, Bioresource Technol. vol. 110, pp. 496–502.

[11] Baumstark R., Schwartz M. (2001) Dispersions for Architectural Coatings - Acrylate Systems Sin Theory and Practice (in German). Vincentz Verlag Hannover, Hannover 2001, p.35, p.124, p 50

[12] Lian B., Chen Y., Zhu L., and Yang R. (2008) Effect of microbial weathering on carbonate rocks," Earth Science Frontiers, vol. 15, no. 6, pp. 90–99

[13] Gysau, D. (2014): Fillers, Vincentz Network GmbH, Hannover, S. 13 ff. (in German)

[14] Schade H., Marchionini A. (1928) The acid mantle of the skin. Berliner Klinische Wochenschrift, Band 7, 1928, S. 12–14, Berlin (in German)

[15] Guggenbichler S., Fey T., and Guggenbichler J. P. (2020) Hospital acquired infections with multiresistant microorganisms: UN Interagency Coordination Group on antimicrobial resistance demands immediate, ambitious, and innovative action, Integrated Biomedical Sciences, vol. 6, no. 1, pp. 84–104

[16] Patent: Zinc molybdate with triclinic crystal structure as antimicrobial agent", EP 3643177A1, Amistec GmbH & Co KG, Kössen/Austria, 2020.

[17] Hausmann K., Kremer B. P. (1993): Extremophiles - microorganisms in unusual habitats, VCH Verlagsgesellschaft mbH, Weinheim, 1993, ISBN 3-527-30026-0 (in German)

[18] Bialevic V., Zachleder V., Bisova K. (2022) The Effect of Variable Light Source and Light Intensity on the Growth of Three Algal Species, Cells MDPI Journal 2022, 11, 1293. https//doi.org/10.3390/cells1111081293

[19] Gorbushina A. A. (2007) Life on the rocks, Environmental Microbiology, vol. 9, no. 7, pp. 1613–1631

[20] Paetzold, P. (2009): Chemistry - An introduction. Walter de Gruyter, Berlin 2009, S. 4 (in German)

[21] Kaim, W. (1991): Bioorganic chemistry, metals at the centre of photosynthesis: magnesium and manganese, Verlag B.G. Teubner Stuttgart, 1991 (in German)

[22] Fuhrkamp J.-H. (2009) Chemical elements and life, Seven molecules, Wiley-VCH Verlag GmbH, S. 278, 1. Edition (in German)

[23] Schreiber U., Bilger W., Neubauer C. (2004): Chlorophyll fluorescence as a nonintrusive indicator for rapid assessment of in vivo photosynthesis, Ecophysiology of Photosynthesis, Springer-Verlag, pp. 49-70

[24] Jander, F. (2001): Mass culture of microalgae with pharmaceutically useful ingredients using CO2 and NaHCO3, obtained from waste gases from a combined heat and power plant, Dissertation Christian-Albrecht-Universität, Kiel, (in German)

[25] Umweltbundesamt (2013): The Federal Environment Agency's air monitoring network (UBA) (in German)

[26] Freystein, K. und Reisser, W. (2011): Algae colonization of facades - influence of fungi on colonization, resistance and control of algae coatings, facade restoration, Helmut Venzmer (Hrsg.). Beuth-Verlag GmbH, 1. Auflage 2011, Berlin, S. 9-16 (in German)

[27] Steinbüchel A., Pötter M., Ewering C., Oppermann-Sanio F. (2013): Microbiology practical course - experiments and theory, ectosymbioses of fungi with green algae or cyanobacteria, pp 304-306, Springer Spektrum, 2. Auflage, ISBN 978-3-642-25150-4 (in German)

[28] Seiffert, F. (2014): Characterization of rock growth and weathering using a model biofilm, Dissertation FU Berlin, 09/2014 (in German)

[29] Baumeister W. (1958): Handbook of plant physiology, total ash content of plants, Springer Verlag, p.7

[30] Burlacot A., Happe Th. (2018): Flavodiiron-mediated CO2 photoreduction – a relay between H2 production and CO2 fixation during the induction of photosynthesis in anaerobic *Chlamydomonas reinhardtii*, Plant Physiology, 2018, DOI: doi.org/10.1104/pp.18.00721

[31] Lohmiller Th., Cox N., Lubitz, W. (2015): http://www.laborundmore.com/archive/685536/Ein-Enzym,-das-die-Welt-veraenderte.html, abgerufen am 13.03.2019

[32] Pirson A. (1952): Minerals and photosynthesis, S.364ff. in „The mineral nutrition of plants “, Springer-Verlag, 1958, p.10 (in German)

[33] Freystein, K., Reisser W. (2010): Influence of particulate matter on algae biofilms, Europäischer Sanierungskalender 2010, Helmut Venzmer (Hrsg.), Beuth Verlag GmbH, Berlin 2010, p. 269-273 (in German)

[34] Annual air quality reports (2021) State Office of Environment, Nature Conservation and Geology, Mecklenburg-Western Pomerania, Güstrow, 2011-2020 (in German). [Online]. Available: www.lung.mv-regierung.de/umwelt/luft/lume.htm. Accessed: Dec. 16, 2021.

[35] Steffgen T. (2019) Experimental studies - building physics, Investigation in condensation water on plaster surfaces,” Pollack Periodica, vol. 14, no. 1, pp. 167–175

[36] Quagliarini E., Gianangeli A., Gregorini B., Osimani A., Aquilanti L., Clementi F. (2019): Effect of temperature and relative humidity on algae biofouling on different fired brick surfaces, Construction and Building Materials 199, Elsevier, pp. 396-405

[37] Bagda E., Spindler G. (2002), Why facades turn grey. Paint and varnish edition 01/2002, Vincentz Verlag Hannover, p 94 (in German)

[38] DIN-Taschenbuch 157 (1993) Colorants, pigments, fillers, dyes, DIN 55943 bis DIN 66131: Normen, Beuth-Verlag Berlin (in German)

[39] Baumstark R., Schwartz M. (2001) Dispersions for Architectural Coatings – Acrylate Systems Sin Theory and Practice (in German). Hannover: Vincentz Verlag Hannover, p124, p35

[40] Court of Justice of the European Union, Press Release 190/22, Judgment of the General Court in Joined Cases T-279/20, T-288/20 and T-283/20 | CWS Powder Coatings and Others v Commission regarding Titan dioxide, 23.11.2023

[41] Heinrich H., Venzmer, H. (2019): Importance of magnesium-containing fillers for the colonization of facade coatings, Chapter 10, Building protection II, Detection methods and applications, Edition Bautenschutz H. Venzmer (Ed.), Insel Poel, ISBN 978-00-063776-6 (in German)

[42] Carl Roth GmbH & Co KG, Safety Dat Sheet Article 0874 (ZnMoO4), Version 1.0 de (29.10.2018), 76185 Karlsruhe/Germany

[43] ISO Standards Handbook, Paints and varnishes, Vol-3 raw materials, ISO 150 – IO 14900, International Organisation for Standardization, Geneve 2002

[44] Patent CA989555A (1972-07-07), Amax Inc. Molybdate corrosion inhibiting pigment and method for preparing same, https://patents.google.com/patent/DE2200654A1/de#citedBy

[45] Patent WO2012007124A1 (19.01.2012), Flame retardant-stabilizer combination for thermoplastic polymers, Inventor: Sebastian HÖROLD, Wolfgang Wanzke, Elke Schlosser, https://patents.google.com/patent/WO2012007124A1/de (in German)

[46] Tetsu T. (2003) Bactericidal effect of an energy storage TiO2-WO3 photocatalyst in dark, Electrochemistry Communications, ELSEVIER, Amsterdam, NL, Bd. 5, Nr. 9, 1. September 2003, pp 793-796, XP002656981, ISSN: 1388-2481, DOI: 10.1016/J.elecom.2003.07.003

[47] Lorenz K. (2011) Anodic TiO2 nanotube layers electrochemically filled with MoO3 and their antimicrobial properties, BIOINTERPHASES, Bd. 6, Nr. 1, 17. März 2011, XP55169086, ISSN: 1934-8630, DOI: 10.1116/1.3566544; pp 16-21

[48] Zollfrank C. (2011) Antimicrobial activity of transition metal acid Mo-Oxid prevents microbial growth on material surfaces, Materials Science and Engineering, ELSEVIER SCIENCE S.A, CH, Bd. 32, Nr. 1, 22. September 2011, XP028112650, ISSN: 0928-4931, DOI: 10.1016/J.MSEC.2011.09.010, pp 47-54

[49] Tétault N. (2012) Biocidal activity of metalloacid-coated surfaces against multidrug-resistant microorganisms, Antimicrobial Resistance & Infection Control, 14. November 2012 (2012-11-14), Seiten 1-6, XP55168973, DOI:10.1186/2047-2994-1-35, URL: http://www.aricjournal.com/content/pdf/2047-2994-1-35.pdf

[50] Shafaei S. (2012) Molybdenum and tungsten oxides as innovative antimicrobial materials, Book of Abstracts, 21. November 2012 (2012-11-21), pp. 314-314, XP55168956, Lissabon, Portugal URL: http://www.formatex.info/icar2012/abstracts/htm/223.pdf

[51] Lackner M. (2013) Polymorphs of molybdenum trioxide as innovative antimicrobial materials", SURFACE INNOVATIONS, Bd. 1, Nr. 4, 5. Oktober 2013 (2013-10-05), Seiten 202-208, XP55168959, ISSN: 2050-6252, DOI: 10.1680/si.13.00021

[52] Tang H. (2013) Highly antibacterial materials constructed from silver molybdate nanoparticles immobilized in chitin matrix, CHEMICAL ENGINEERING JOURNAL, vol. 234, 5 September 2013, pages 124-131, XP55393557, CH ISSN: 1385-8947, DOI: 10.1016/j.cej.2013.08.096

[53] Qianping Wang (2008) Method for preparing three-component coprecipitation molybdate antimicrobial by using microwave heating, In: "EPODOC Database", 24 September 2008, XP55393560, pages 1-2, & CN 101 268 784 A (UNIV HEBEI POLYTECHNIC [CN]) 24 September 2008

[54] Hofbauer W., Fitz C., Krus M., Sedlbauer K., Breuer K. (2006) Prediction method for biological infestation by algae, fungi and lichens on building component surfaces. Building research for practice, Band 77, Fraunhofer IRB Verlag, ISBN-13 978-3-8167-7102-9, p. 23 (in German)

[55] DIN EN 16492:2014, Paints and varnishes - Evaluation of the surface disfigurement caused by fungi and algae on coatings, German version (in German), DIN Deutsches Institut für Normung e.V., Beuth Verlag GmbH, Berlin, 2014.

[56] DIN EN 15458:2014, Paints and varnishes – Laboratory method for testing the efficacy of film preservatives in a coating against algae; German version EN 15458:2014, Beuth Verlag GmbH, 10772 Berlin.

[57] Cole M., Bond C.P. (1972): Recent advances in automatic image analysis using a television system, Journal of Microscopy vol. 96, https://doi.org/10.1111/j.1365-2818.1972.tb03747.x

[58] Al-Azawi M. (2013): Image Thresholding using Histogram Fuzzy Approximation, https://doi.org/10.5120/14480-2781, International Journal of Computer Applications, pp36-40

[59] ImageJ, Image processing and analysis in Java, 2018. [Online]. Available: https://imagej.nih.gov/ij/index.html. Accessed: December 27, 2021.

[60] Beer S., Vilenkin B., Weil A., Veste M., Susel L., Eshel, A. (1998): Measuring photosynthetic rates in seagrasses by pulse amplitude modulated (PAM) fluorometry. Mar. Ecol. Prog. Ser., 164: 293 – 300.

[61] Geel C. (1997): Photosystem II electron flow as a measure for phytoplankton gross primary production, Dissertation, University Wageningen.

[62] Eggert A., Häubner N., Klausch S., Karsten U., Schumann R. (2006): Quantification of algal biofilms colonising building materials: chlorophyll-a measured by PAM-fluorometry as a biomass parameter, Biofouling, 22:02, pp 79-90, DOI: 10.1080/08927010600579090

[63] Von Werder J., Venzmer H. (2012): "The potential of pulse amplitude modulation fluorometry for evaluating the resistance of building materials to algal growth," International Biodeterioration & Biodegradation, vol. 84, pp. 227–235, 2012.

[64] Von Werder J., Venzmer H., Cerny R. (2015) Application of fluorometric and numerical analysis for assessing the algal resistance of external thermal insulation composite systems, Journal of Building Physics, vol. 38, no. 4, pp. 290–316

[65] Wehr J.D., Sheath R.G. (2003) Freshwater algae of North America: ecology and classification. 1st Edition Amsterdam & Boston, Academic Press

[66] Szymanski N., Dabrowski P., Sabochnicka-Swiatek M., Panchal B., Lohse D., Kalaji H.M. (2017): Taxonomic classification of algae by the use of chlorophyll a, Scientific Review – Engineering and Environmental Sciences (2017), 26 (4), 470–480, DOI 10.22630/PNIKS.2017.26.4.45

[67] Vandamme D., Foubert I., Fraeye I., Meeschaert B., Muylaert K. (2012): Flocculation of Chlorella vulgaris induced by high pH: Role of magnesium and calcium and practical implications, Bioresour. Technol., vol. 105, pp. 114–119

[68] Leentvaar, J., Rebhun, M. (1982) Effect of Magnesium and Calcium Precipitation on coagulation-flocculation with lime, Water Research Vol. 16, pp. 655-662, Pergamon Press Ltd., Great Britain

[69] Barros A., Goncalves A., Simoes M., Pires J.C.M. (2015) Harvestings techniques applied to microalgae: A review, Renewable and Sustainable Energy Reviews 41, 1489-1500

[70] Vogel M. (2011) For the uptake and binding of uranium (VI) by the green alga Chlorella vulgaris (in German), Doctoral Dissertation, Technische Universität Dresden

[71] Van der Hoek C., Mann D.G., Jahns H.M. (1995) Algae. An Introduction to Phycology. Cambridge University Press, Cambridge

[72] Smith B., Davis R. (2012) Sedimentation of algae flocculated using naturally-available, magnesium-based flocculants. Algal Research 2012; 1:32-9

[73] Modak J. M., Natarajan K. (1995): Biosorption of metals using non-living biomass, Environmental Science, https://doi.org/10.1007/BF03403102

[74] Schopf W. (1983) Evolution on earth`s earliest ecosystems, recent progress, and unsolved problems, in earth`s earliest biosphere, Princeton Univ. Press, New Jersey, pp.361-384

[75] Costerton J.W., Donlan R.M. (2002) Biofilms: survival mechanisms of clinically relevant microorganisms, Clinical Microbiology Rev. 15, pp. 167-193

[76] Flemming H.C., Wingender J. (2002) What fits biofilms together. Proteins, polysaccharides. Chemistry in our time, pp. 30-42 (in German)

[77] Parrilli E., Tutino M.L., Marino G. (2022) Biofilm as an adaption strategy to extreme conditions, Rendiconti Lincei. Szeinze Fisiche e Naturali, 33:527-536, https://doi.org/10.1007/s12210-022-01083-8

[78] Bock E., Krumbein W.E (1989) Activities of microorganisms and possible consequences for the rock of architectural monuments, special issue on building protection and restoration, pp. 34-37

[79] Motzke, G. (2004): Algae fungi facades, A legal allocation problem taking into account the new material defect concept of the modernization of the law of obligations, C. Maurer Druck und Verlag, Geisslingen, S.19 (in German)

[80] Krus M., Sedlbauer K., and Lenz K. (2003) Influence of different measures on the undershooting of the dew point on exterior surfaces" (in German), Special Edition 4. Dahlberg-Kolloquium, Wismar, Germany, H. Venzmer, Ed., Huss-Medien GmbH, Verlag Bauwesen, Berlin, pp. 83–94.

[81] Künzel H.M., Fitz C., Krus M. (2011): Moisture protection of various facade systems, facade renovation, Helmuth Venzmer (ed.), Beuth-Verlag GmbH Berlin, 1st edition 2011, S.29-51, (in German)

[82] Dubosc A., Escadeillas G., Blanc PJ. (2001) Characterization of biological stains on external concrete walls and influence of concrete as underlying material. Cement and Concrete Research 2001;31(11):1613-7

[83] Cerman, Z. (2007) Superhydrophobicity and self-cleaning: Mode of action, efficiency, and limitations in defence against microorganisms. Dissertation, Rheinische Friedrich-Wilhelms-Universität Bonn (in German)

[84] Leonhard, H, & Sinnesbichler, H. (2000) Investigation of the long-wave thermal radiation behaviour of facade coatings in winter. IBP-Report RK-ES-05/2000 (in German)

[85] Krus, M., Fitz C., Sedlbauer K., (2008) Latent heat storage additives and IR paints to reduce the risk of overheating on external facades. Altbausanierung 2 (Ed. H. Venzmer), Beuth Verlag GmbH, Berlin, 91-101 (in German)

[86] R. Schwerdt (2001) Durability of Biocidal Agents in Architectural Coatings in a Multi-year Field Trial (in German). vol. 8, Research Results from Building Physics. Stuttgart: Fraunhofer Verlag

[87] Hashimoto K., Irle H., Fujishima A. (2005) TiO2-photocatalysis – A historical overview and future prospects. Japanese Journal of Applied Physics Part 1, Vol. 44, No. 12, 8269-8285

[88] Bagda E., (1998) Preservation of emulsion paints. Active ingredients - Effect - Analysis - Emissions. Band 509, TAE Esslingen, expert Verlag Renningen-Malmsheim, p. 2 (in German)

[89] Wunder T., (2003) Biocide selection to prevent algae and fungi. Renovation of old buildings 5/6 (Ed. H Venzmer), Verlag Bauwesen, HUSS-Medien GmbH, Berlin, 149-157 (in German)

[90] Lindner W., (2000) On the chemistry of biocides on facades, in: Biocides in architectural coatings (Ed. J. Bartz), TAE expert Verlag, Band 545, pp. 53-66 (in German)

[91] Kaup T., Boos M. (2008) Possibilities and limitations in the formulation of functional facade coatings. Biofilms and functional building material surfaces (Ed. H. Venzmer), Beuth Verlag GmbH, Berlin, 129-141 (in German)

[92] Bagda E., (1998) Preservation of emulsion paints. Active ingredients - Effect - Analysis - Emissions. Band 509, TAE Esslingen, expert Verlag Renningen-Malmsheim, pp. 5-8 (in German)

[93] Lindner W. (2005) Surface Coatings. In Paulus W. (Ed.): Directory of Microbicides for the Protection of Materials, Springer New York, pp. 347-376

[94] International Standard ISO 2296:2011(E), Measurement of antibacterial activity on plastics and other non-porous surfaces, Second Edition 01-08-2011

[95] Brenner T. (2010) Vigilant germ killers, paint and varnish, Issue 06/2010, Vincentz Network, Hannover, 3p (in German)

[96] Brühwasser C., Heinrich H., Lass-Flörl C., Mayr A. (2017) Self-disinfecting surfaces and activity against Staphyloccocus aureus ATCC 6538 under real-life conditions. JOURNAL OF HOSPITAL INFECTION 97: 2 pp. 196-199, 4 p.

[97] Patent DE 10 2017 010 366 A1, Heinrich H. (Inventor), Resin composition, resin coating, laminates and impregnates containing them, and process for their manufacture, German Patent and Trademark Office DPMA, publication 2019 (in German)

[98] Mayr A., Orth-Höller D., Heinrich H., Hinterberger G., Wille I., Naschberger V., Lass-Flörl C., Binder U. (2019) Galleria mellonella as a Model to Study the Effect of Antimicrobial Surfaces on Contamination by Staphylococcus aureus, Archives of Clinical and Biomedical Research Vol. 3 No. 5 – October 2019. [ISSN 2572-9292], DOI:10.26502/acbr.50170076

[99] Herrmann D., (2020) Neue DIN 55699: TSR-Wert beachten, Malerblatt (online), https://www.malerblatt.de/technik/was-besagt-der-tsr-wert vom 20.02.2020 (19:30h)

[100] Garcia-Pichel F., Castenholz R. W. (1991): Characterization and biological implications of scytonemine, a cyanobacterial sheath pigment. Journal of Phycology, pp 395–409, DOI: 10.1111/j.0022-3646.1991.00395.

[101] Pentecost A., Whitton B. A. (2012): Subaerial Cyanobacteria, Ecology of Cyanobacteria II, Springer Science + Business Media B.V., Chapter 10, p 299. DOI: 10.1007/978-94-007-3855-3_10.

[102] Böhringer D. (2011) Barrierefreie Gestaltung von Kontrasten und Beschriftungen, IRB Fraunhofer Verlag, ISBN 10-3816784453, p. 126

[103] Sous S., (2018) AIBAU, Aachen, VHV-Building experts, p. 88, https://www.vhv-bauexperten.de/aktuelles/downloads/vortraege-bautage2018

[104] TORSO-Verlag e.K., Obere Grüben 8, 97877 Wertheim, www.torso.de

[105] IUQ Institut für Umweltschutz und Qualitätssicherung Dr. Krengel GmbH, 23936 Grevesmühlen/Germany, Prüfbericht-Nr. 21-00507/09396 v. 18.02.2021

[106] Ahnert F. (1996) Introduction to Geomorphology (in German). Verlag Eugen Ulmer Stuttgart, 1996, p.82

[107] Bagda E., Spindler G. (2002) Why façades turn grey. Paint & varnish Edition 01/2002, p 94, Vincentz Verlag, Hannover (in German)

[108] Vasavada N. (2016) One-way ANOVA with post-hoc Tukey HSD (Honestly Significant Difference) test calculator for comparing multiple treatments. [Online]. Available: https://astatsa.com/OneWay_Anova_with_TukeyHSD/. Accessed: December 27, 2021.

[109] Brechet E., McStay D., Wakefield R.D., Campbell I. (1998). A novel blue LED based scanning hand-held fluorometer for detection of terrestrial algae on solid surfaces. DOI:10.1117/12.323527

[110] Eggert A., Häubner N., Klausch S., Karsten U., Schumann R. (2006) Quantification of algal biofilms colonising building materials: chlorophyll a measured by PAM-fluorometry as a biomass parameter. Biofouling. 2006;22(1-2):79-90. DOI: 10.1080/08927010600579090. PMID: 16581672, DOI:10.1080/08927010600579090

[111] Tang Y.Z., Dobbs F.C. (2007) Green autofluorescence in dinoflagellates, diatoms, and other microalgae and its implications for vital staining and morphological studies. Appl Environ Microbiol. 2007 Apr;73(7):2306-13. doi: 10.1128/AEM.01741-06. Epub 2007 Feb 2. PMID: 17277199; PMCID: PMC1855647.

[112] Venzmer H., Von Werder J., Lesnych N., & Koss L. (2008). Algal defacement of façade materials—results of long-term natural weathering tests obtained by new diagnostic tools. In Proceedings of the 8th Symposium on Building Physics in the Nordic Countries (Vol. 1, pp. 277-284). DTU.

[113] Gustavs L., Schumann R., Eggert A., & Karsten U. (2009). In vivo growth fluorometry: accuracy and limits of microalgal growth rate measurements in ecophysiological investigations. Aquatic microbial ecology, 55(1), 95-104.

[114] Konkol N., McNamara C.J., Mitchell R. (2009) Fluorometric detection and estimation of fungal biomass on cultural heritage materials. Journal of Microbiological Methods. 2010 Feb;80(2):178-82. DOI: 10.1016/j.mimet.2009.12.008. E-pub 2009 Dec 22. PMID: 20026363.

[115] Johansson S. (2011). Biological growth on rendered façades Lund University, Division of Building Materials, PhD-Thesis, Sweden

[116] Gazulla M. F., Sánchez E., González J. M., Portillo M. C., Orduna M. (2011). Relationship between certain ceramic roofing tile characteristics and biodeterioration. Journal of the European Ceramic Society, 31(15), 2753-2761.

[117] Gladis F., & Schumann R. (2011). Influence of material properties and photocatalysis on phototrophic growth in multi-year roof weathering. International biodeterioration & biodegradation, 65(1), 36-44.

[118] Cement Concrete Composition 36 (2013) 93–100, https://doi.org/10.1016/j.cemconcomp.2012.08.030.

[119] Von Werder, J., Venzmer, H. (2013). The potential of pulse amplitude modulation fluorometry for evaluating the resistance of building materials to algal growth. International biodeterioration & biodegradation, 84, 227-235.

[120] Blanco S. M., de Cea A. A., Pérez I. S., De Belie N. (2014). Bioreceptivity optimisation of concrete substratum to stimulate biological colonisation (Doctoral dissertation, Universitat Politècnica de Catalunya).

[121] Manso S., De Muynck, W., Segura I., Aguado A., Steppe K., Boon N., De Belie N. (2014). Bioreceptivity evaluation of cementitious materials designed to stimulate biological growth. Science of the Total Environment, 481, 232-241.

[122] Ferrari C. (2015) Review on the influence of biological deterioration on the surface properties of building materials: Organisms, Materials, and Methods, Int. J. of Design & Nature and Ecodynamics. Vol. 10, No. 1, 21–39

[123] Eyssautier-Chuine S., Vaillant-Gaveau N., Gommeaux M., Thomachot-Schneider C., Pleck J., & Fronteau G. (2016) Chlorophyll fluorescence and colorimetric analysis for monitoring the algal development on biocide-treated stone. In The Open Conference Proceedings Journal (Vol. 7, No. 1).

[124] Vojtková H. (2017) Algae and their biodegradation effects on building materials in the Ostrava industrial agglomeration, IOP Conf. Ser.: Earth Environ. Sci. 92 012073, DOI 10.1088/1755-1315/92/1/012073

[125] Vázquez-Nion D., Silva B., Prieto B. (2018) Bioreceptivity index for granitic rocks used as construction material, Science of The Total Environment, Volume 633, Pages 112-121, ISSN 0048-9697, https://doi.org/10.1016/j.scitotenv.2018.03.171.

[126] Wang-Choi Y. (2018) Advances in Materials Science and Engineering, Volume 2018, Article ID 1892127, 8 pages, https://doi.org/10.1155/2018/1892127

[127] Prieto B., Montoro Á., Fuentes E., Aguiar U., Sanmartín P. (2019) Functional properties and biodeterioration behaviour of new formulations of lime technical mortars. In Geophysical Research Abstracts (Vol. 21).

[128] Sanmartín P., Grove R., Carballeira R., Viles H. (2020) Impact of colour on the bioreceptivity of granite to the green alga Apatococcus lobatus: Laboratory and field testing. Sci. Total Environ. 2020 Nov 25; 745:141179. DOI: 10.1016/j.scitotenv.2020.141179. Epub 2020 Jul 22.

[129] Stefanova A., Pichaya I., Caldwell G., Stephen G., Bridgens B., Armstrong R. (2021) Photosynthetic textile bio composites: Using laboratory testing and digital fabrication to develop flexible living building materials, Science and Engineering of Composite Materials, vol. 28, no. 1, 2021, pp. 223-236. https://doi.org/10.1515/secm-2021-0023

[130] Fuentes E., Prieto B. (2021) International Biodeterioration & Biodegradation, Volume 164, 2021, 105295, ISSN 0964-8305, https://doi.org/10.1016/j.ibiod.2021.105295.

[131] Hedwigia Nova (2022) 114(3-4):303-320, DOI:10.1127/nova_hedwigia/2022/0691

[132] Crawford A., Pichaya I., Caldwell G., Armstrong R., Bridgens B. (2022) Clay 3D printing as a bio-design research tool: development of photosynthetic living building components, Architectural Science Review, 65:3, 185-195, DOI: 10.1080/00038628.2022.2058908

[133] Stohl L., Manninger T., von Werder J., Dehn F., Gorbushina A., Meng B. (2023) Bioreceptivity of concrete: A review. Journal of Building Engineering, 107201.

[134] Hoff V. (2017) Variation in benthic colonization on tile and in leaf degradation-results from a flume experiment in Norway (master's thesis, Norwegian University of Life Sciences, Ås).

[135] Morin V., De Larrard F., Dubois-Brugger I., Horgnies M., Duchand S., Vacher S., Lapinski M. (2018). Concrete with improve of bioreceptivity. In Conference: Final Conference of RILEM TC.

[136] Heinrich H., Venzmer H. (2020): Multifunctional detection method for the differentiated in-situ analysis of supramural biofilms during renovation measures on building component surfaces, Chapter 3 (eBook), Building Preservation III Detection methods and applications, Edition Bautenschutz, Ingenieur-Kontor Prof. H. Venzmer, Ostseebad Insel Poel, ISBN 978-3-00-066509-7 (in German)

[137] Romani M., Adouane E., Carrion C., Veckerlé C., Boeuf D., Fernandez F., Lami R. (2021). Diversity and activities of pioneer bacteria, algae, and fungi colonizing ceramic roof tiles during the first year of outdoor exposure. International Biodeterioration & Biodegradation, 162, 105230.

[138] Bellopede R., Balestra V., De Regibus C., Isaia M., Marini P., Nicolosi G., Vigna B. (2022). Biocorrosion of speleothems driven by lampenflora: preliminary observations in Bossea show cave (NW-Italy). In " Geosciences for a Sustainable Future" SGI-SIMP Congress, Torino 19-21 September 2022-Abstract Book (p. 550). Società Geologica Italiana.

[139] Morin V., Duchand S., Dubois-Brugger I., Perrot M., Lapinski M., & Vacher S. (2022). Development of laboratory tests to measure the growth kinetic of micro-algae of concrete in marine environment and comparison to in-situ experiments. In IOP Conference Series: Materials Science and Engineering (Vol. 1245, No. 1, p. 012002). IOP Publishing.

[140] Reboah P., Bolou-Bi C. B., Nowak S., & Verney-Carron A. (2023). Influence of climatic factors on cyanobacteria and green algae development on building surface. Plos one, 18(3), e0282140.

[141] Heinrich H., Len A., Venzmer H. (2023). Investigation of façade coatings containing algae-prone fillers. Pollack Periodica, 18(1), 55-59.

[142] Drakard V. F., Brooks P. R., & Crowe T. P. (2023) Colonisation after disturbance on artificial structures: The influence of timing and grazing. Marine Environmental Research, 187, 105956.

[143] Chong K.H., Volesky B. (1995) Description of two-metal biosorption equilibria by Langmuir-type models. Biotechnology Bioengineering 47, 451-460

[144] Schlie F. (1898-1902) Die Kunst- und Geschichtsdenkmäler des Großherzogtums Mecklenburg-Schwerin, Schwerin